CHAPTER 3

ASSEMBLY OF EMPTY CORE-LIKE PARTICLES AND DOUBLE-SHELLED, VIRUS-LIKE PARTICLES OF AFRICAN HORSESICKNESS VIRUS BY CO-EXPRESSION OF FOUR MAJOR STRUCTURAL PROTEINS

3.1. INTRODUCTION

In order to increase our understanding of the assembly of the capsid proteins of AHSV, for the development of subunit vaccines and to study viral morphogenesis, it is necessary to investigate the interaction of the four major structural proteins of AHSV in the absence of other AHSV proteins and the viral genome. To investigate particle formation it was necessary to synthesise the proteins of interest in significant quantities using an appropriate expression system, in a near to native conformation.

The formation of complex structures such as viruses often requires the synthesis and interaction of several gene products. For example, seven structural proteins in different molar proportions are needed for the assembly of mature African horsesickness virus particles. Viral structures which contain multiple proteins encoded by separate genes or mRNA species and involving non-equimolar ratios of proteins present a more difficult and challenging objective to the study of viral morphogenesis. The AHSV and BTV cores present a puzzle of how a large complex, containing mismatched symmetry, can assemble (Roy, 1992; Roy, 1996; Roy *et al.*, 1997). Viruses of the family Reoviridae have received considerable attention from structural biologists. The structure of at least one member of each of the four major genera, Rotavirus, Orthoreovirus, Orbivirus, and Aquareovirus, has been determined using cryo-electron microscopy. Most of the structure-related research and the assembly of orbivirus particles have been carried out with BTV. The atomic structure of the core of BTV has recently been resolved by X-ray crystallography (Grimes *et al.*, 1998).

The assembly of the two major core proteins of BTV, VP3 and VP7, was demonstrated by simultaneous expression of the two proteins, using a dual gene recombinant baculovirus consisting of duplicated polyhedrin promoters of *Autographa californica* nuclear polyhedrosis virus. Recombinant baculoviruses synthesising both proteins produced core-like particles distributed throughout the infected insect cells. The BTV CLPs appeared to be similar in size and appearance to cores prepared from BTV. In the case of BTV, baculovirus multigene vectors have been developed to co-synthesise up to five BTV proteins in the same cell (Balyaev & Roy, 1993; Balyaev *et al.*, 1995).

For optimum synthesis of BT VLPs a quadruple gene expression vector, which utilises the polyhedrin and p10 promoters of AcNPV, has been used to synthesise the BTV VP2, VP3, VP5 and VP7 proteins. The expressed proteins assembled into virtually homogenous double capsid particles (French *et al.*, 1990).

In comparison to BTV, very little is known about the assembly of the structural proteins of AHSV and most of the focus has been on protective antigens and the development of subunit vaccines (Martinez-Torrecuadrada *et al.*, 1996). Until very recently a number of the genes that encode the capsid proteins had either not yet been cloned or had not been expressed. No work on the assembly of AHS VLPs has been published. One of the aims in AHSV research has been to clone, characterise and express all the genes that encode AHSV structural proteins, in order to identify potentially important differences between BTV and AHSV capsid proteins. Furthermore, to reveal common structural elements in cognate proteins of related orbiviruses, that can provide us with a better understanding of how the structure of individual proteins relates to their function. All ten different genome segments of AHSV, including VP1, VP3, VP4, VP5 and VP6 have now been cloned, sequenced and successfully expressed using recombinant baculoviruses. Subsequent structural and functional analysis of these recombinant proteins have provided information concerning the assembly, coding properties and replication of AHSV. The natural progression of future studies will be the examination of multiprotein structures such as the core-like and virus-like particles.

The assembly of virus-like particles by the co-expression of the four major structural proteins of AHSV presents several research opportunities. For example, the stages of viral assembly, the contribution of individual components to the assembly process and the nature of viral protein interactions can be investigated. An increased understanding in viral morphogenesis may aid in the development of antiviral agents, which specifically interfere with the assembly process. In addition, it is anticipated that the availability of large quantities of intact VLPs due to the authenticity in their biological and immunological properties could prove useful as viral vaccines, as they lack any genetic material and cannot replicate. The use of baculovirus-expressed subviral particles as vaccines against AHSV has potential advantages over attenuated viral vaccines since they are non-infectious in the target host.

Virus assembly within infected cells involves a precise sequence of macromolecular interactions. To unravel the individual steps involved in the assembly of the complete virion of AHSV, Maree *et al.* (1998) engineered the first of a series recombinant baculoviruses to make multicomponent structures resembling AHSV structure (CLPs). AHSV VP3 and VP7 were simultaneously expressed using two recombinant baculoviruses expressing each gene respectively. As in the case of BTV, the assembly of AHSV VP3 and VP7 into CLPs was self-primed and their structure resembled empty authentic

AHSV cores. The fine structure of the AHSV CLPs remains to be investigated and in order to accomplish this aim it is necessary to co-express large amounts of AHSV VP3 and VP7, using a dual vector. In the long term we hope to make the correlation between structural and functional differences of the individual viral proteins of AHSV and BTV. From a vaccine development point of view, CLPs may prove to be of great practical value. Firstly, the CLPs may provide the necessary scaffold for the correct conformational presentation of the relevant neutralising epitopes of VP2. Therefore, the co-expression of the CLPs with the outer capsid polypeptides of AHSV and their possible self-primed assembly into VLPs may prove to be important in eliciting a neutralising immune response in horses against AHSV. BTV VLPs were found to be highly immunogenic, even at low doses, compared to VP2 alone or mixtures of VP2 and VP5. Secondly, CLPs can be developed as an antigen delivery system expressing/carrying foreign epitopes on the surface of the CLPs. Chimeric BTV CLPs containing foreign epitopes of up to 39 amino acids were able to elicit humoral or T helper cell responses, depending on the epitope. In order to accomplish the aims of using the AHSV CLPs as antigen delivery systems, there is a requirement for a dual recombinant vector expressing large amounts of both major core proteins simultaneously and in the correct molar ratio.

Therefore, the objectives for this part of the investigation were, firstly to investigate the structure and assembly of AHSV major core proteins, VP3 and VP7, by co-expression of the two proteins in insect cells, and secondly to determine whether the outer capsid proteins of AHSV will spontaneously assemble on the CLPs to form VLPs.

3.2. MATERIALS AND METHODS

3.2.1. Materials

The baculovirus transfer vector, pFastbacDual, was obtained from Life Technologies. The late Prof. D. Botes of the Department of Biochemistry, University of Cape Town synthesised the oligonucleotide primers used in this section. The Klenow DNA polymerase enzyme, rapid DNA ligation kit and plasmid or PCR high pure purification kits were supplied by Boehringer Mannheim. Qiagen supplied the Qiagen^{R} plasmid mini-kit, while the Nucleobond^{R} and Wizard^{TM} columns were obtained from Macherey-Nagel and Promega, respectively. Life Technologies also supplied *E. coli* DH5α cells. AmpliTaq^{R} DNA polymerase FS, was supplied in the ABI PRISM^{TM} Big Dye Terminator Cycle Sequencing Ready Reaction kit (Perkin Elmer).

3.2.2. DNA manipulations and construction of dual transfer vectors

3.2.2.1. Insertion of AHSV-9 VP3 and VP7 genes into pFastbacDual

cDNA copies representing the complete coding sequences of the AHSV-9 segment 3 (S3) and segment 7 (S7) were cloned and manipulated for expression in the baculovirus system by Mr. S Durbach and Mrs. S Maree respectively in the laboratory of Prof. H. Huismans (Maree *et al.*, 1998). S. Durbach expressed the VP3 gene in

E.coli. The VP7 gene and a PCR-cDNA hybrid VP3 gene was constructed and expressed by S. Maree.

The PCR-tailored VP7 gene (Maree *et al.*, 1998) was excised from pBR-S7PCR by *Bgl*II digestion and cloned into the dephosphorylated, isocaudameric *Bam*H1 site of the dual baculovirus transfer vector, pFastbac-dual, using standard cloning procedures as described in Materials and Methods in chapter 2. *E.coli* XL1-Blue cells were used in the transformation and propagation of plasmids. Ampicillin and gentamycin resistant transformants were selected. The derived recombinant plasmids, which appeared larger than wild type pFastbac-Dual on a 1% agarose gel, were further characterised by restriction enzyme mapping. The plasmids were digested with *Sac*I to identify VP7 gene inserts and simultaneously digested with *Bam*H1 and *Hind*III to determine the orientation. A representative recombinant, containing the VP7 gene in the correct orientation for transcription of sense-RNA to be directed by the polyhedrin promoter, was selected (pFBd-S7.9).

The full length AHSV-9 PCR-cDNA VP3 hybrid gene (Maree *et al.*, 1998) suitable for cloning in the baculovirus transfer vector, was subsequently excised from the parent vector, pBR-S3Hyb, by *Bgl*II restriction. Following denaturing of the enzyme by heating at 65°C, nucleotides were added to the overhang termini by use of the Klenow DNA polymerase enzyme (Boehringer Mannheim). Typically 2 U of enzyme was incubated for 30 min in a total volume of 20 µl incubation buffer (50 mM Tris-HCL, 10 mM $MgCl_2$, 1 mM dithioerythritol pH 7.5) containing 0.5-1.0 µg digested DNA and 50 µM of each dNTP. The enzyme was denatured by heating at 65 °C for 5 min and removed by Geneclean™ purification of the fragments following electrophoresis. Alternatively the Klenow enzyme was removed by purification through PCR high pure purification kit (Boehringer Mannheim). The VP3 hybrid gene was blunt end ligated into the dephosphorylated *Sma*I site of pFBd-S7.9. Ligation was performed at 22°C overnight as described in section 2.2.8.3 using an insert:vector ratio of higher than 10:1. Transformation was performed using competent *E. coli* XL1-Blue cells according to the $CaCl_2$/heat shock method (section 2.2.4.1). Ampicillin and gentamycin resistant transformants were selected and a clone containing the VP3 hybrid gene under control of the p10 promoter (pFBd-S3.9-S7.9), was selected by restriction enzyme mapping with *Hind*III and/or *Eco*R1. The full-length status and orientation of the two genes in the pFastbac-Dual plasmid were verified by means of PCR, using VP3 and VP7 specific end primers (table 3.1), and automated cycle sequencing (section 4.2.5) with Ppolh and Pp10 specific primers. The PCR protocol followed was denaturation at 94°C for 3 min followed by 30 cycles of 1 min denaturation at 94°C, annealing for 45 sec at 55°C and elongation for 2 min (3 min for VP3 gene) at 72°C, for both amplification of VP3 and VP7 genes.

3.2.2.2. Insertion of AHSV-9 or AHSV-3 VP2 genes with AHSV-9 VP3 into the dual transfer vector

The recombinant pBS plasmids, pBS-AHSV3.2 and pBS-AHSV9.2, containing full length copies of AHSV-3 and AHSV-9 segment 2 genes respectively, cloned *Bam*H1/*Bgl*II in the T7 orientation were provided by Mr. Frank Vreede and Mr. Grant Napier (Department of Genetics, University of Pretoria). Both genes were proven to be full-length. Restriction enzyme mapping of the segment 2 gene of the two serotypes was performed to verify the orientation. The pBS-AHSV9.2 plasmid was digested with *Hind*III, and pBS-AHSV3.2 with *Xba*I, both enzymes cut asymmetrically once in the gene and once in the vector.

The first step in the construction of a dual vector containing both the VP3 and AHSV-9 or 3 VP2 genes was to clone the AHSV VP3 gene into the pFastbac-Dual vector using the cloning strategy as described in the previous section. A representative recombinant, which contained the gene of interest in the correct orientation for transcription of the sense RNA to be directed by the p10 promoter, was selected and designated pFBd-S3.9. Full-length AHSV-9 VP2 was recovered from pBS-AHSV9.2 by a triple digestion with *Sal*I, *Xba*I and *Sca*I in the

same incubation buffer and purified with the Geneclean™ kit. AHSV-3 VP2 (Vreede & Huismans, 1994) was cut out with *Sma*I, *Sal*I and *Sca*I digestions in the recommended salt buffers for the enzymes and gel purified. Plasmid pFBd-S3.9 was linearised by double digestion with *Sal*I and *Xba*I for cloning of AHSV-9 VP2 under control of the polyhedrin promoter. Alternatively, pFBD-S3 was digested with *Xba*I followed by Klenow repair of the sticky ends, chloroform extraction (2.2.5.1) and *Sal*I digestion for cloning of AHSV-3 VP2. The linearised plasmids were ligated to the full-length *Sal*I/*Xba*I restricted AHSV-9 segment 2 or *Sal*I/*Sma*I AHSV-3 segment 2 DNA, respectively. Ligation was performed using rapid DNA ligation kit (Boehringer Mannheim) which utilises T4 DNA ligase (2.2.8.3) together with ligase buffer and 1x DNA dilution buffer.

The ligation mixtures were used to transform *E. coli* DH5α cells, which were made competent by a modification/extension of the $CaCl_2$-based procedure (section 2.2.3.1.) as described by Hanahan *et al.* (1983 & 1991). An overnight culture of DH5α cells were grown in LB medium at 30°C until the OD_{550} reaches 0.4. The cells were collected and dispersed in $^1/_3$ volume CCMB80 transformation buffer (80 mM $CaCl_2$, 20 mM $MnCl_2$, 10 mM $MgCl_2$, 10 mM K.acetate). The cells were pelleted, supernatant decant and resuspended in a 1/12 of original volume CCMB80. After transformation with the ligation mix the culture was grown for 4 h in LB or SOC medium before plating out on LB-agar plates containing amp, tet and gent. Colonies with amp^R and $gent^R$ phenotype were isolated and characterised by restriction analysis. Recombinant plasmids with the correct transcriptional orientation of segment 2 relative to the polyhedrin promoter were selected and designated pFBd-S2.9-S3.9 and pFBD-S2.3-S3.9. The full-length status and orientation of segment 3 and segment 2 genes in the pFastbac-Dual plasmids were verified by means of PCR, using VP3 and VP2 specific end primers (table 3.1.), and automated cycle sequencing with Ppolh and Pp10 specific primers. The PCR protocol followed was 30 cycles of denaturation (96°C for 2 min), primer annealing (50°C for 45 sec) and elongation (29 cycles for 4 min and 1 cycle for 10 min at 72°C).

3.2.2.3. Cloning of AHSV VP5 and VP7 genes into the dual transfer vector

A recombinant pBS plasmid, pBS-AHSV9.6 containing the full length copy of AHSV-9 VP5 gene, cloned in the T7 orientation into the *Bam*H1 site of the vector, was obtained from Mrs. M du Plessis (Department of Microbiology, University of Pretoria) (Du Plessis & Nel, 1997). The AHSV-3 VP5 gene, previously cloned into pBS (pBS-AHSV3.6), was provided by Mr. Frank Vreede. The full-length status of the VP5 genes was verified with *Bam*H1 and *Hind*III or *Bgl*II digestions.

The AHSV-9/-3 VP5 genes was retrieved with *Bam*H1 digestion and purified using the Geneclean™ kit. The purified fragments were then ligated to dephosphorylated *Bam*H1-restricted pFastBAC-Dual, using the rapid DNA ligation kit according to the manufacturers' instructions. DH5α cells, made competent by the $CaCl_2$/$MnCl_2$ based method (3.2.1.2), were transformed and selected for amp and gent resistance. Possible recombinants which appears larger than pFastbac-Dual on a 1% agarose gel were characterised by restriction enzyme mapping with *Bam*H1, *Hind*III and *Bgl*II digestions. Representative recombinants (pFBd-S6.9 and pFBd-S6.3) containing the PCR-tailored serotype 9 and 3 VP5 genes in the correct orientation for transcription of the sense RNA from the polyhedrin promoter was selected.

The PCR-tailored AHSV-9 segment 7 DNA was recovered from pBS-S7 (T3 orientation) with simultaneous digestion with *Sma*I and *Xho*I in the recommended salt buffers and restriction conditions specified by the manufacturer. The plasmids pFBD-S6.9 and pFBd-S6.3 were also double digested with *Sma*I and *Xho*I and the effective digestion of both enzymes analysed by self-ligation of the linearised plasmid and transformation into

competent DH5α cells. The plasmid was only used for ligation if there was a significant reduction in the number of colonies compared to a positive control, where the same amount of *Sma*I cut plasmid was used. The purified *Sma*I/*Xho*I restricted VP7 fragment was ligated into the vector using rapid DNA ligation kit or an alternative protocol, using the condensing reagent PEG 8000 (15% of reaction volume) which suppresses intramolecular ligation and accelerate the rate of ligation of blunt-ended DNA described by Sambrook & Maniatis, 1988.

Transformation was performed using competent *E. coli* SURE cells. The cells were made competent using the TFB/FSB method (Hanahan *et al.*, 1983 & 1991). SURE cells grown at 30°C to mid log-phase were collected and made competent as described in the previous section using the TFB/FSB buffer (100 mM KCl, 42 mM $MnCl_2$, 10 mM $CaCl_2$, 3 mM $CoCl_3$ or $RuCl_2$ and 10 mM K.Acetate) or TSB/TSBG. After 4 h at 27-30°C incubation in LB medium containing tetracyclin, transformants were plated out on LB agar plates containing amp, tet and gent and incubated for at least 36 h at 27-30°C. Plasmids from a number of colonies were isolated, screened with dot blot hybridisation (2.2.5.2) and characterised by restriction analysis. Recombinant plasmids with the correct transcriptional orientation of the VP7 gene relative to the p10 promoter were selected by *Sac*I and *Bam*H1 restriction mapping and designated pFBd-S6.9-S7.9 and pFBd-S6.3-S7.9. The full-length status and orientation of the respective genes in the pFastbac-Dual plasmid were verified by means of PCR, using VP5 and VP7 specific end primers (Table 3.1.), and automated cycle sequencing with polh and p10 specific primers. The PCR protocol followed and automated cycle sequencing is described in sections 3.2.1.1 and 4.2.5, respectively.

Table 3.1. *Primers used for PCR identification of the different AHSV genes used in the construction of dual recombinant baculoviruses.*

Gene Target	End Specific	Oligonucleotide sequence	Denatu-ration	Annea-ling	Elonga-tion
AHSV-3 VP2	5' specific (PP1) 3' specific (PP2)	5'-CAC**AGATCT**GTTTAATTCACCATGGCTTCG-3' 5'-GAG**AGATCT**GTAAGTTGATTCACTTGGAGC-3'	96 °C 2 min	50 °C 45 s	72 °C 4 min
AHSV-9 VP2	5' specific (PP1) 3' specific (PP2)	5'-CAC**AGATCT**GTTTAATTCACCATGGCTTCG-3' 5'-GAG**AGATCT**GTAAGTTGATTCACTTGGAGC-3'	96 °C 2 min	50 °C 45 s	72 °C 4 min
AHSV-9 VP3	5' specific (SI5) 3' specific (SI3)	5'-GG**AGATCT**ATGCAAGGGAATGAAAGAATAC-3' 5'-GG**AGATCT**GGCTGCTAAA**T**CGTTGGTCG-3'	94 °C 1 min	55 °C 45 s	72 °C 3 min
AHSV-9 VP5	5' specific (PP7) 3' specific (PP8)	5'-CCA**GGATCC**GTTTATTTTTCCAGAGACC-3' 5'-CCA**GGATCC**GTATGTGTTTTTCCCCGC-3'	94 °C 1 min	53 °C 45 s	72 °C 2 min
AHSV-9 VP7	5' specific (SP2) 3' specific (SP3)	5'-CAC**AGATCT**TTCGGTTAGGATGGACGCG-3' 5'-CAC**AGATCT**GTAAGTGTATTCGGTATTGAC-3'	94 °C 1 min	55 °C 45 s	72 °C 2 min

* Unique restriction enzyme sites are shown in bold

3.2.3. Generation and selection of recombinant baculoviruses

Since the methods used here to generate dual recombinant baculoviruses differed in some aspects to the methods described in chapter 2 it is explained briefly.

3.2.3.1. Construction of composite bacmid DNA by transposition

Construction of recombinant baculovirus DNA was done by modification of the methods described in section

2.2.12. *E. coli* DH10BAC™ cells, containing the bacmid genome and helper plasmid were grown up in small overnight cultures at 27-30°C and made competent using the PEG/DMSO method (Chung & Miller, 1988). DH10BAC cells were grown to early log phase (OD_{550} = 0.5) in LB-broth supplemented with kanamycin and tetracyclin. Cells were pelleted and resuspended in $^1/_{10}$ volume of ice-cold LB-broth supplemented with 10% (w/v) PEG, 5% (v/v) DMSO, 10 mM $MgCl_2$ and 10 mM $MgSO_4$ (TSB medium). Cells were then kept on ice for 20 min. Aliquots of 200 µl of competent cells were placed in a test tube, approximately 0.5-1.0 µg of the recombinant donor plasmids (pFBd-S3.9-S7.9, pFBd-S2.9-S3.9, pFBd-S2.3-S3.9, pFBd-S6.9-S7.9 and pFBd-S6.3-S7.9) were added and incubated on ice for 30 min. To this was added 800 µl of TSBG medium (TSB-medium to which is added 20 mM glucose) and the mixture was incubated in a shake incubator at 27-30°C for 4 h to allow transposition and expression of plasmid-encoded antibiotic resistance genes to occur. Between 100 and 150 µl of transformed cells were then plated out onto LB-agar plates containing kanamycin, gentamycin, tetracyclin, X-gal and IPTG (section 2.2.12.2.) for selection. Plates were incubated inverted for 36 h to allow for expression of the blue/white phenotypes. If transposition of *Tn7* element into the bacmid occurs the *lacZ* gene is disrupted and recombinant colonies will be white versus non-recombinants, which are blue (2.2.12.2). White colonies were picked and streaked on identical plates to confirm their white phenotype.

3.2.3.2. Isolation and selection of composite bacmid DNA

The isolation of composite bacmid DNA was done following a protocol specifically developed for isolation of large plasmid DNA (> 100 kb) as was adapted for isolation of high molecular weight bacmid DNA (Amemiya *et al.*, 1994). Cell pellets from 1 ml suspension cultures were resuspended in 300 µl solution 1 (2.2.5), followed by the addition of 300 µl solution 2 (0.2 N NaOH, 1% SDS). Each tube was gently inverted and incubated at RT for 5 min. Following this, 300 µl of 3 M K.acetate pH 5.5 was added and the samples cooled on ice for 5-10 min. Each sample was centrifuged at maximum speed for 10 min and 800 µl absolute isopropanol was added to each supernatant. After 20 min at -20°C, DNA was pelleted and washed with 70% ethanol. Pellets were air dried and resuspended in 30 µl sterile ddH_2O and kept at 4°C. The solution was not to be vortexed or subjected to mechanical stress, as this may lead to shearing of the high MW bacmid DNA.

The potential recombinant bacmid DNA were selected further by means of PCR amplification. End specific primers or polh and p10 specific primers in combination with pUC/M13 amplification primers were used to amplify the different AHSV genes under the same conditions as described in section 3.2.2, using 5 µl of each recombinant bacmid DNA. As controls wild type bacmid DNA preparations and the recombinant pBS plasmids containing each gene of interest were also used as templates in separate reactions. In some cases dot blot hybridisation (section 2.2.6) was also used for selection of potential recombinant bacmid DNA. Approximately 200 ng of each potential recombinant bacmid DNA was denatured and dot spotted onto Hybond-N nylon membrane as described in section 2.2.6.2. The DNA was fixed with UV irradiation for 5 min and then hybridised using gene specific probes.

3.2.3.3. Transfection of Sf9 cells with bacmid DNA

Following isolation of the recombinant bacmid DNA, 0.9 x 10^6 cells were seeded in 35 mm six-well tissue culture plates (Nunclon™). Cells were allowed to attach for 1h at 27°C during which time transfection mixtures containing composite bacmid DNA were prepared as follows: 8 µl of recombinant bacmid DNA (1.5-2 µg) was diluted into 100 µl Grace's medium without serum or antibiotics, as this could inhibit uptake of exogenous DNA. A second solution containing 8 µl lipofectin™ or cellfectin™ reagent (Gibco BRL) or DOTAP (Boehringer Mannheim) in 100 µl Grace's medium without serum or antibiotics was also prepared, after which the two solutions were gently mixed and incubated at RT for 45 min. The cells were washed twice with 2 ml Grace's medium without serum or antibiotics. Then 800 µl of medium was added to the tubes, containing the DNA-lipid

complexes and the cells were overlaid with the lipid-DNA complexes. Cells were incubated for 6 h in a 27°C incubator to allow uptake of the recombinant bacmid DNA, after which time the transfection mixtures were removed and 2 ml Grace's medium containing serum and antibiotics was added. Cells were then incubated for a further 96 h, after which the viral supernatant was harvested. Preparation of high titre virus stocks was done as described in section 2.2.11.4 and the viruses designated DBac-S3.9-S7.9, DBac-S2.9-S3.9, DBac-S2.3-S3.9, DBac-S6.9-S7.9 and DBac-S6.3-S7.9.

3.2.3.4. *In vivo* mRNA hybridisation

Transcription of AHSV-9 genes in insect cells was tested using an *in situ* hybridisation method (Paeratakul *et al.*, 1988). Monolayers of Sf9 cells in 24 mm wells (3×10^5 cells/well) were either mock-infected or infected with the selected dual recombinant baculovirus (DBac-S2.9-S3.9, DBac-S2.3-S3.9, DBac-S6.9-S7.9 and DBac-S6.3-S7.9) at a MOI of 10 p.f.u./cell. The infected cells were harvested 48 h p.i., washed and kept in 300 µl PBS at -20°C. Approximately 1×10^5 cells were spotted onto Hybond C-extra nitrocellulose membranes (Amersham), prewetted in PBS, using a dot-blot microfiltration apparatus. Equal volumes of each sample were blotted in duplicate for detection of either the AHSV-9 VP3 or VP2 mRNA (infection with DBac-S2.9-S3.9) or the AHSV-9 VP7 or VP5 mRNA (infection with DBac-S6.9-S7.9). Cells were fixed onto the membranes at 4°C for 1 h in 1% gluteraldehyde, 3% NaCl, 10 mM NaH_2PO_4, 40 mM Na_2HPO_4 (pH 7.4) and rinsed three times with proteolitic buffer (50 mM EDTA, 0.1 M Tris-HCL, pH 8.0). Cells were digested in proteolitic buffer containing proteinase K (20 µg/ml) at 37°C for 30 min. Memebranes were air dried and immersed in prehybridisation buffer (50% formamide, 5 x SSPE, 0.1% milk powder) for 1 h followed by hybridisation with the AHSV-9 or -3 gene-specific radiolabelled probe. Radiolabelled probes were prepared as described in section 2.2.6.1. The probes were prepared from pBS-AHSV9.2, pBS-S3Hyb, pBS-AHSV9.6 and pBS-S7PCR recombinant plasmids.

3.2.4. Co-expression of AHSV capsid proteins in insect cells and purification of multimeric particles comprising different combinations of AHSV proteins

3.2.4.1. Analysis of polypeptides synthesised in infected insect cells

Monolayers of Sf9 cells were infected with the VP3/VP7, VP2/VP3 or VP5/VP7 dual recombinant baculoviruses at a MOI of 5 to 10 pfu/cell of each virus, as described in section 2.2.12. Sf9 cells were also mock infected or infected with the parent virus. Infected cells were harvested at 48 or 72 h p.i., pelleted, washed and resuspended in 1x PBS. Prior to electrophoretic analysis, protein samples were mixed with an equal volume 2x PSB (2.2.12). Proteins were resolved by 12% or 10% SDS-PAGE analysis (2.2.10.3). The time course for maximal protein expression was determined by repeating the infection and radiolabelling of the infected cells at time intervals 36 h, 42 h, 48 h and 54 h p.i., described in section 2.2.12.

3.2.4.2. Co-expression of different combinations of AHSV capsid proteins in insect cells and purification of expressed multimeric particles

S. frugiperda cells were infected at a multiplicity of 10-15 pfu with either the dual recombinant baculovirus or wild type virus or mock infected. Cells were harvested at 48-72 h post-infection, washed with 1 x PBS and lysed at 4°C in 50 mM Tris-HCL (pH 8.0), 150 mM NaCl, 0.5% Nonidet P-40 (TNN buffer) at a concentration of 2×10^7 cells/ml followed by mechanical shearing through a dounce apparatus. Nuclei were removed by low speed centrifugation at 1000 rpm for 5 min and washed twice in small volumes of TNN buffer. The cytoplasmic

fractions were pooled and subjected to differential centrifugation for 30 min at 5000 rpm in a J-21 Beckman centrifuge. The expressed particles were purified from the supernatant either by banding on a discontinuous sucrose gradient (40% and 68% (w/v) in 150 mM NaCl, 0.2 M Tris-HCl pH 8.0) after centrifugation at 35 000 rpm in a SW50.1 Beckman rotor (85 000 x g) for 3 h or on a self forming CsCl (35%) density gradients after centrifugation at 140 000 g for 18 h. Fractions forming at the 40% to 68% interface were collected (0.7-1.0 ml volume), diluted to 5 ml volume in 150 mM NaCl, 0.2 M Tris-HCl (pH 8.0) and pelleted at 85 000 g for 30 min. The particles were analysed by SDS-PAGE and examined by electron microscopy.

Sf9 cells were also co-infected with the AHSV-9 VP3/VP7 dual recombinant baculovirus and an AHSV-9 VP5 or VP2 single gene recombinant baculovirus at multiplicities of 5 pfu/cell. Similar co-infections were performed with the VP3/VP2 dual and VP7 single recombinant baculoviruses and VP5/VP7 dual and VP3 single recombinant baculoviruses. For the production of VLPs the co-infection were repeated using VP2.3/VP3 or VP2.9/VP3 in combination with VP5.9/VP7 dual gene recombinant baculoviruses or VP2.3/VP5.3 and VP3/VP7 recombinant baculoviruses at a MOI of not more than 10^5 pfu/cell. The assembled particles were recovered and purified through a 40 to 68% discontinuous sucrose gradients, centrifuging for 2 h at 4°C and 85 000 g or alternatively on an 10-40% (w/v) continuous sucrose gradient. The protein components of the fractions forming the 40% to 68% interface were collected, analysed by SDS-PAGE and examined by electron microscopy.

3.2.4.3. Stoichiometry of VP3 to VP7

Monolayers of Sf9 cells were infected with the dual-recombinant baculovirus at a multiplicity of 10 pfu per cell and incubated at 28°C for 2 h after which the inoculum was replaced with fresh Grace's medium to synchronise the infection. The infected cells were incubated for a further 24 to 36 h. Radiolabelling of the viral proteins was achieved as described in section 2.2.12. The cells were then harvested and washed in 1 x PBS and the expressed particles were purified on discontinuous sucrose gradients as already described. The particles were pelleted and mixed with protein dissociation buffer and the samples of various amounts were subjected to SDS-PAGE. After electrophoresis the gel was stained with Coomassie Blue, destained in 5% acetic acid and 5% methanol, dried and autoradiographed. The bands of VP3 and VP7 were excised from the dried gel and their activities (counts per minute) were determined after incubation in a liquid scintillation cocktail. The experiment was performed twice, and the results were pooled.

3.2.5. Electron microscopy of purified particles

Purified synthetic AHSV particles were adsorbed onto copper 400-mesh Formvar carbon-coated 400-mesh grids by floating the grids on droplets of the material for 2 min. After being washed twice with 150 mM NaCl, 0.2 M Tris-HCl (pH 8.0), the particles were negatively stained for 30 s on droplets of 2% (w/v) uranyl acetate. For immunodecorating studies, particles obtained from simultaneous expression of dual recombinant virus expressing CLPs and single recombinant virus expressing VP2 or VP5 were adsorbed to carbon-filmed grids and incubated in a 1:100 dilution of AHSV-3 VP5 or AHSV-9 VP2 monospecific antibodies for 30 min. The unbound antibody was washed briefly at the end of the interaction and the grid was then negatively stained as described. All grids were examined in a JEOL electron microscope at room temperature at 60 kV. Low dose micrographs were recorded at a 60 000x magnification. Controls included omission of the primary antibody as well as the dual virus alone.

3.3. RESULTS

3.3.1. Expression of the genes encoding the four major structural proteins of AHSV-9 in insect cells using dual recombinant baculovirus vectors

In order to produce CLPs, partial VLPs and VLPs, the different AHSV structural genes were cloned in different combination into the dual baculovirus donor vector (pFastbac-Dual). The dual constructs used to produce recombinant baculoviruses, that express the AHSV structural proteins, are summarised in table 3.2. The interaction of the structural proteins was investigated by means of co-infection experiments. The construction of the different dual vectors is described in this section.

Table 3.2: *Summary of the plasmid DNA constructs made for usage in the expression of the four major structural proteins of AHSV.*

pFastbac-dual construct	**Foreign genes and AHSV serotypes**	**Promoter**	Constructed by
pFBdS3.9-S7.9	AHSV-9 VP3 and AHSV-9 VP7	p10 polyhedrin	Francois Maree
pFBdS2.9-S3.9	AHSV-9 VP2 and AHSV-9 VP3	polyhedrin p10	Francois Maree
pFBdS2.3-S3.9	AHSV-3 VP2 and AHSV-3 VP3	polyhedrin p10	Francois Maree
pFBdS6.9-S7.9	AHSV-9 VP5 and AHSV-9 VP7	polyhedrin p10	Francois Maree
pFBdS6.3-S7.9	AHSV-3 VP5 and AHSV-9 VP7	p10 polyhedrin	Francois Maree
pFBdS2.3-S6.3	AHSV-3 VP2 and AHSV-3 VP5	polyhedrin p10	Renate Filter
pFBd-S6.9	AHSV-9 VP5	polyhedrin	Francois Maree
pFB-S2.9	AHSV-9 VP2	polyhedrin	Grant Napier

3.3.1.1. Construction of an AHSV-9 VP3 and VP7 dual-recombinant baculovirus transfer vector

The dual expression transfer vector, pFastbac-Dual, facilitates the introduction of two heterologous foreign genes, under control of the very late polyhedrin and p10 promoters, into a single recombinant virus. The strategy employed (*Figure 3.1A*) for the cloning of the full-length AHSV-9 VP3 and VP7 genes into pFastbac-Dual, was as follows. PCR tailored copies representing the complete coding sequences of the AHSV-9 segment 3 and segment 7 genes were used for co-expression in the BAC-TO-BAC baculovirus system. Both the VP3 and VP7 genes contain internal *Bam*H1 sites and the vector-specific *Bam*H1 site downstream of the polyhedrin promoter was therefore utilised in the first cloning step. A PCR-tailored copy of the VP7 gene was previously cloned by dG/dC-tailing into pBR322 by S. Maree and the recombinant plasmid pBR-S7PCR was utilised to obtain the full length VP7 gene of AHSV-9. The PCR-tailored VP7 gene was excised from pBRS7PCR by *Bgl*II digestion and cloned into the dephosphorylated *Bam*H1 site of the pFastbac-Dual vector under control of the polyhedrin promoter. The derived recombinant plasmids were characterised by restriction enzyme mapping with *Sac*I, which cleaves twice in the VP7 gene at position 250 and 1045, and simultaneous digestions *with Bam*H1 and *Hind*III, which respectively cleaves the DNA ca. 100 bp from the 5' end of the gene and in the multiple cloning site downstream of the polyhedrin promoter. A representative recombinant, yielding three fragments of 5.5 kb, 850 bp and 100 bp in the first digestion and two fragments of 5.3 kb and 1000 bp in the second digestion was selected. This clone contained the VP7 gene in the correct orientation for transcription of the sense-RNA to be directed by the polyhedrin promoter. The recombinant was designated pFBd-S7.9 and was used to insert the AHSV-9 VP3 gene.

A PCR tailored copy of the VP3 gene of AHSV-9, containing *Bgl*II restriction sites at the 5' and 3' termini, was cloned by homopolymer dG/dC tailing in pBR322 by Steven Durbach. A VP3 chimeric gene (pBR-S3Hyb) was constructed by Sonja Maree, in which the central 2.0 kb part of the PCR copy was replaced by the corresponding cDNA region. The VP3 chimeric gene was subsequently recovered from pBR-S3Hyb by *Bgl*II restriction and the ends filled up with Klenow. The VP3 chimeric gene was blunt end cloned into the dephosphorylated *Sma*I site of pFBd-S7.9 plasmid. Many of the derived plasmids were the same size, while some were smaller than pFBd-S7.9 when the ccc forms were compared, which implied that deletions had occurred. Many of the deletions involved the gent^R gene, which made the future selection on gentamycin essential. Plasmids which appeared larger than pFBd-S7.9 were further characterised by asymmetrical restriction with *Bam*H1, *Hind*III and/or *Eco*R1 in order to identify the full length VP3 and VP7 specific inserts as well as the correct transcriptional orientation of the VP3 hybrid gene. The VP3 gene specific *Hind*III site is located at ca. 2.3 kb and the *Eco*R1 site at ca. 300 bp from the 5' end and at vector-specific sites, downstream of the polyhedrin promoter (MCS). Plasmids yielding two fragments of ca. 4 kb and 5.1 kb with *Hind*III digestion and

two fragments of ca. 2 kb and 7.1 kb with *Eco*R1 digestion and three fragments of ca. 1.9 kb, 2.1 kb and 5.1 kb with simultaneous digestion with both enzymes were regarded as recombinant (*Figure 3.1B, C*). A representative clone containing the VP3 hybrid gene under control of the p10 promoter, was selected and designated pFBd-S3.9-S7.9. The yield of recombinants with VP3 in the correct transcriptional orientation was about 1-2% of all colonies screened, using the described strategy.

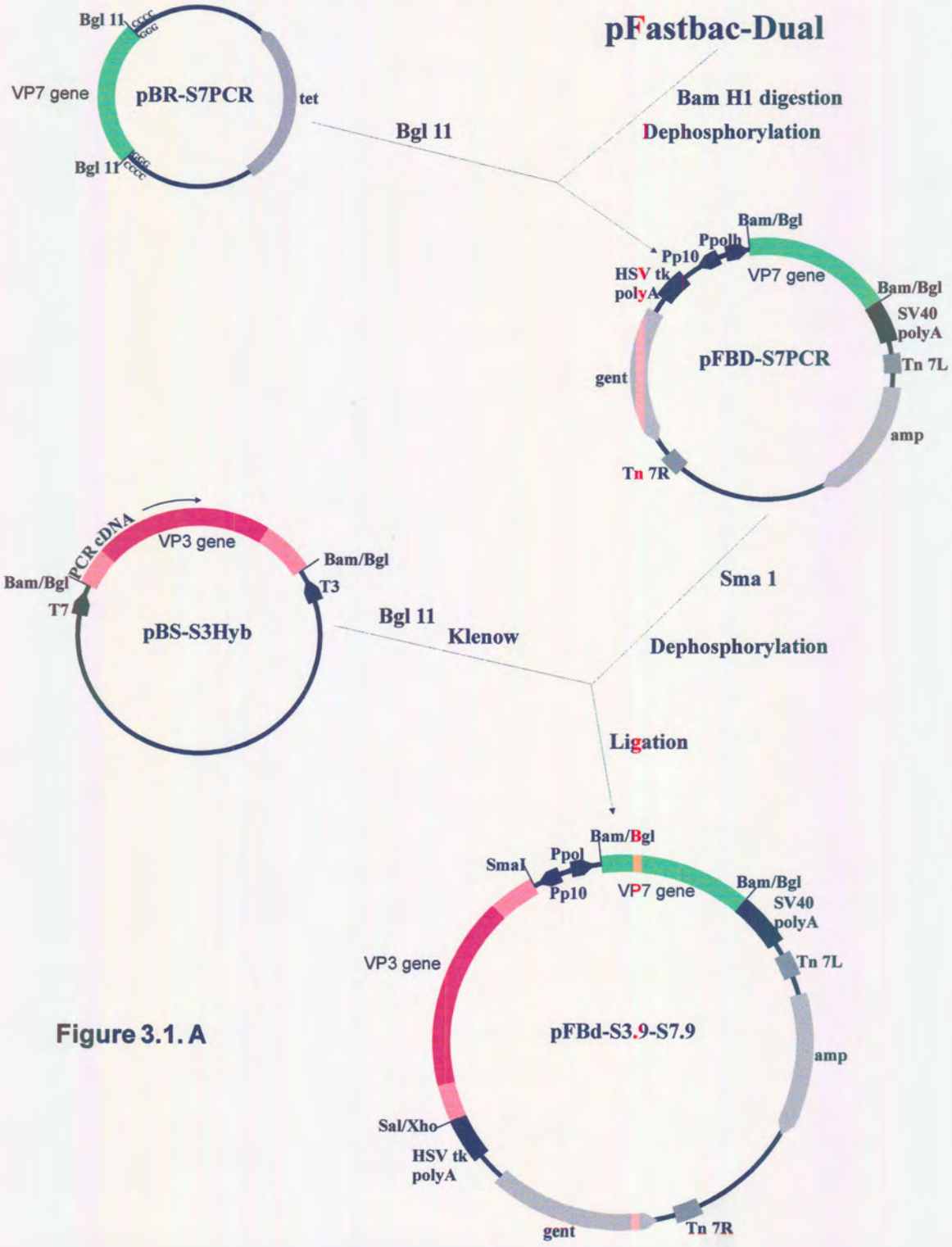

Figure 3.1. A

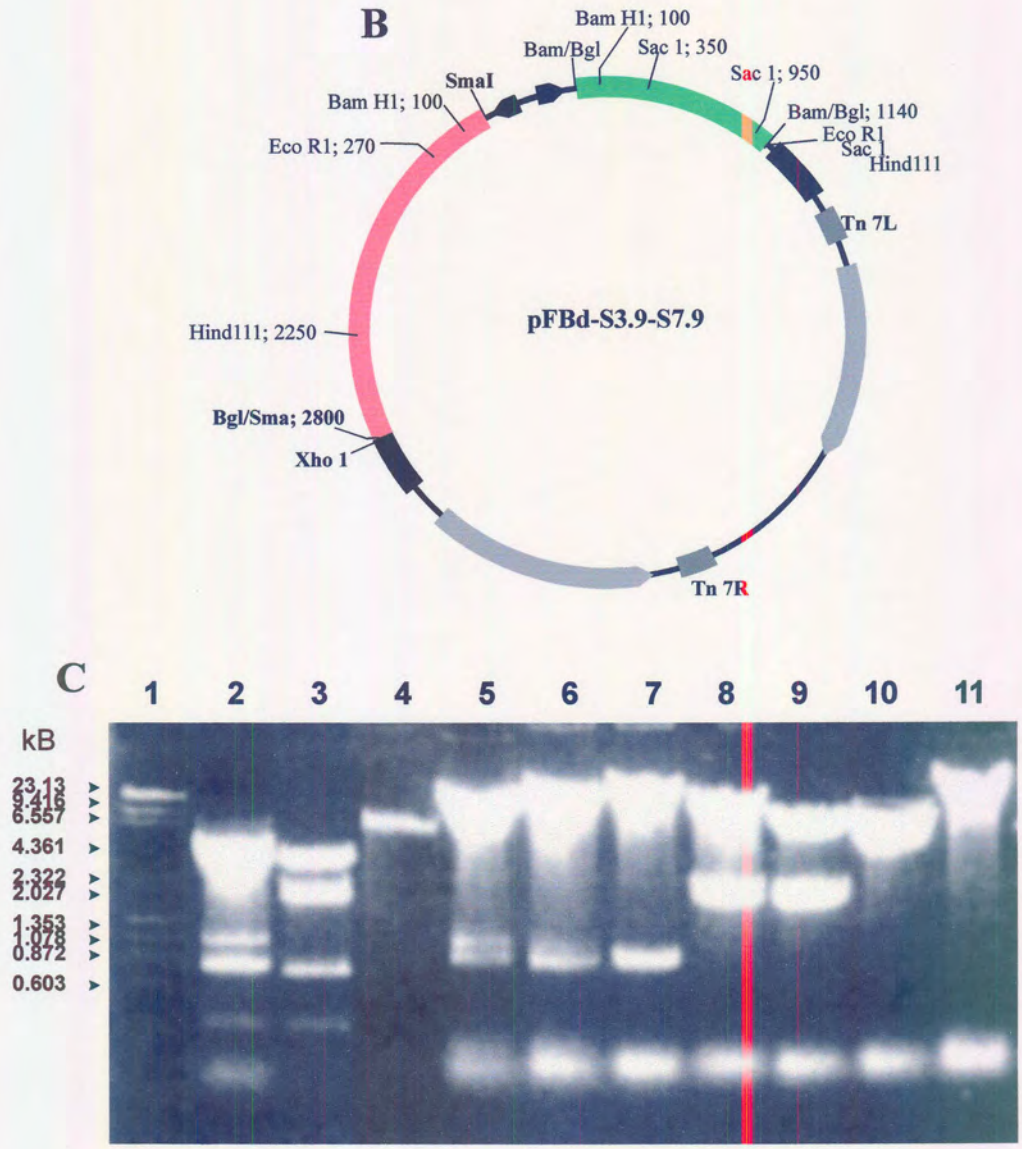

Figure 3.1: (A) A schematic diagram showing the strategy for cloning both AHSV-9 VP3 and VP7 genes into the dual expression transfer vector, pFastbac-Dual. The AHSV-9 VP3 and VP7 genes is shown in red and green, respectively. (B) A schematic representation of a partial restriction map of the dual recombinant plasmid, pFBd-S3.9-S7.9. (C) Agarose gel electrophoretic analysis of pFBd-S3.9-S7.9. The plasmids pBS-S7PCR (lane 2) and pBS-S3Hyb (lane 3) were digested with *Sac*I and *Hind*III/*Eco*R1, respectively. This, together with molecular weight markers MW11 and ϕx174 (lane 1) and linearised pFBd (lane 4), function as controls. Lane 5 represents pFBd-S7 digested with *Sac*I. Lanes 6-11 represent pFBd-S3.9-S7.9 digested with *Sac*I, *Bam*H1, *Eco*R1, *Hind*III/*Eco*R1, *Hind*III and *Sal*I, respectively. The sizes of the molecular weight markers are indicated to the left of the figure.

3.3.1.2. Construction of a dual-recombinant baculovirus transfer vector containing either AHSV-3 or AHSV-9 VP2 and AHSV-9 VP3 genes

The strategy employed for the cloning of both the full length VP2 gene of two AHSV serotypes and the VP3 gene into the dual transfer vector was as follows (*Figure 3.2*): In the first step the VP3 gene was cloned into the *Sma*I site of the pFBdual vector under control of the p10 promoter, essentially as described above. A representative recombinant, which contain the VP3 chimeric gene in the correct orientation for transcription of the sense RNA to be directed by the p10 promoter, was selected and designated pFBd-S3.9.

Secondly, the VP2 gene of both AHSV-3 and AHSV-9 were respectively cloned under control of the polyhedrin promoter, using two somewhat different strategies for each VP2 gene. Briefly, full length AHSV-9 segment 2 was recovered from pBS-AHSV9.2 (a PCR-cDNA chimeric copy of the AHSV-9 VP2 gene; cloned and constructed by Grant Napier) by triple digestion with *Sal*I, *Xba*I and *Sca*I. The strategy was aimed at separating the 3.2 kb VP2 gene from the pBS vector. *Sca*I cuts in the amp^R gene of pBS and digest the 3.2 kb vector into two shorter fragments of ca. 1.2 kb and 2.0 kb, which could be separated from the VP2 gene in a triple digestion. AHSV-9 VP2 was directionally cloned into the *Sal*I/*Xba*I sites of pFBd-S3.9. The identity and orientation of the AHSV-9 VP2 gene, with respect to the polyhedrin promoter, of recombinants was verified by restriction analysis with *Eco*R1 and/or *Hind*III (*Figure 3.3 A, B*). A plasmid yielding 750 bp, 2x 1.2 kb and 7.1 kb fragments with *Eco*R1 digestion and 2.4 kb, 3.7 kb and 5.1 kb fragments with *Hind*III digestions was selected and called pFBd-S2.9-S3.9.

The strategy for the cloning of AHSV-3 VP2 into pFBd-S3.9 differed as follows. A 3.2 kb fragment, representing the full length AHSV-3 VP2 gene was obtained by triple digestion of pBS-AHSV3.2 with *Sal*I, *Sma*I and *Sca*I. The VP2 gene was directionally cloned into pFBd-S3.9 and the correct orientation determined by restriction analysis with *Hind*III, *Eco*R1, *Xba*I and *Bam*H1. This was achieved on the basis of a AHSV-3 segment 2-specific *Xba*I site and *Bam*H1 site which cuts asymmetrically in the gene 2700 bp and 30 bp from the 5' terminus respectively and a vector-specific *Xba*I site downstream from the polyhedrin promoter or *Bam*H1 site 150 bp from the 5' terminus of the VP3 gene. Thus a plasmid yielding two XbaI fragments of approximately 9.8 kb and 500 bp and two *Bam*H1 fragments of 800 bp and 9.4 kb was selected and designated pFBd-S2.3-S3.9 (*Figure 3.4 A, B*).

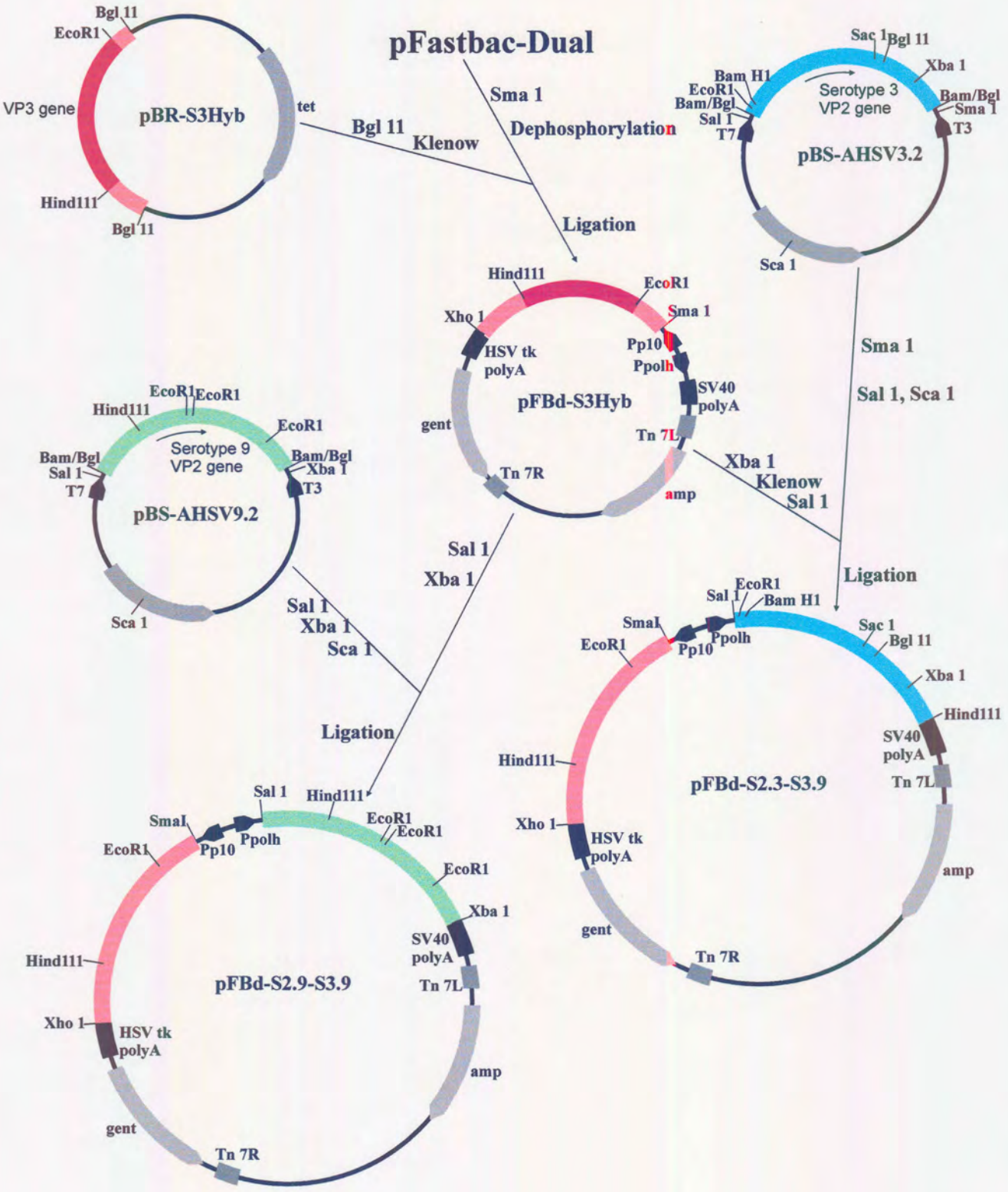

Figure 3.2: A schematic diagram of the strategy employed for the respective cloning of AHSV-3 and AHSV-9 VP2 genes in combination with AHSV-9 VP3 into the transfer vector pFastbac-Dual.

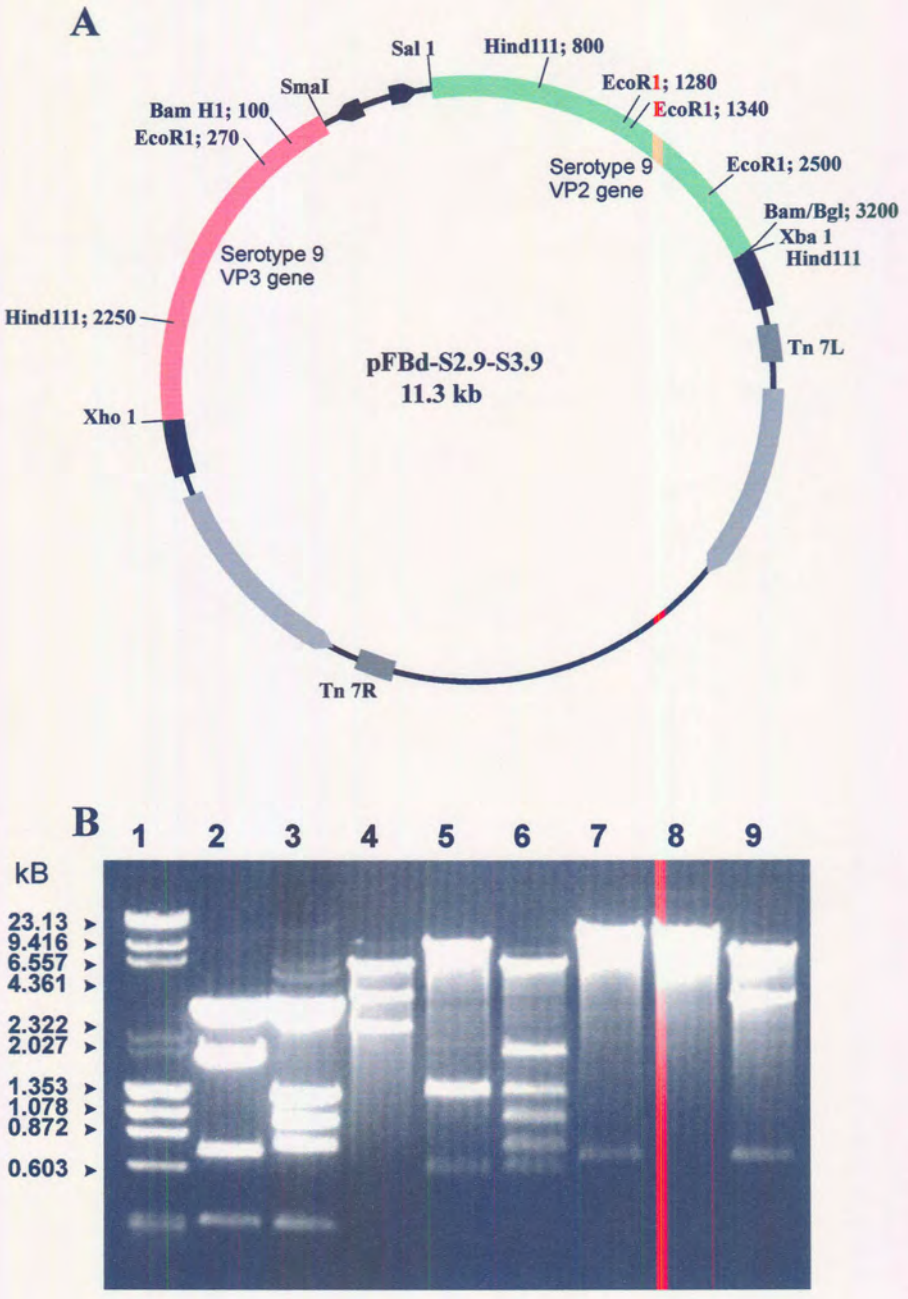

Figure 3.3: (A) A schematic representation of a partial restriction map of the plasmid pFBd-S2.9-S3.9, containing AHSV-9 VP2 and VP3 genes in the correct transcriptional orientation for expression by the polyhedrin and p10 promoters, respectively. The distance from the 5'end of the gene is indicated in bp next to each restriction enzyme site. (B) A restriction analysis of pFBd-S2.9-S3.9. The plasmids pBS-S3Hyb (lane 2) and pBS-AHSV9.2 (lane 3) digested with *Hind*III/*Eco*R1 were included as controls. Lanes 4-9 shows the fragments obtained after restriction with *Hind*III (4), *Eco*R1 (5), *Hind*III/*Eco*R1 (6), *Bam*H1 (7), *Xba*I (8) and *Bam*H1/*Xba*I (9), respectively. Lane 1 shows molecular weight markers with the sizes in kb indicated to the left of the figure.

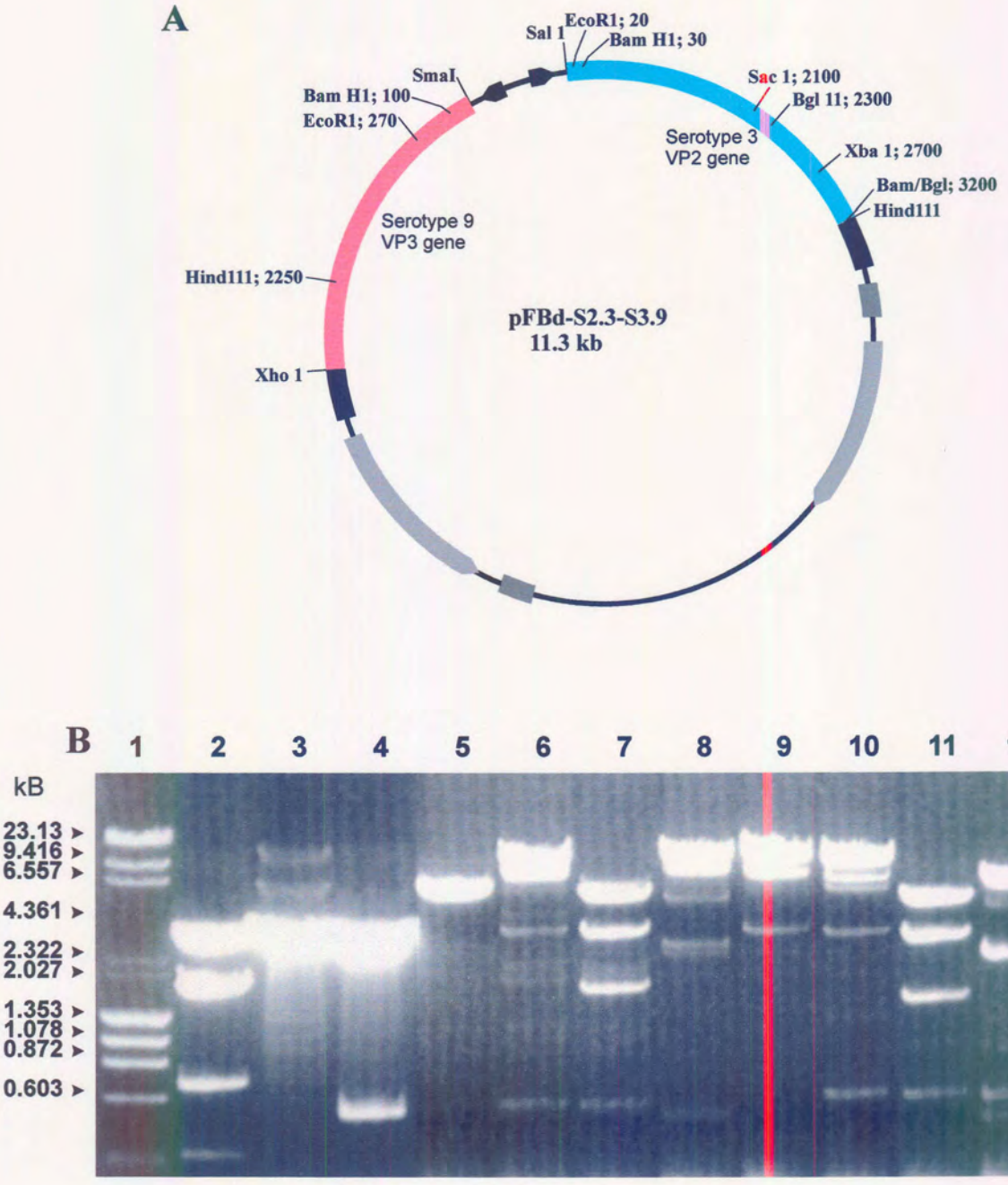

Figure 3.4: (A) A schematic representation of a partial restriction map of the plasmid pFBd-S2.3-S3.9, containing AHSV-3 VP2 and AHSV-9 VP3 genes in the correct transcriptional orientation for expression by the polyhedrin and p10 promoters, respectively. (B) A restriction analysis of pFBd-S2.3-S3.9. The plasmids pBS-S3Hyb (lane 2) digested with *Hind*III/*Eco*R1 and pBS-AHSV3.2 (lanes 3 and 4) digested with *Hind*III/*Eco*R1 and *Bam*H1/*Xba*I were included as controls. Lanes 5-12 shows the fragments obtained after restriction with *Hind*III (5), *Eco*R1 (6), *Hind*III/*Eco*R1 (7), *Xba*I (8), *Sal*I (9), *Bam*H1 (10), *Hind*III/*Bam*H1 (11) and *Bam*H1/*Xba*I (12), respectively. Lane 1 contains molecular weight markers and the sizes are indicated to the left of the figure.

3.3.1.3. Construction of recombinant baculovirus transfer plasmids containing both AHSV VP5 and VP7 genes

Different strategies were used for the construction of a dual transfer vector containing both the VP5 and VP7 genes of AHSV. Cloning of these two genes together in pFastbac-Dual was extremely inefficient and clones were exceptionally unstable. The only successful cloning strategy (*Figure 3.5 A*) that resulted in a recombinant, containing both AHSV-9 VP5 and VP7 genes, is described with specific reference to procedures that were found to be essential for the success of the cloning procedure.

In the first step AHSV-9 or AHSV-3 VP5 gene was cloned into pFastbac-Dual transfer vector. The VP7 gene contains an internal *Bam*H1 site and the vector-specific *Bam*H1 site, downstream of the polyhedrin promoter was therefore utilised in the first cloning step. The PCR-tailored DNA copies of AHSV-9 or -3 VP5 genes were recovered from pBS-AHSV9.6 and pBS-AHSV3.6 respectively and recloned into the dephosphorylated *Bam*H1 site of pFastbac-Dual. Recombinant plasmids, identified by *Bam*H1 digestion and yielded 1.5 kb fragments, were subjected to *Hind*III or *Bgl*II digestion in order to determine the orientation of the VP5 gene in pFastbac-Dual relative to the polyhedrin promoter. Restriction with *Hind*III cleaves the gene ca. 1000 bp from the 5' terminus and the plasmid within the multiple cloning site downstream of the polyhedrin promoter. *Bgl*II cuts in the gene, approximately 300 bp from the 5' end and twice in the vector at positions 2646 and 3116. A plasmid yielding two *Hind*III fragments of ca. 1000 bp and 5.7 kb and three *Bgl*II fragments of 2.4 kb, 2.7 kb and 470 bp was selected, pFBd-S6.9 (*Figure 3.5 C*). This cloning resulted in more than 55% recombinants of which approximately $^1/_3$ were in the desired orientation.

The PCR-tailored VP7 gene cloned in the T7 orientation of pBS (S. Maree) was excised from pBS-S7PCR by restriction with *Sma*I and *Sal*I, purified and cloned into the *Sma*I/*Xho*I site downstream of the p10 promoter of pFBd-S6.9 and pFBd-S6.3. (*Figure 3.5 B, C*). Dual recombinants were selected with *Sac*I, *Bam*H1, *Hind*III and *Eco*R1/*Xho*I digestions. Plasmids that yielded fragments of 850 bp and 7.0 kb (*Sac*I), 550 bp, 1.5 kb and 5.0 kb (*Bam*H1), 500 bp and 7.3 kb (*Hind*III) and 300 bp, 850 bp and 1.7 kb (*Eco*R1/*Xho*I) in the respective digestions were selected (pFBd-S6.9-S7.9 and pFBd-S6.3-S7.9). More than 50% of the derived plasmids were smaller than pFBd-S6.9 when ccc forms were compared, which implies that major deletions occurred. The emergence of this rearrangement or homologous recombination events could be reduced, using *E. coli* SURE cells with recombination deficient (*uvrC*$^-$, *umuC*$^-$ and *recB* and *recJ* mutations) and restriction negative (*mcrA*$^-$, *mcrCB*$^-$) phenotypes. The preparation of competent cells and transformation at < 30°C and selection of transformants on both ampicillin and gentamycin also played a role in reducing the number of deletions, since a great number of the recombinational events involved the gentamycin gene as

analysed by restriction enzyme mapping (results not shown). The presence of both AHSV-9 VP5 and VP7 genes were incompatible or homologous with sequences in the plasmid which cause the dual recombinant plasmid to be extremely unstable and deletions were detected with each generation of bacterial growth.

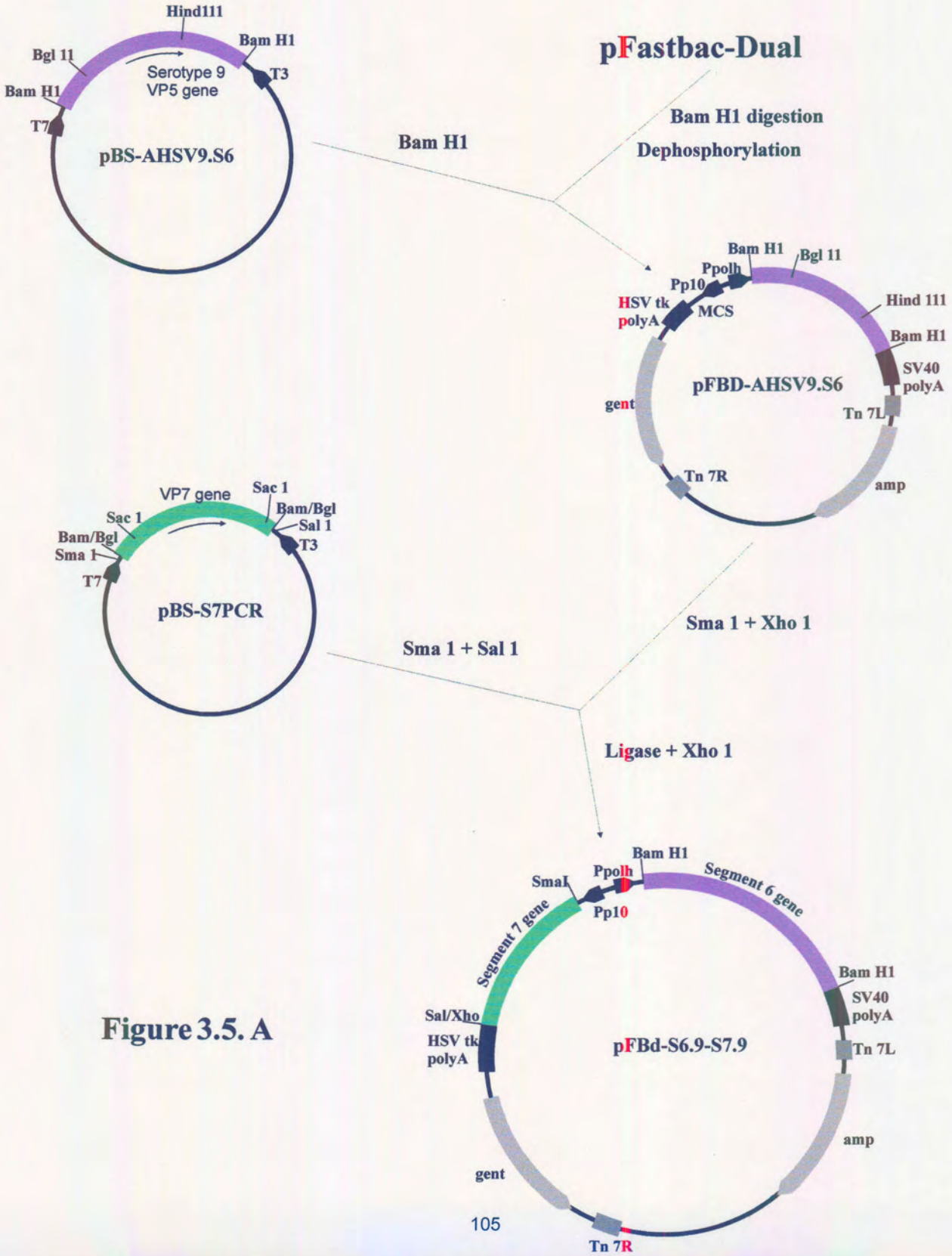

Figure 3.5. A

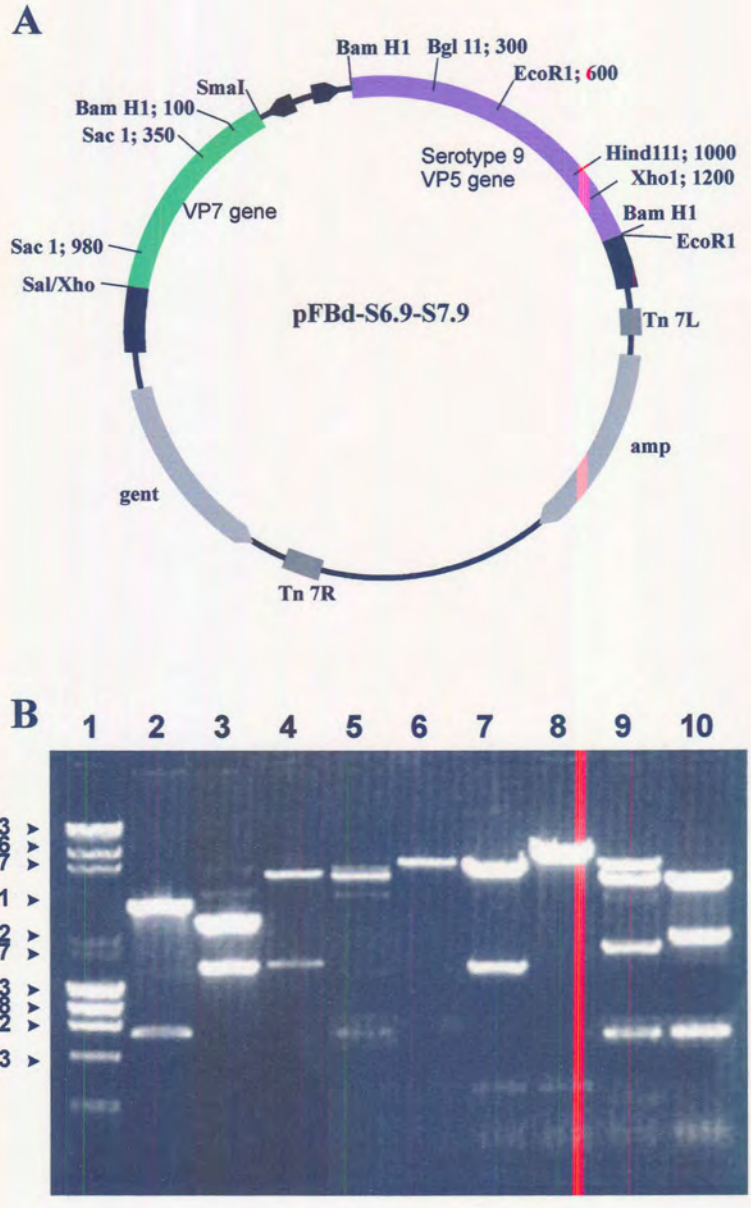

Figure 3.5: (A) A schematic diagram showing the cloning strategy for inserting both AHSV-9 VP5 and VP7 into the dual expression transfer vector, pFastbac-Dual. (B) A schematic representation of a partial restriction map of the recombinant dual transfer vector, pFBd-S6.9-S7.9, containing both genes in the correct transcriptional orientation for expression as non-fused proteins by the polyhedrin and p10 promoters, respectively. The distance in bp from the 5' end of each gene is shown next to the R.E site. (C) An agarose gel electrophoretic analysis of the dual recombinant plasmid, pFBd-S6.9-S7.9. The plasmid was restricted with *Bam*H1 (lane 7), *Hind*III (lane 8), *Eco*R1/*Xho*I (lane 9) and *Sac*I (lane 10) for identification and determining of orientation of the two genes. The pBS-S7PCR (lane 2) and pBS-AHSV9.6 (lane 3) plasmids, digested with *Sac*I and *Bam*H1, respectively, were included as controls together with the molecular weight markers MW11 and ϕx174 (lane 1). Lanes 5-6 represent pFBd-S6.9 digested with *Bam*H1, *Eco*R1/*Xho*I and *Hind*III.

3.3.1.4. Production of dual recombinant shuttle vectors (bacmids)

The next step in constructing dual recombinant baculoviruses expressing different combinations of the major structural proteins of AHSV-9 and AHSV-3 involves producing recombinant bacmids in *E. coli*. Plasmids pFBd-S3.9-S7.9, pFBd-S2.9-S3.9, pFBd-S2.3-S3.9, pFBd-S6.9-S7.9, pFBd-S6.3-S7.9 and pFBd-S6.9 (table 3.2) were transformed into competent *E.coli* DH10Bac cells containing the tetracyclin resistant helper plasmid, which supplies the Tn7 transposase functions and the bacmid DNA (kanamycin resistant). Putative infectious recombinant baculoviral DNA or composite bacmid DNA, containing two heterologous genes under control of the polyhedrin and p10 promoters respectively, was isolated. To confirm that each of the bacmids constructed, contained the respective genes of interest, selected regions of the bacmid DNA were amplified, using the AHSV gene specific primers (summarised in table 3.2) and the polyhedrin and p10 specific primers in combination with pUC/M13 amplification primers. The pUC/M13 primers are directed at sequences on either side of the mini-*att*Tn7 site, within the *lacZ*α-complementation region of the bacmid. The presence of amplified products of the correct size was determined by agarose gel electrophoresis (results not shown). PCR amplification of the respective composite bacmids containing the AHSV structural genes, produced PCR fragments, which corresponded to the VP2, VP3, VP5 and VP7 amplified gene products in the positive controls. These amplified products confirm that the bacmid DNA contained the complete genes of interest.

3.3.1.5. Construction of dual-recombinant baculoviruses

The final step to generate recombinant baculoviruses capable of replicating in insect cells and expressing the heterologous AHSV genes requires the composite bacmid DNA of the four different dual bacmids to be transfected into Sf9 insect cells using a cationic lipid reagent. Three different lipofection reagents were compared for their efficiency of transfection during the course of this investigation. Cellfectin was found to yield the best results (results not shown). Cells were harvested four days post-infection with transfection supernatants, and the proteins analysed by SDS-PAGE.

The transfected cell supernatants were subjected to plaque purification prior to the preparation of high tittered recombinant viral stocks. The viral stocks were titrated and used to re-infect cells at a known MOI of between 5-20 pfu/cell, as described in the following sections. Although it is not strictly necessary to include a plaque purification step, it was found that one round of plaque purification significantly enhanced the stability of protein expression. Viruses from different plaques had different levels of protein expression, varying from no expression to relative high levels of expression. This indicates that the transfection supernatant consist of a heterogeneous population of viruses, each showing different levels of expression. Plaque purification also decreased the amount of defective particles that compete with the complete virion for the cellular machinery and resulted in decreased protein expression from the recombinant viruses.

3.3.1.6. Detection of heterologous RNA synthesised in recombinant baculovirus-infected cells

To established whether active transcription of the foreign genes takes place, dual recombinant baculovirus infected cells were assayed for VP3 and VP2 or VP5 and VP7 mRNA production using an established *in situ* hybridisation procedure. Sf9 cells infected with DBac-S2.9-S3.9 and DBac-S6.9-S7.9 were harvested at 44 h p.i., the optimum time for high level synthesis of mRNA from the very late baculoviral promotors. Cells infected with the VP2/VP3 dual viruses were hybridised to the VP3.9- or VP2.9-specific radiolabelled probes, while those infected with the VP5/VP7 dual recombinants were hybridised to the VP7.9- or VP5.9-specific probes (*Figure 3.6*). Hybridisation of all the VP2/VP3 recombinant infected cell lysates with the VP3-specific probe yielded positive signals. VP2.9-specific probe only detected RNA from cells infected with AHSV-9 VP2/VP3 dual (DBac-S2.9-S3.9). RNA from insect cells infected with DBac-S6.9-S7.9 hybridised to both the VP7.9- and VP5.9-specific probes. These results indicated that active transcription of all the genes under control of either the p10 or polh promotors takes place.

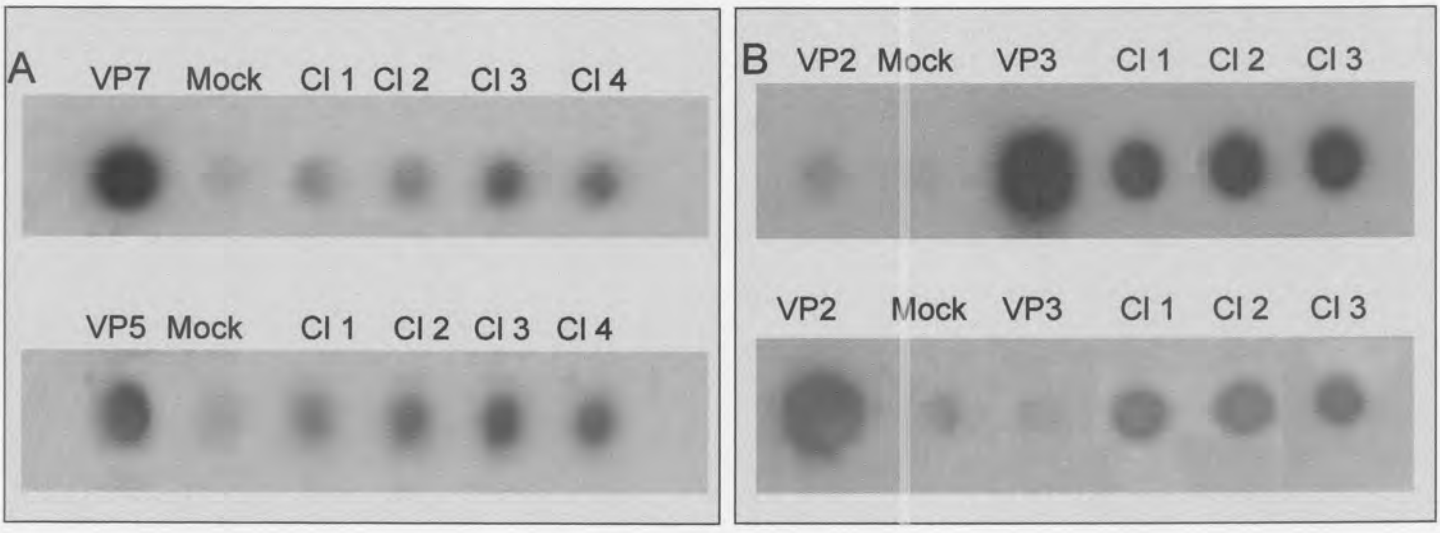

Figure 3.6: In situ Northern blot analysis of Sf 9 cells infected with dual recombinant baculoviruses. Infected cells were harvested 44 h p.i. (A) RNA from DBac-S5.9-S7.9 infected cells were hybridised to VP5(9) and VP7(9)-specific radiolabelled probes (synthesised from pBS-S7PCR and pBS-AHSV9.6 plasmids) and (B) DBac-S2.9-S3.9 infected cells were hybridised to VP2(9) and VP3(9) probes (derived from pBS-AHSV9.2 and pBS-S3Hyb plasmids). For comparison mock-infected cells (negative control) were included in the assay. Plasmid DNA containing the genes of interest served as positive controls.

3.3.2. Investigation of heterologous gene expression in Sf9 cells

In order to determine whether AHSV-9 VP3 and VP7 proteins were expressed from the dual baculovirus recombinant, *S. frugiperda* cells were infected with the VP3 and VP7 dual recombinant baculovirus (DBac-S3.9-S7.9). SDS-PAGE analysis of the infected cell polypeptides revealed that two unique protein bands which co-migrated with AHSV-9 VP3 (90 kDa) and VP7 (38 kDa) derived from recombinant baculoviruses which express VP3 or VP7 individually, were synthesised (*Figure 3.7 A*). No similar bands were observed in the wild-type or mock-infected Sf9 cells. The sizes of the expressed proteins agreed with those expected for VP3 and VP7 on basis of their amino acid compositions (i.e., 103 269 and 38 464 Dalton), respectively. Radioactive labelling of the infected cell polypeptides and comparison with authentic AHSV-infected polypeptides (*Figure 3.7 B*) provided confirmation that the expressed proteins represented authentic AHSV polypeptides and further confirmation was obtained from investigation of their ability to form CLPs. Western immunoblot analysis with antisera raised to AHSV-9 was not possible because the serum does not recognise the linear amino acid chains of VP3 and VP7.

The amount or yield of VP3 and VP7 protein produced by the recombinant baculoviruses was estimated and compared to previously reported levels of expression of these proteins in insect cells. In order to estimate the amount of VP3 and VP7 produced, lysates of recombinant virus infected cells (MOI = 10) at 72 h p.i., were subjected to SDS-PAGE along with various known amounts (0.25-1.0 mg) of Rainbow^{TM} marker (Amersham). Proteins were visualised by Coomassie blue staining. The yield of expressed AHSV-9 VP3 was estimated to be approximately 1-2 $\mu g/10^6$ cells while that of VP7 was in the order of 20-25 $\mu g/10^6$ cells (results not shown). The dual expression of VP3 and VP7 resulted in a yield lower than expression of the individual proteins (8-10 $\mu g/10^6$ for VP3 and 0.8-1.0 $mg/10^6$ for VP7). The level of expression of AHSV-9 VP3 was nevertheless higher than previously reported in the case of AcRP23-*lacZ* baculovirus expression (S. Durbach, 1998). The much higher level of VP7 (ca. 20-25 $mg/10^6$ cells) versus VP3 expression is in agreement with the *in vitro* results (Maree *et al.*, 1998). The ratio of VP3 versus VP7 expression was determined and it was found to be approximately 2:15, which is about the same molar ratio found for the BTV core (2:13). VP7 aggregated into large crystals in the cytoplasm identical to the crytalline structures described by Chuma *et al.* (1992) and Burroughs *et al.* (1994).

In order to determine if AHSV-3 VP2 and VP3, AHSV-9 VP2 and VP3 and AHSV-9 VP5 and VP7 were co-synthesised in recombinant virus-infected cells, monolayers of *S. frugiperda* cells were infected with the respective dual recombinant baculoviruses (DBac-S2.9-S3.9, DBac-S2.3-S3.9, DBac-S6.9-S7.9 and Dbac-S6.3-S7.9) and pulse labelled with ^{35}S-methionine from 32 to 36 h p.i. Mock and wild type baculovirus infected Sf9 cells and cells infected with recombinant baculoviruses expressing VP2, VP3, VP5 and VP7 individually were similarly prepared as controls. Following harvesting of the cells, the proteins in the cell lysates were resolved by SDS-PAGE and visualised by autoradiography. The results are shown in *Figure 3.8*. Discreet protein bands of approximately 116

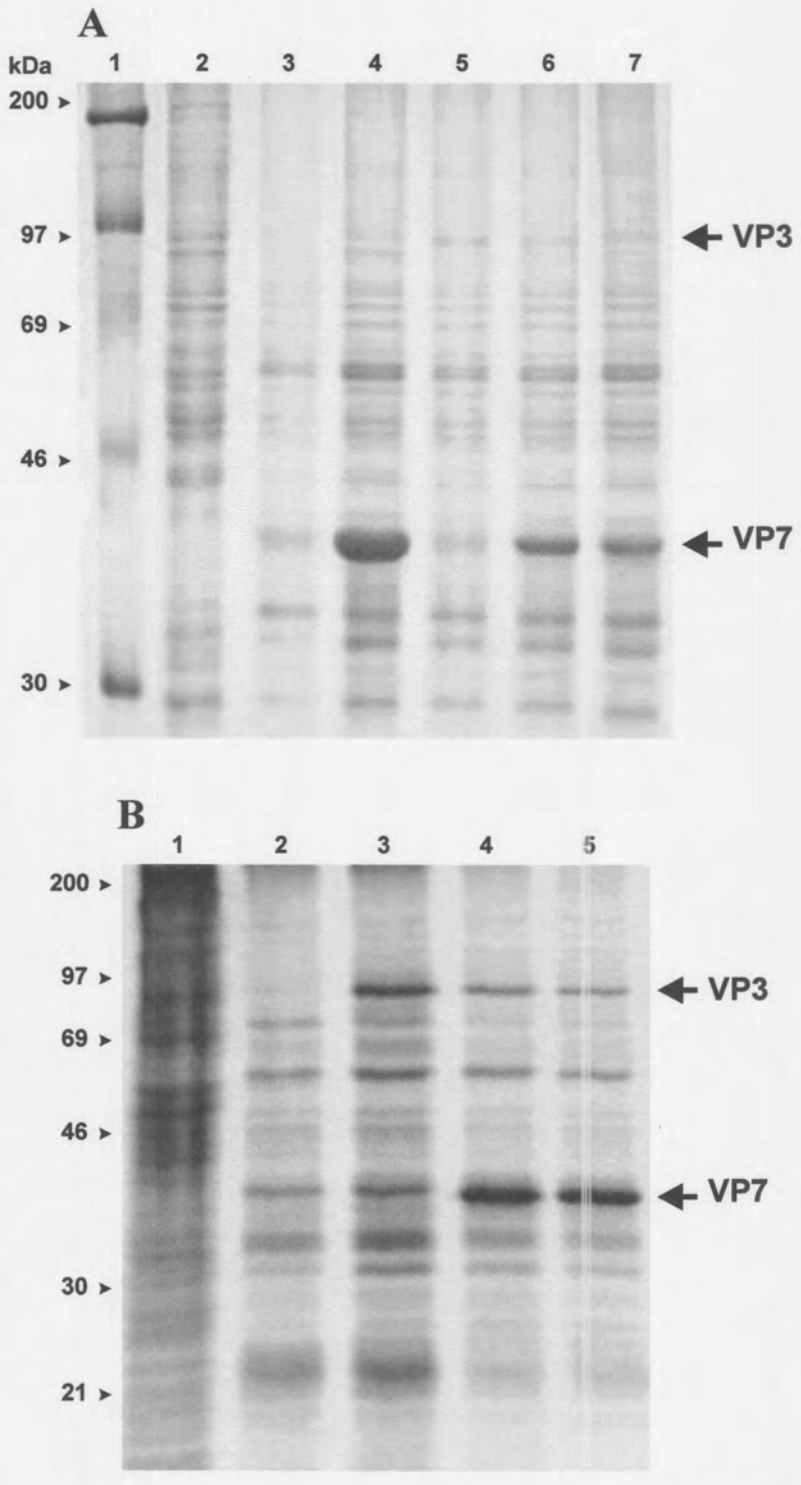

Figure 3.7: (A) SDS-PAGE analysis of cell lysates of insect cells infected with recombinant and wild-type baculoviruses. Lane 1, protein molecular weight marker; Lane 2, mock-infected Sf9 cells; Lane 3, wild type baculovirus; Lane 4, AHSV-9 VP7 recombinant baculovirus; Lane 5, AHSV-9 VP3 recombinant baculovirus; Lane 6 and 7, AHSV-9 VP3 and VP7 dual recombinant baculoviruses. Sizes of protein markers are indicated in kDa at the left of the figure. (B) Autoradiograph of ^{35}S-methionine labelled proteins separated by SDS-PAGE. Lane 1, mock-infected Sf9 cells; Lane 2, wild type baculovirus; Lane 3, AHSV-9 VP3 recombinant baculovirus; Lane 4 and 5, AHSV-9 VP3 and VP7 dual recombinant baculoviruses.

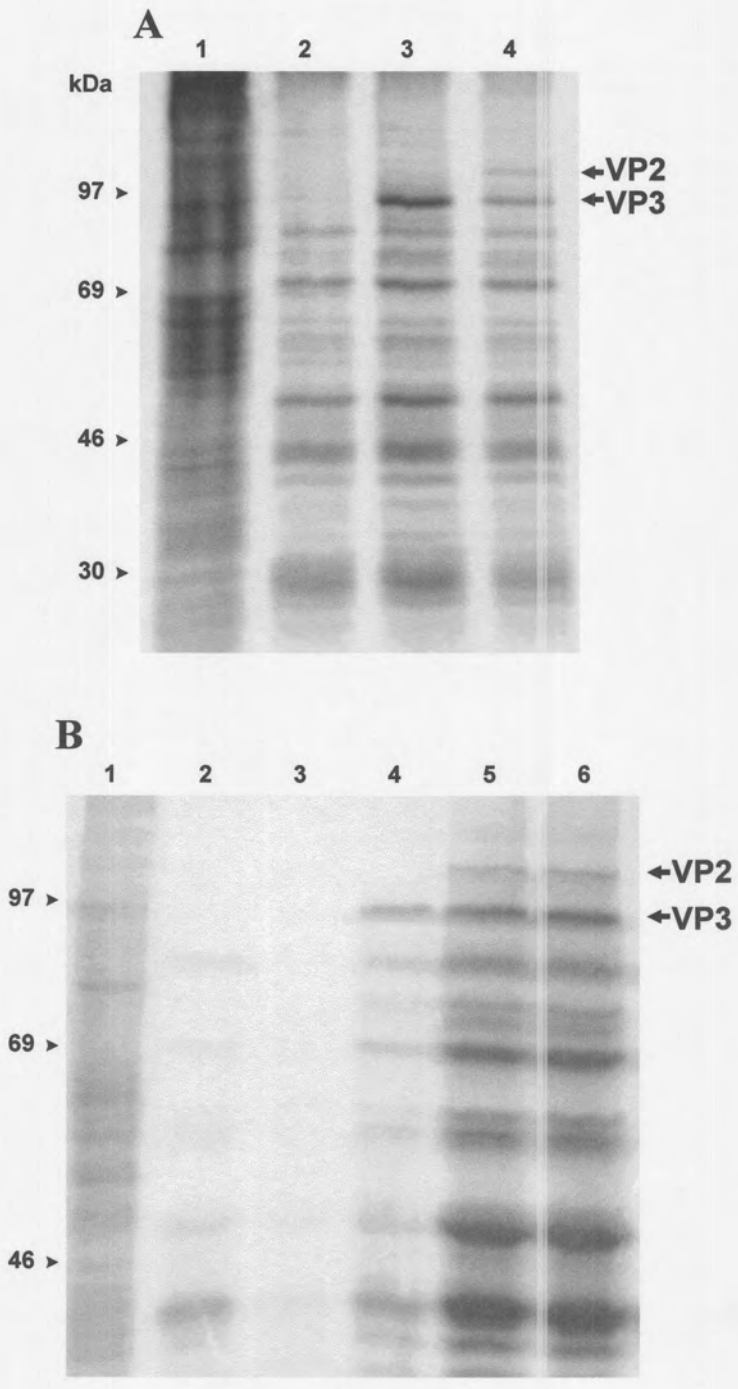

Figure 3.7: Autoradiograph of SDS-PAGE analysis of ^{35}S-methionine labelled proteins from cell lysates of insect cells infected with VP3/VP2 dual recombinant and wild-type baculoviruses. (A) Lane 1, mock-infected Sf9 cells; Lane 2, wild type baculovirus; Lane 3, AHSV-9 VP3 recombinant baculovirus; Lane 4, AHSV-9 VP2 and VP3 dual recombinant baculovirus. (B) Lane 1, mock-infected Sf9 cells; Lane 2, wild type baculovirus; Lane 3, AHSV-3 VP2 recombinant baculovirus; Lane 4, AHSV-9 VP3 recombinant baculovirus; Lane 5 and 6, AHSV-3 VP2 and VP3 dual recombinant baculoviruses.

kDa and 97 kDa that co-migrated with VP2 and VP3 in the positive controls, but were absent in mock and wild type infected cells, were present in both DBac-S2.9-S3.9 and DBac-S2.3-S3.9 infected cells. In DBac-S6.9-S7.9 and DBac-S6.3-S7.9 infected cells, two unique protein bands with approximate sizes of 64 and 38 kDa, respectively, were identified after separation on 10% SDS-PAGE and autoradiography, in the cell lysate (*Figure 3.9*). These proteins corresponded to VP5 and VP7 in the positive controls. The sizes of the expressed proteins agreed with those expected for VP2, VP3, VP5 and VP7 calculated from their amino acid compositions. Since the levels of expression were below that which could be determined with certainty by staining, confirmation that the expressed proteins represented authentic AHSV proteins was provided by immunoprecipitation with antisera raised to AHSV serotypes 9 and 3 (results not shown). The putative VP2 and VP3 proteins as well as VP5 were shown to react specifically with anti-AHSV serum, while no reaction was detected with mock-infected or wild-type infected cells. Immunoprecipitation of VP7 was non-specific since VP7 also precipitated in the control without serum as a result of the natural occurring large VP7 crystals.

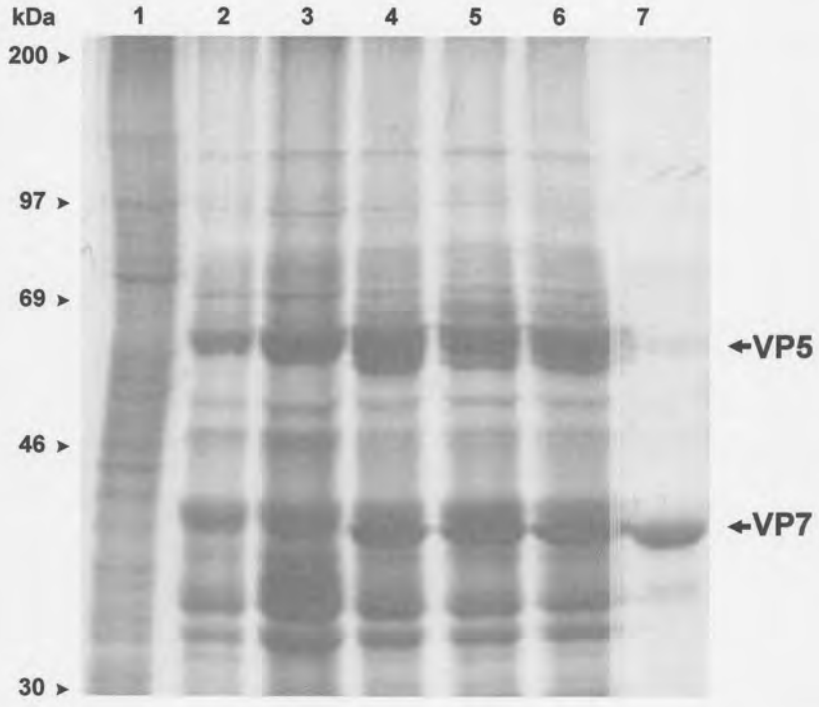

Figure 3.9: Autoradiograph of SDS-PAGE analysis of ^{35}S-methionine labelled proteins from cell lysates of insect cells infected with VP5/VP7 dual recombinant and wild-type baculoviruses. (A) Lane 1, mock-infected Sf9 cells; Lane 2, wild type baculovirus; Lane 3, AHSV-9 VP5 recombinant baculovirus; Lanes 4 and 5, AHSV-9 VP5 and VP7 dual recombinant baculoviruses; Lane 6, AHSV-3 VP5 and AHSV-9 VP7 dual; Lane 7, AHSV-9 VP7 recombinant baculovirus.

3.3.3. Co-expression, purification and electron microscopic evaluation of assembled particles

In order to produce CLPs, partial VLPs and VLPs, the different dual recombinant baculovirus constructs were used to infect or co-infect SF9 cells with the aim to express different combinations of the AHSV structural proteins. The co-infection experiments together with the various purification protocols followed, are summarised in table 3.3.

Table 3.3: *Summary of infections or co-infections performed with the various recombinant baculoviruses and particle purification methods (differential centrifugation, DC; discontinuous (DSG) and continuous (CSG) sucrose gradient; caesium chloride gradient, CsCl) used.*

Recombinant baculoviruses Dual (d) or single (s)	Foreign proteins (VP) AHSV serotypes	Possible assemblies	Purification methods
DBac-S3.9-S7.9	VP3/9 and VP7/9	CLPs	DSG, CSG, CsCl
DBac-S3.9-S7.9 DBac-S6.9 or 3	VP3/9 and VP7/9 VP5/9 or VP5/3	Partial VLPs (CLP + VP5)	DC, CSG
DBac-S3.9-S7.9 Bac-S2.9	VP3/9 and VP7/9 VP2/9	Partial VLPs (CLP + VP2)	DC, CSG
DBac-S2.9-S3.9 DBac-S6.9-S7.9	VP2/9 and VP3/9 VP5/9 and VP7/9	Homologous VLPs	DC, DSG
DBac-S2.3-S3.9 DBac-S6.3-S7.9	VP2/3 and VP3/9 VP5/3 and VP7/9	Heterologous VLPs	DC, DSG
DBac-S3.9-S7.9 DBac-S2.3-S6.3	VP3/9 and VP7/9 VP2/3 and VP5/3	Heterologous VLPs	DC, CSG, CsCl

3.3.3.1. Particles formed by assembly of VP3 and VP7 in insect cells

In order to determine whether expressed AHSV-9 VP3 and VP7 proteins could interact with each other and form complex structures, *S. frugiperda* cells were infected with the VP3 and VP7 dual recombinant baculovirus. Particles formed by the self-assembly of AHSV-9 VP3 and VP7 were purified on the basis of differences in their sedimentation rates (S) in a sucrose gradient. The particles were isolated by lysing infected Sf9 cells with a non-ionic detergent and purified on discontinuous sucrose gradients or self-forming CsCl gradients. After fractionation of the sucrose gradient and analysis by SDS-PAGE, the VP3 and VP7 complexes were identified in the region of

250 S, which is in agreement with previous results (Maree et al., 1998). In the CsCl, the particles banded at a density of 1.30 g/cm^3. Both the sedimentation coefficient and the density of the expressed particles was approximately half that of AHSV core particles derived from complete virions (Oellerman *et al.*, 1969; Huismans *et al.*, 1987; Burroughs *et al.*, 1994). This is expected since the particles do not contain any minor structural proteins or dsRNA. When examined by electron microscopy, the material was found to consists of core-like particles whose size and appearance were similar to those of authentic AHSV core particles prepared from AHSV-infected BHK cells (Burroughs *et al.*, 1994). The electron microscopic images of the empty synthetic particles revealed a dark central region with typical icosahedral symmetry (*Figure 3.10*). This was surrounded by a less electron dense layer with knobby morphological protrusions extending outwards. The particles appeared uniform in size and shape with an average diameter of 72 nm.

Capsomeres radiating 7.0 nm from the icosahedral subcore are clearly visible and appear as elongated tripods/prisms. The ring-like arrangement of the capsomeres (VP7 trimers) onto the VP3 subcore is also visible with five to six trimers in a circular arrangement. This indicated the pentameric arrangement of the capsomere on the surface of the CLPs. The distance between the trimers was approximately 7.0 nm and the trimers were arranged with its bottom domain onto the VP3 scaffold and its top domain facing outwards. Inside the CLP the VP3 layer appeared smooth and forms an icosahedral scaffold with six 5-fold axes visible. The VP3 and VP7 layer of the CLP is approximately 9.0 nm in diameter. The interaction of VP3 and VP7 were verified by antibody decoration, using monoclonal antisera raised against AHSV-3 VP7 (Van Wyngaard *et al.*, 1992). Electron micrographs revealed that each particle of interest was masked by a dark shadow resulting from the specific interaction of monoclonal VP7 antibodies with the VP7 outer shell (*Figure 3.10 B*). A few contaminating empty baculovirus capsids were present which were not captured by the VP7 monoclonal antibodies and therefore served as negative controls (results not shown).

The yield of CLPs produced was very low. Using 2 x 10^8 cells infected with plaque purified dual recombinant viruses at a MOI of 10-15 pfu/cell yielded only 1-2 μg of VP7 after purification on a sucrose gradient. This resulted in 1 to a maximum of 6 CLPs observed in a block on an electron microscope grid. Aggregations of CLPs and baculovirus proteins were also present. To increase the yield of CLPs the purification process was optimised, using the purification method described by Burroughs *et al.* (1994) with a few minor changes. Partial purification of CLPs from infected cell culture media was achieved using combinations or individual detergent treatments (0.05 - 0.5%Triton X-100, 0.1 - 0.5% Nonidet-P40 and 0.5 - 1.0% sodium N-lauroyl sarcosine (NLS)), with protease inhibitors and differential centrifugation using the procedure described in material and methods. This resulted in a reasonable detectable yield of VP3 and VP7 protein which were approximately 70% purified as analysed by SDS-PAGE. The presence of protease inhibitors made a significant

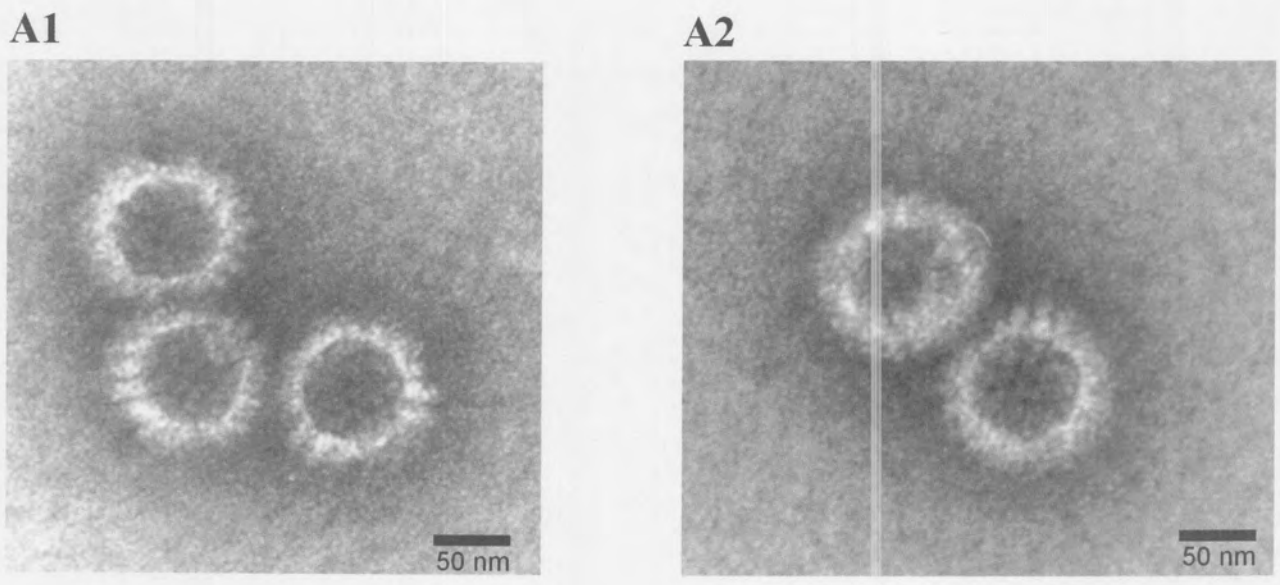

Figure 3.10: (A) Electron micrographs of empty AHSV CLPs synthesised in insect cells by a recombinant baculovirus expressing the two major AHSV core proteins VP3 and VP7. The expressed particles were purified on self-forming CsCl gradients and negatively stained with 2% aqueous uranyl acetate. (B) Negative contrast electron micrographs of the purified CLPs bound to VP7 monoclonal antibodies.

difference in the yield of CLPs recovered after purification. However, the CLPs were still contaminated with a large number of empty baculovirus capsids and baculovirus expressed tubules. Purification of this partial purified material by discontinuous sucrose gradient centrifugation still resulted in contaminating baculovirus structures, although free of cellular proteins and VP7 crystals. Maintenance of CLPs in 0.2% NLS or 0.2% Nonidet-P40 was essential to prevent irreversible aggregation. Although up to five or six CLPs could be found in an E.M field at 50 000 enlargement, this was not enough for high resolution structural studies using In-lense FESEM or for use in a subunit vaccine. Highly purified CLPs were obtained with CsCl centrifugation, although approximately 40% of the particles were lost during this procedure. The particles purified this way formed a sharp white band with a density of 1.30 g/ml.

The stability of the particles under different physicochemical conditions was also investigated. A purified preparation of CLPs were adsorbed onto E.M grids and treated with different solutions prior to negative staining. Treatment of the particle with a low salt buffer (< 50 mM NaCl) or high salt buffer (>1 M NaCl or $MgCl_2$) resulted in the loss of the capsomeres leaving a smooth inner subcore-like particle (SCLP). The CLPs appeared to be unstable at $MgCl_2$ concentrations higher than 1 M, which is in agreement with the results of Burroughs *et al.* (1994) and Mertens *et al.*, 1987 on the stability of AHSV and BTV cores, respectively. Like BTV and AHSV cores, the CLPs were stable in a wide range of pH conditions from about 6.0 to 9.0. A reducing agent (10 mM DTT) was used by Burroughs *et al.* (1994) for purification of complete AHSV virions. The stability of AHSV CLPs in the presence of DTT was also investigated, with no significant effect on the structure and was later incorporated during the purification process of VLPs.

3.3.3.2. Assembly of VP2 or VP5 proteins onto CLPs

To determine whether VP2 or VP5 can assemble onto cores in an *in vivo* system, the VP3/VP7 dual recombinant baculovirus and an AHSV-9 VP2 (Bac-AH9.2; constructed by G. Napier) or VP5 (pFBD-S5/9; section 3.3.1.3) single recombinant baculoviruses were employed to infect Sf9 cells, in order to co-express the three relevant genes in insect cells. The cells were co-infected with either Dual-S3.S7 and Bac-S6/(9 or 3) or Dual-S3.S7 and Bac-AH9.2 at strictly 5 pfu/cell of each recombinant virus. Protein complexes synthesised in infected cells were separated on the basis of differences in their sedimentation rates (S) in a sucrose gradient. The gradient was fractionated and the fractions analysed by SDS-PAGE. Three of the lower fractions contained very faint bands corresponding to the predicted sizes of VP3, VP5 and VP7 or VP2, VP3 and VP7 (result not shown). These fractions were pooled and the assembled particles recovered by high-speed centrifugation.

To analyse the morphology of these particles, both multimeric structures (one containing VP2, VP3 and VP7, the other VP5, VP3 and VP7) were examined by negative staining electron microscopy. In

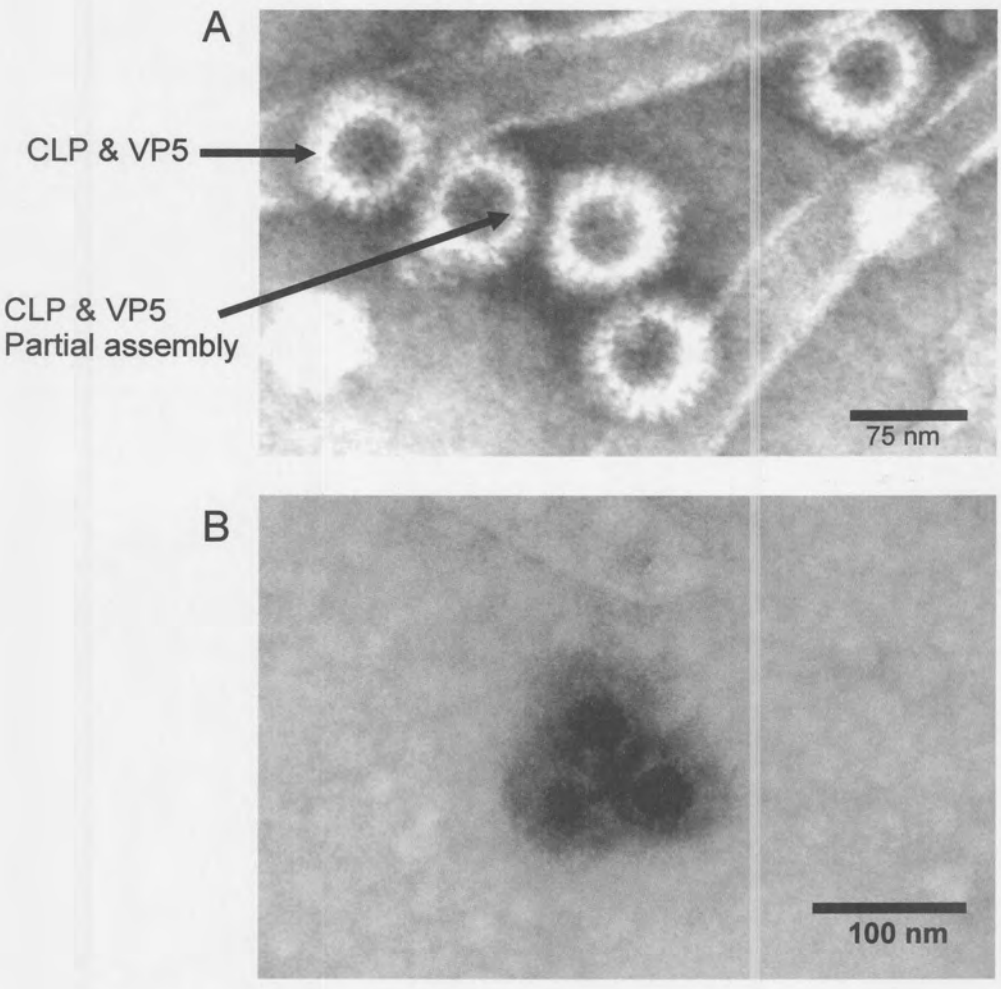

Figure 3.11 (A) Electron micrograph of partial VLPs synthesised in insect cells by co-infection of a dual VP3/VP7 recombinant baculovirus and a VP5 single recombinant baculovirus. Some partially assembled particles were also observed. The particles were purified on either a 30-68% discontinuous sucrose gradient or a 20-50% continuous sucrose gradient. (B) Negative contrast electron micrographs of the purified partial VLPs (CLPs & VP5) decorated with VP5 monospecific antisera and stained with uranyl acetate.

preparations from infections involving the VP3/VP7 dual recombinant vector, the only structures observed were CLPs. In contrast, the co-expression of VP3 and VP7 with either VP2 or VP5 proteins resulted in the formation of double-shelled particles (containing an additional protein layer) resembling authentic empty AHS virions (*Figure 3.11A & 3.12*). However, these double-shelled particles had a somewhat smaller diameter than reported for AHS virions, although larger than CLPs. These partial-VLPs with only one outer capsid protein (VP2 or VP5) had an approximate diameter of 76 to 78 nm, whereas the complete virion containing both outer capsid proteins measure approximately 82-84 nm. The electron microscopic images also indicated that the empty synthetic partial VLPs were characterised by a dark central region with typical icosahedral symmetry, identical to the empty CLPs. These empty partial VLPs were lacking the knobby protrusions characteristic of the surface of CLPs and cores, but were surrounded by a diffuse outer layer. The data were substantiated by a study using monospecific antibodies raised against VP5 or polyclonal serum against AHSV-9 (*Figure 3.11B & 3.12*). Conclusive results were obtained demonstrating that both VP2 and VP5 attach to the CLPs independently of each other.

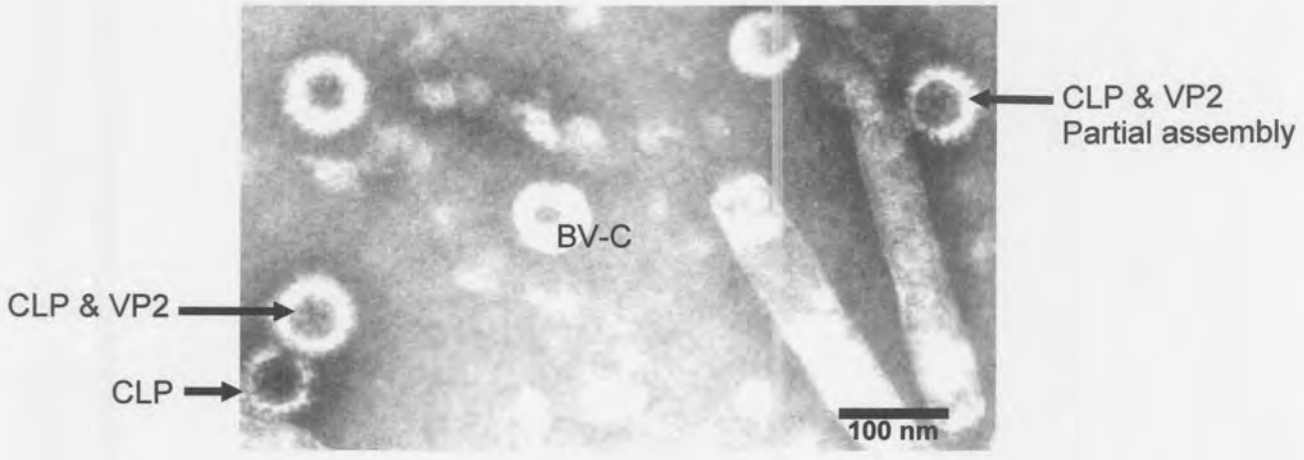

Figure 3.12: Electron micrograph of partial VLPs synthesised in insect cells by co-infection of a dual VP3/VP7 recombinant baculovirus and a VP2 single recombinant baculovirus. VP2 assembles spontaneously onto preformed CLPs in the absence of VP5. Partial assembled intermediates were also present in the sample (*right*). The particles were purified on either a 30-68% discontinuous sucrose gradient or a 20-50% continuous sucrose gradient.

3.3.3.3. Co-expression of four major structural proteins of AHSV in insect cells

To assess the interaction of the four major structural proteins of AHSV, insect cells were co-infected with both the VP2/VP3 and VP5/VP7 dual recombinant baculoviruses, in order to co-express VP2, VP3, VP5 and VP7. The cells were harvested at 48 h p.i. and lysed with a non-ionic detergent Nonidet-P40 under reducing conditions (DTT) in the presence of proteinase inhibitors, and the released particles were purified to homogeneity by centrifugation on discontinuous sucrose gradients. When examined by the electron microscope, some empty double-shelled particles were observed consisting of an electron dense core surrounded by a thick outer capsid. The yield of these particles was extremely low. SDS-PAGE analysis of fractions containing the particles failed to recognise the presence of the four major structural proteins. No more than 1 particle was visible in a number of fields under the electron microscope and most of these were partial CLPs. A few partial VLPs were observed, shown in *Figure 3.13*. Reasons for the low yield in VLP production is explained later.

The next step in the production of VLPs was to co-infect insect cells with the VP3/VP7 dual recombinant baculovirus and a VP2/VP5 (serotype 3) dual recombinant baculovirus. The latter was constructed by Renate Filter in the lab of H. Huismans. The expressed proteins made in infected cells assembled into double capsid particles the same as described above. Some simple CLPs were also observed in the preparation. Their diameters were estimated to be of the order of 72 nm and they exhibit similar morphology described in section 3.3.3. Most of all a range of intermediate structures

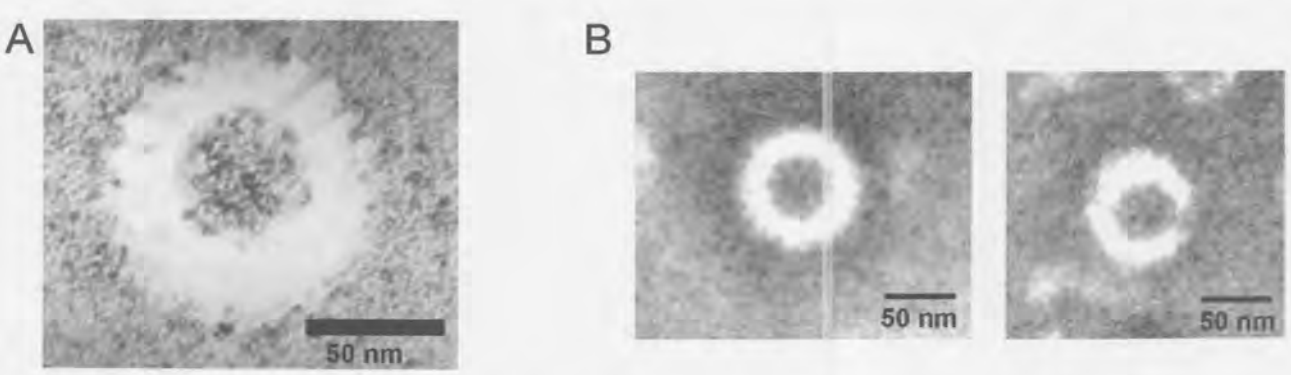

Figure 3.13: Electron micrograph of VLPs synthesised in insect cells. In (A) the particles were synthesised by co-infection of a VP2/VP3 and a VP5/VP7 dual recombinant baculoviruses. Self-assembly of all four major structural proteins of AHSV was observed. The yield of these VLPs was low and partial assembled intermediates were present in abundance. In (B) the empty AHSV double-shelled VLPs were synthesised by the co-infection of a VP2/VP5 and a VP3/VP7 dual recombinant baculoviruses. The particles were purified on either a 30-68% discontinuous sucrose gradient or a 20-50% continuous sucrose gradient.

were also observed, apparently with various amounts of the outer capsid proteins attached. These may reflect different stages in particle assembly. The centres of all types of particles (CLPs, VLPs, intermediate VLPs) exhibited an icosahedral configuration. The diameters of the largest particles were estimated to be in the order of 82 nm.

The yield of these VLPs was still extremely low which made the investigation of the fine structure difficult. Large distinctive crystals, which is formed by the accumulation of VP7 in the cytoplasm of infected cells, were observed. These crystals appeared similar to the crystalline structures found in AHSV-4 infected cells when observed under the light microscope (Chuma *et al.*, 1992; Burroughs *et al.*, 1994).

3.4. DISCUSSION

The primary objective of this study was to increase the understanding of the assembly of the four major structural proteins of AHSV by establishing whether the four proteins can interact spontaneously in the absence of other AHSV proteins and the viral genome. In order to study these aspects it was necessary to synthesise the proteins of interest in significant quantities using an appropriate expression system. Therefore, in this part of the investigation the aim was first of all to establish a useful model for studying protein-protein interaction in virus assembly and secondly to develop a system that could be used for the presentation of foreign antigenic determinants, including the VP2 protein of AHSV in its desired conformation. The first step towards the production of AHS VLPs was to produce CLPs to act as a scaffold for the assembly of the two outer capsid proteins.

Recently Maree *et al.*, (1998) were able to demonstrate the self assembly of AHSV-9 VP3 and VP7 by co-infection of insect cells with recombinant baculoviruses expressing each gene respectively. They laid the foundation for the assembly of AHS VLPs. However, the resulting CLPs were heterogeneous with respect to the amount of visible capsomeres, indicative of the formation of partially assembled particles. Partial assembly could be expected, because the strategy used relied upon co-infection of cells with individual VP3 and VP7 recombinant baculoviruses (Burroughs *et al.*, 1995). The multiplicity of infection of each recombinant virus varies from cell to cell which correlates with the level of protein expression (Maree *et al.*, 1999). A further disadvantage of co-infection is that the yield of CLP formation was extremely low. To overcome this variation in the ratio of VP3 to VP7 expression and the low yield of CLPs, an attempt was made to synthesise CLPs by simultaneous expression of the two major core proteins, VP3 and VP7, using a dual recombinant baculovirus. To express both proteins simultaneously in infected insect cells use was made of the Bac-to-Bac™ baculovirus expression system (Life Technologies).

The dual expression transfer vector, pFastbac-dual, utilises both the polyhedrin and p10 promoters for the expression of two heterologous foreign genes. The first strategical step involved the cloning of different combination of AHSV structural proteins, including proteins from different serotypes, in the dual transfer vector, each under control of its own promoter. The tailored DNA copies of AHSV segment 3 and 7 were cloned into pFastbac-dual under control of the p10 and polyhedrin promoters respectively. In an attempt to investigate the interaction of both outer capsid proteins with CLPs, two dual transfer vectors were constructed. In one dual vector either the AHSV-3 or 9 VP2 gene and the AHSV-9 VP3 gene were cloned under control of the polyhedrin and p10 promoter respectively, while the AHSV-3 or 9 VP5 gene and AHSV-9 VP7 gene were inserted in a second dual transfer plasmid. The use of different AHSV serotypes for the outer capsid proteins provide the means to investigate the formation of heterologous VLPs. This strategy, using a dual with VP2/VP3 and one with VP5/VP7 was followed for two reasons. First of all each of the major core proteins (VP3 and VP7) and outer capsid proteins (VP2 and VP5) will be directed from the same promoter, which means that each protein will be in the correct ratio for optimum particle formation. Secondly, when co-infected, cells infected with only one dual will form no particles and the only particles will be produced when both dual recombinants are present in the same cell. This will overcome the problem of intermediate structures formed by the co-infection of a VP3/VP7 dual and VP2/VP5 dual (French *et al.*, 1990). Dual recombinant composite bacmid DNA was constructed in *E. coli* cells by site-specific transposition of the genes and flanking regulatory sequences from the transfer vector into the bacmid genome with the aid of a helper plasmid. Recombinant baculoviruses were obtained by transfection of this composite bacmid DNA into *Spodoptera frugiperda* cells (Luckow *et al.*, 1993).

To investigate the assembly of AHSV VP3 and VP7, insect cells were infected with the VP3/VP7 dual recombinant baculovirus and VP3/VP7 complexes were purified from infected cells and analysed by electron microscopy. Expressed VP3 and VP7 were found to interact spontaneously to form core-like particles of the same size, appearance and stoichiometric arrangement of VP3 to VP7 as in authentic AHSV cores. This confirms the result from Maree et al. (1998). Uniform particles with a diameter of 72 nm, which structurally resembled cores prepared from AHSV-4 (Burroughs *et al.*, 1994) were visible with negative staining. The diameter is in agreement with that of BTV CLPs (Hewat et al., 1992) obtained from cryoelectron microscopic images. Native BTV cores are 69 nm in diameter (Prasad *et al.*, 1992), which is slightly smaller than that of BTV CLPs for an unknown reason. Only VP3 and VP7 were identified as the protein components of the expressed particles. Also the molar ratios of the two proteins were similar to those of VP3 and VP7 derived from infectious AHSV and also similar to the ratio found for BTV CLPs (Burroughs *et al.*, 1994). In contrast to virus-derived cores, the CLPs appeared empty, since it lacks nucleic acids and the minor structural proteins. This explains the lower density and sedimentation rate of the CLPs in comparison to complete virions

(Huismans *et al.*, 1987). The CLPs have a knobby surface structure, similar to cores derived from virus by removal of VP2 and VP5 (Burroughs *et al.*, 1994). This outer core layer is probably composed of VP7 trimers as for BTV (Grimes *et al.*, 1995). The VP7 capsomeres are easily removed from CLPs with a low salt buffer, resulting in a ring-like structure composed solely of VP3. Expression of VP3 in the absence of VP7, failed to identify any recognisable structure or SCLPs.

Assembly of these core-like particles from VP3 and VP7 demonstrated that these proteins provide the structural integrity of the core and that their formation in insect cells is not dependent on the presence of AHSV dsRNA or the minor core proteins. In addition, it can be concluded that the AHSV non-structural proteins are not required to either assist or direct the assembly of these empty particles. It should be noted that VP7 aggregates into large hexagonal crystals in infected cells, even when co-expressed with VP3, which could impede incorporation into particles. The functional significance of the VP7 crystals, if any, remains to be determined. It is postulated that these crystals represent a by-product, rather than an essential component of the AHSV replication process (Burroughs *et al.*, 1994).

Initial co-infection experiments with a dual vector containing BTV VP3 and VP7 and a recombinant vector with either BTV VP2 or VP5 failed to demonstrate the assembly of the individual capsid proteins onto the CLPs (French *et al.*, 1990). Liu *et al.* (1992) demonstrated *in vitro* the interaction of BTV VP2 and VP5 onto preformed CLPs. Whether the outer capsid proteins of AHSV or other orbiviruses can interact independently with the core was not previously known. Using the dual recombinant baculovirus expression vector containing AHSV VP3 and VP7 and a recombinant baculovirus containing either AHSV-3 VP5 or AHSV-9 VP2, a co-infection experiment was performed. The results demonstrated that the outer capsid proteins of AHSV, VP2 and VP5, do interact separately with CLPs *in vivo*. The VP2 and VP5 do interact only with the VP7 protein of the core. These data was confirmed by the co-expression of VP2 and VP3 or VP5 and VP3. Analysis of infected cell lysates with sucrose gradient centrifugation failed to obtain these proteins in the same fraction, which indicate that there was no association of VP2 or VP5 onto VP3 scaffolds in the absence of VP7. Further evidence that the multimeric structures represented empty CLPs with assembled VP2 or VP5 was provided by their ability to react with monospecific antisera. Liu *et al.* (1992) demonstrated that the level of interaction of VP2 to the CLP is much less when expressed in the absence of VP5. It is likely that during morphogenesis of the virus the proteins stabilise each other in the virion structure.

In a attempt to attach both outer capsid proteins to CLPs, experiments were performed involving co-infection of *S. frugiperda* cells with two dual recombinant baculoviruses, each containing two major structural proteins of AHSV. The one recombinant expressing VP2 and VP3 and another VP5 and

VP7, respectively were used to co-infect insect cells. This strategy of producing VLPs was used in order to eliminate the variable amount of CLPs and outer capsid proteins, which would lead to intermediate structures. This strategy resulted in a very poor yield of CLPs, possibly because the VP7 protein, in the presence of all four major structural proteins, still aggregates into crystals in infected cells. This could inhibit the incorporation into particles. It was also demonstrated by Maree *et al.* (1998) that variable amounts of VP7 incorporate during intracellular assembly as a direct result of the variation in the ratio of VP3 to VP7 expression in insect cells co-infected with VP3 and VP7 single recombinant baculoviruses. The absence of the full complement of the knobby protrusions or capsomeres on the CLPs surface may result in the failure of VP2 and VP5 to associate with the CLPs. To verify this statement it was also indicated, by the co-expression of VP2 and VP3 or VP3 and VP5, that VP5 and VP2 associate with VP7 trimers and not with the VP3 subcore. To overcome this problem, another co-infection experiment was performed, this time using the VP3/VP7 dual recombinant in combination with a VP2/VP5 dual recombinant.

Protein complexes comprising all four structural proteins corresponding to the estimated sizes of AHSV-9 VP2, VP3, VP5 and VP7 were isolated. Electron micrographic images of negatively stained complexes indicated that these particles largely resembled AHS virions. Unlike the native AHS virions, the empty double-shelled particles consisting of a core surrounded by a thick outer capsid. This outer capsid was visible as a diffuse layer in electron micrographs, similar to that of BT VLPs (French *et al.*, 1990; Hewat *et al.*, 1994), since these images show little surface detail. The diameter of the largest particles were estimated to be in the order of 81 to 84 nm, i.e., comparable to those of AHS virions (Oellerman *et al.*, 1969; Burroughs *et al.*, 1994) and BTV virions and VLPs (Huismans *et al.*, 1987; French *et al.*, 1990; Hewat *et al.*, 1994). A striking feature unique to the synthetic particles, is the empty centre, since it lacks the genome and minor core proteins. The VLPs appeared to vary with respect to the quantity of VP2 and VP5 on the outer layer, which confers in intermediate VLPs. This may be due to the variable amount of VP2 and VP5 incorporated during intracellular assembly as a direct result of the variation in the ratio of VP3 and VP7 expression to VP2 and VP5 expression in insect cells co-infected with the VP3/VP7 and VP2/VP5 recombinant baculoviruses. A similar range of particles were obtained with BTV when the production of VLPs relied on the co-infection of two dual expression vectors (French *et al.*, 1990; Hewat *et al.*, 1994) and only very few particles appeared complete.

Data obtained from Hewat *et al.* (1994) revealed that the outer capsid of BT VLPs exhibited a well-ordered morphology that contrasted strongly with that deduced by conventional staining methods. In the BT VLP it was observed that globular structures were located underneath sail-shaped surface structures. The globular proteins, presumed to be VP5, were located on the six-membered rings of the VP7 trimers of the BTV core and CLPs. The sail-shaped spikes were situated above the VP7

trimers and form 60 triskeleton-type motifs, which cover all but 20 of the VP7 trimers in the virion. It is likely that these spikes are the VP2 (Hewat *et al.*, 1992; Hewat *et al.*, 1994).

In this part of the investigation it was demonstrated that the co-expression of all four AHSV major structural proteins in insect cells, resulted in the intracellular formation of virus-like particles (VLPs) which structurally resembled AHS virions. These results confirm that all four major capsid proteins of AHSV are capable of self-assembly into the correct structure, as for the native virus capsid, when simultaneously expressed in cells. The low proportion of complete particles produced by the two recombinant baculoviruses is probably due to suboptimal expression ratios of the four proteins as well as the crystallisation of VP7. Given that (a) the AHSV CLPs assembled spontaneously by co-expression of VP3 and VP7, (b) coexpression of VP3, VP7 and VP5, or VP3, VP7 and VP2 gives rise to spherical intermediate particles which lose the VP2 or VP5 easily, leaving a CLP, and (c) co-expression of VP2, VP3, VP5 and VP7 resulted in the assembly of double-shelled VLPs, it appears that VP2 and VP5 interact separately of each other to VP7. According to Hewat *et al.* (1994) the presence of both outer capsid proteins are necessary for the incorporation of the VP7 trimers around the five-fold axis, while Liu *et al.* (1992) demonstrated that the two proteins stabilise each other in the complete virion.

The observation of the spontaneous formation of complete AHSV VLPs in the absence of the nonstructural proteins implies that the nonstructural proteins are not necessary for the formation of the viral capsid. However, they may be involved in the control of dsRNA packaging and/or prevention of RNA transcription during assembly, but more important they may be involved in optimising the assembly process for more efficient capsid formation.

CHAPTER 4

EFFECT OF SITE DIRECTED INSERTION MUTATION ON THE CRYSTAL FORMATION, SOLUBILITY AND CLP FORMATION OF AHSV-9 VP7

4.1. INTRODUCTION

AHSV VP7 is composed of 349 amino acids with a calculated M_r of 38 kDa and its sequence is highly hydrophobic (Roy *et al.*, 1991). Although the BTV VP7 also contains a high percentage of hydrophobic residues, BTV VP7 synthesised by recombinant baculoviruses is soluble in the trimeric form (Basak *et al.*, 1992). In contrast to BTV, AHSV VP7 aggregates in infected cells in large, flat hexagonal crystals with a maximum dimension of about 6 μm (Buroughs *et al.*, 1994; Chuma *et al.*, 1992). Such large structures represent a feature unique to AHSV among the orbiviruses investigated. The building block for the AHSV VP7 crystals is a trimeric molecule containing three VP7 subunits. The subunits interact with each other via hydrophobic contacts. Hydrophobic residues involved in these contacts probably contribute to the tendency of the protein to aggregate (Basak *et al.*, 1996). It has been reported that AHSV-4 VP7 also forms crystalline structures when expressed in insect cells (Roy *et al.*, 1991). The X-ray crystallographic structure of the top domain of AHSV VP7 has recently been resolved to a 2.3 Å resolution and was found to be very similar to that of the BTV VP7 trimers (described in chapter 1), as expected from the high degree of sequence similarity of the BTV and AHSV VP7 proteins (Basak *et al.*, 1996).

The AHSV VP7 crystals, purified from BHK cells infected with AHSV-9, were shown to be highly immunogenic, elicited a strong immune response and were effective as a subunit vaccine in a mouse model (Wade-Evans *et al.*, 1997; Wade-Evans *et al.*, 1998). Passive transfer of antibodies from immunised mice failed to protect syngeneic recipients from AHSV challenge, which indicates that an antibody response is unlikely to represent the primary mechanism involved in the protection induced by vaccination with VP7 crystals. It is therefore possible that immunisation with VP7 induces a protective T-cell response. Furthermore, the conformation and possibly the assembly of the VP7 into crystals appear to be important in the mechanism of protection against the heterologous serotype challenge. Based on these findings and reports that VP7 of BTV contains immunodominant, serotype cross-reactive T-cell epitopes (Angove *et al.*, 1998), it was decided to investigate the potential of baculovirus-expressed AHSV-9 VP7 as a particulate antigen delivery system for the presentation of foreign peptides. Expression of VP7 crystals as an antigen delivery

system in insect cells has several advantages. Baculovirus expression will provide an entirely satisfactory source of recombinant crystals for vaccine purposes. These particles present no risk of contamination with infectious virus and the disc-shaped crystals are easily purified in a one step ultracentrifugation process. The aim of this part of the investigation was to investigate the possibility of developing the major core structural protein, VP7, of AHSV as a particulate vaccine delivery system for presenting small peptides to the immune system.

VP7 protein is also the major constituent of the virus core and when co-expressed with VP3 assembles into CLPs (chapter 3). Alternative to the use of CLPs as scaffolds for the presentation of VP2 in its correct conformation, the CLPs also have the potential to be used as antigen delivery systems by the insertion of foreign immunogenic epitopes into VP7 under conditions that do not disrupt CLP assembly. The use of AHSV CLPs, to provide protection against AHSV has never been investigated, partly because of the low yield of CLPs produced (chapter 3). In the case of BTV, partial protection against BTV challenge was afforded by CLP vaccination (Roy *et al.*, 1994). Although extension mutants of BTV VP7, containing 48 amino acids of hepatitis B virus preS2 region at the N-terminus were able to form chimeric CLPs, these CLPs were quite unstable. These chimeric particles were indeed highly immunogenic, but the results indicated that the suitability of the N-terminus of BTV VP7 for the insertion of foreign epitopes, is relatively restricted (Le Blois & Roy, 1993; Belyaev and Roy, 1992). On the other hand in-frame addition of sequences at the C-terminus of BTV VP7 abolishes CLP formation, presumably due to lack of trimer-trimer interactions (Le Blois & Roy, 1993). Certain internal sites of BTV VP7, Ala145 and Gln238, have also been investigated as target sites for the insertion of foreign epitopes on the basis that both sites were located on exposed loops of VP7 and thus on the surface of the trimers and CLPs. Insertion of foreign epitopes into the BTV VP7 Gln238 site abrogated CLP formation. However, chimeric BTV CLPs were produced when sequences of variable lengths of up to 29 amino acids have been inserted into the Ala145 site. These CLPs were shown to elicit strong humoral immune responses against these epitopes.

The aims of this part of the investigation were first of all to identify regions in the VP7 top domain, which can be used as insertion sites for the display of epitopes or peptides. Secondly, to modify the AHSV-9 VP7 gene by means of site-specific insertion mutations, in order to create restriction enzyme sites to facilitate the insertion of foreign epitopes and to analyse the insertion mutants with respect to solubility, trimerisation and the ability to form hexagonal crystals as well as CLPs. Thirdly, to construct VP7/TrVP2 chimeras that express an immunogenic region of AHSV-9 VP2, on the surface of the VP7 protein.

4.2. MATERIALS AND METHODS

4.2.1. Materials

The oligonucleotide primers used in this section were obtained from Boehringer Mannheim. The pMOSBlue PCR cloning kit was supplied by Amesham and the TaKaRa Ex Taq™ polymerase Gibco BRL (Life technologies). Qiagen supplied the Qiagen® plasmid mini-kit tip 20, the high pure plasmid purification kit was obtained from Boehringer Mannheim, the Nucleobond® columns from Macherey-Nagel and Wizard™ columns from Promega. ABI PRISM™ Big Dye Terminator Cycle Sequencing Ready Reaction kit was purchased from Perkin Elmer Biosystems.

4.2.2. Site-directed insertion mutagenesis of VP7 and the construction of recombinant transfer vectors

To introduce an AHSV-9 VP2 epitope into the two identified hydrophilic domains of the AHSV-9 VP7 protein necessitated the insertion of unique restriction sites in both regions. Two VP7 insertion mutants with 18 additional nucleotides at positions 548 to 549 and 617 to 618 were constructed by a polymerase chain reaction method (PCR). The 18 additional nucleotides represents three unique restriction enzyme recognition sites that were inserted into the sequence that encode two conserved hydrophilic regions of the cloned and tailored DNA copy of the VP7 gene of AHSV-9. Each of the VP7 site-specific insertion mutants were constructed by making use of two different PCR approaches, which are outlined in *Figure 4.3* and *Figure 4.5*, respectively. In the more laborious method, the insertions were generated after ligation of selectively amplified fragments of the VP7 gene. Four primers and two separate PCR reactions were used for each insertion mutation. A set of external oligonucleotide primers specific for the 5' and 3' regions of the VP7 gene containing *Bgl*II sites at each terminal, was used to introduce *Bgl*II sites at both ends of the VP7 sequence. For each insertion mutation a set of two mutagenic primers were designed, which contained the specific restriction enzyme sites (*Hind*III, *Xba*I and *Xba*I, *Sal*I) to be inserted between nucleotide positions 548 and 549 and 617 and 618, respectively. The strategy of creating the insertion mutants involved amplifying the VP7 gene as two VP7-specific segments, which were then ligated to create a complete gene. The sequences of the mutagenic primers as well as 5'- and 3'-specific primers, both of which included *Bgl*II linker sequences are shown in Table 4.1. and the annealing temperatures of the respective primers are summarised in Table 4.2. The plasmid pBR-VP7PCR (obtained from S. Maree), containing the complete coding sequence of the AHSV-9 VP7 gene, was used as a template in the polymerase chain reaction.

Briefly, the two PCR reactions for each insertion mutation were performed using the cool start method. The separate reaction mixtures of 50 µl each, consisted of 5 µl 10 x TaKaRa Ex Taq™ polymerase buffer (20 mM $MgCl_2$, 500 mM KCl, 250 mM TAPS pH 9.3, 10 mM 2-mercaptoethanol), 8 µl of a 2.5 mM dNTP mixture, 0.5-5 ng of template plasmid (pBR-S7PCR), 100 pmol (950 ng) of each oligonucleotide primer and 2 U of TaKaRa Ex Taq™ polymerase (Life technologies). The PCR reactions were subjected to 30 cycles of amplification in an ABI termal cycler 9600 PCR machine. The thermal parameters used for the PCR were 2 min hold at 94°C, 30 sec at 94°C, 30 sec at 52°C, 1 min at 72°C for 5 cycles, 30 sec at 94°C, 30 sec at 58°C, 1 min at 72°C for 10 cycles, 30 sec at 94°C, 30 sec at 64°C, 1 min at 72°C for 15 cycles, and 10 min hold at 72°C (Table 4.2).

TABLE 4.1: *Sequences of PCR primers used for the construction of VP7 insertion mutants*

Mutation	Position, polarity and type of primer	Oligonucleotide sequence
ins177-178	548-549; -; insertion	5'-GC**TCTAGAAAGCTT**CCTTGGGGCTAGCAGCGC-3'
	548-549; +; insertion	5'-GC**TCTAGAGTCGAC**AGGGGGGACGCAGTCATG-3'
ins200-201	617-618; -; insertion	5'-GC**TCTAGAAAGCTT**GCACCTTGAGGATCAC-3'
	617-618; +; insertion	5'-GC**TCTAGAGTCGAC**TCACTTGAGAGCGCTCC-3'
External:	+; 5' end-specific	5'-CAC**AGATCT**TTCGGTTAGGATGGACGCG-3'
	-; 3' end-specific	5'-CAC**AGATCT**GTAAGTGTATTCGGTATTGAC-3'

* Unique restriction enzyme sites to be inserted are shown in bold

TABLE 4.2: *The annealing temperatures (T_m), including and excluding the extra bases, of the above primers are summarised.*

Primer	Number of nucleotides	T_m excluding	T_m including
mt177Rev (-)	32 bp (18 G+C)	62 °C	73 °C
mt177For (+)	32 bp (20 G+C)	60 °C	74 °C
mt200Rev (-)	31 bp (18 G+C)	54 °C	69 °C
mt200For (+)	31 bp (16 G+C)	54 °C	72 °C
VP7-5'For (+)	28 bp (15 G+C)	56 °C	61 °C
VP7-3'Rev (-)	30 bp (12 G+C)	55 °C	59 °C

Amplification was followed by cloning the amplicons into the PCR cloning vector, pMOSBlue (Amersham). Following electrophoresis of samples of each reaction mixture in a 1.0% agarose gel, the amplified PCR products were recovered from the respective reaction mixtures using Geneclean™ procedure (section 2.2.4.2) or alternatively extracted with chloroform/isoamylalcohol (section 2.2.4.1), to remove residual DNA polymerase. The PCR fragments were ligated in a 1:10 ratio to the T-vector using the reagents supplied by the manufacturer. The ligation mixtures were transformed into ultra-competent MOS*Blue* cells according to the manufacturer instructions. Recombinant plasmids were isolated from white recombinant colonies with amp^R and tet^R phenotype and identified by restriction enzyme mapping. Orientation of each fragment was determined using *Sac*I.

Full-length VP7 insertion mutants at positions 548-549 (amino acids 177-178; VP7mt177) and 617-618 (amino acids 200-201; VP7mt200) were reconstructed by a two step directional cloning procedure in

pFastbac1 so as to enable expression of the resultant product by means of the BAC-TO-BAC™ expression system. First the 5'-terminal domain of both VP7 mutants was recovered from pMB-177/5' and pMB-200/5' with *Bgl*II and *Xba*I and ligated into the *Bam*H1 and *Xba*I sites of pFastbac1 and recombinants selected by *Sac*I digestion. The 3'-terminus was cut from pMB-177/3' with *Xba*I and *Kpn*I and cloned into the pFB-177/5' containing the modified 5' region of VP7. The 3'-terminus of insertion mutant 200 was retrieved from pMB-200/3' with *Xba*I digestion and ligated into the dephosphorylated *Xba*I site of pFB-200/5' and recombinants with the correct orientation of the 3' fragment selected with *Sal*I and *Sac*I digestions. Recombinant pFastbac1 plasmids containing the two modified VP7 genes were selected with *Sac*I, *Hind*III, *Xba*I and *Sal*I digestions. The VP7 insertion mutant genes in pFastbac1 were designated pFB-VP7mt177 (containing insertion between amino acids 177 and 178) and pFB-VP7mt200 (containing insertion between amino acids 200 and 201). The insertion of the three restriction enzyme sites in both modified VP7 recombinant plasmids were verified by automated dye terminator cycle sequencing (section 4.2.4), before expression of the modified VP7 proteins.

In the second method, the VP7 insertion-specific mutants were constructed by a modification of the polymerase chain reaction method as described by Imai *et al.*, (1991). In this method two oligonucleotide primers, designed to amplify the target DNA in inverted tail-to-tail directions, were used to amplify the cloning vector together with the target VP7 sequence in one PCR reaction and thereby generating the desired insertions. The plasmid pBS-VP7PCR, containing the full-length tailored VP7 gene in the T7 orientation, was used as template and the set of two mutagenic primers containing the unique restriction enzyme sites, described above (table 4.1), were used for priming the reaction. Briefly, the PCR reaction mixtures consisted of 10 µl of 10 x Ex Taq™ buffer, 8 µl of a 2.5 mM dNTP mixture, 0.5-5 ng of template plasmid (pBS-S7PCR), 85 pmol of the sense and antisense primers and 2 U of TaKaRa Ex Taq™ polymerase (Life technologies). The thermal parameters used for the PCR were the same as described above except the elongation at 72 °C were extended to 4.5 min in each cycle. The amplicons were gel purified digested with *Xba*I, self-ligated and transformed into competent *E. coli* XI1Blue cells. The two resultant VP7-specific clones, designated pIM177 and pIM200, was characterised by *Sac*I, *Hind*III, *Xba*I and *Sal*I digestions and automated sequencing (section 4.2.4). The two modified VP7 genes were recovered by *Eco*R1 and *Kpn*I digestions and recloned into the *Eco*R1/*Kpn*I site of pFastbac1 which were designated pFB-InM177 and pFB-InM200, respectively. These recombinant transfer vectors were used to express the modified VP7 proteins in eukaryotic cells.

4.2.3. Insertion of AHSV-9 VP2 epitopes in the VP7-encoding DNA and construction of recombinant baculovirus transfer vectors

The introduction of an AHSV-9 VP2 epitope into the two identified hydrophilic domains of the AHSV-9 VP7 protein, were performed using the two modified VP7 genes containing the unique restriction sites. These modifications allows the insertion of sequences with complementary 5' and 3' overhangs into the target sites. Sequences representing AHSV-9 VP2 immunogenic epitopes can now be cloned directionally in the correct reading frame of the VP7 sequences encoding the hydrophilic regions. Seeing as the cloning strategy followed by Samantha Hopkins in producing the two chimeric VP7/TrVP2 proteins, using the two insertion mutants, has not been documented elsewhere, it is included in this section for reference purposes. The strategy followed for generating the chimeric proteins was as follows: the first step was to clone a 2.3 kb region of VP2, which contain the epitope of interest (amino acids 385 to 415 and nucleotides 1167 to 1257), into the *Hind*III site of VP7 mutant 200. The VP2 specific *Hind*III site at position 957 is in the correct reading

frame to the *Hind*III site inserted at position 548-549 of AHSV-9 VP7 gene.

The plasmid pBS-AHSV9.2 was digested with *Hind*III and the 2.3 kb DNA fragment representing the AHSV-9 VP2 was excised from the gel and purified by Geneclean™ extraction (section 2.2.4.2). The plasmid pFB-mt200 was linearised with *Hind*III and then ligated to the purified 2.3 kb *Hind*III-restricted AHSV-9 segment 2 specific DNA. Following transformation into competent *E. coli* XL1Blue cells, plasmids from a number of amp^+ and tet^+ colonies were isolated and characterised by restriction analysis. A recombinant plasmid with the correct orientation of the *Hind*III truncated segment 2, inserted into the *Hind*III site of pFB-VP7mt200, was selected. This intermediate mt200/VP2 chimera was completely restricted with *Xba*I and partially restricted with *Eco*R1 for 1h using 2-3 μg of DNA. The enzymes were heat-inactivated at 65 °C for 15 min and the ends filled up using Klenow DNA polymerase and 50 μM dNTPs (section 3.2.1.1). Filling up of the overhang termini was necessary to correct the reading frame as well as to enable the ligation of two incompatible ends. The restricted fragments were separated on a 0.7% agarose gel and the approximately 6.3 kb DNA band was excised from the gel and purified by Geneclean™ extraction. The DNA was self-ligated, transformed into XL1Blue cells and plated out as above. Plasmid DNA from a large number of colonies was isolated and the covalently closed circular form compared to that of pFB-VP7mt200 before further characterisation with restriction enzyme digestions. The VP7mt200 with VP2-specific insert (mt200/TrVP2) were sequenced to confirm the segment 2 status of the insert and the correct reading frame (section 4.2.4).

The second chimera was constructed by retrieving the segment 2 specific insert from pFB-200/VP2 by *Hind*III and *Sal*I digestion in the appropriate RE buffer. The 300 bp fragment was cloned directionally into the corresponding sites of pFB-mt177 to create pFB-mt177/TrVP2.

4.2.4. Construction of recombinant pFastbacDual transfer vectors containing AHSV-9 VP3 and recombinant VP7 genes

The recombinant dual transfer vector, pFBd-S3.9-S7.9, was utilised for the cloning of the recombinant VP7 genes with VP3. The plasmid pFBd-S3.9-S7.9 was partially digested with *Bam*H1 (section 2.2.10) and completely digested with *Pst*I. The recombinant and chimeric VP7 genes were obtained by simultaneous restriction with *Bam*H1 and *Pst*I in a suitable salt buffer of plasmids pFB-mt177, pFB-mt200, pFB177/TrVP2 and pFB200/TrVP2. Ligation, transformation and selection was performed as described in section 3.2.1.1. Recombinant pFastbacDual transfer vectors were used to construct dual recombinant baculoviruses.

4.2.5. Dye terminator cycle sequencing of the VP7 insertion mutants

All sequencing reactions were done by cycle sequencing using dye-labelled terminators. Amplification of template strands was done using AmpliTaq^R DNA polymerase FS, a mutant form of Taq DNA polymerase, which has essentially no 5'□3'exonuclease activity as well as drastically reduced discrimination against incorporation of dideoxynucleotides, leading to much lower concentrations of dye-labelled terminators having to be used. AmpliTaq^R DNA polymerase FS, was supplied in the ABI PRISM™ Big Dye Terminator Cycle Sequencing Ready Reaction kit (Perkin Elmer). Kits were stored at -20°C with the dye terminator solutions being shielded from light.

4.2.5.1. Template purification and quantitation

Recombinant pFastbac1 and pBS vectors containing the desired fragments were purified using one of the following plasmid purification kits to ensure optimal quality of DNA template for automated sequencing: the Qiagen^{R} plasmid mini-kit tip 20 (Qiagen), high pure plasmid purification kit (Boehringer Mannheim), Nucleobond (Macherey-Nagel) and Wizard columns (Promega). Manufacturers instructions were followed for all plasmid purifications. All these purification methods are based on a modified alkaline lysis procedure (section 2.2.4), followed by binding of the plasmid DNA either to an anion-exchange resin under appropriate low salt and pH conditions or to the surface of glass fibres or silica materials in the presence of a chaotropic salt. In both cases the binding process is specific for nucleic acids and the bound DNA is purified from salts, proteins and other cellular impurities, prior to elution.

The quality and quantity of the DNA templates were analysed using at least two of the following three methods. A 1% analytical agarose gel comparing a dilution series of the appropriate linearised plasmid DNA with a DNA standard size marker with known concentration. Secondly, the optical density of each sample was measured spectrophotometricly at 260 nm, 280 nm and 320 nm, using a Beckman DU® 64 spectrophotometer. The concentration of the DNA was calculated from the 260 nm reading, using the extinction coefficient for dsDNA as $1A_{260}$ = 50 μg/μl, while the 260 nm to 280 nm ratio gave an indication of the purity of the sample. The reading at 320 nm is an indication of the amount of salts present in the sample. The third method is based on the measurement of the change in fluorescence characteristics of Bizbenzimide (Hoechst 33258) in the presence of DNA, using the Hoefer DyNA Quant^{TM} 200 fluorometer. Measurements were done according to the manufacturer's instructions using 2 μl of the unknown DNA sample in 2 ml of assay solution (0.1 μg/ml Hoechst in 0.2 M NaCl, 10 mM Tris-HCL, 1 mM EDTA, pH 7.4). The final concentration was determined using the formula for a straight line (y = mx + b).

4.2.5.2. Cycle sequencing reactions

For PCR based cycle sequencing reaction, 3.2 pmole of the polyhedrin-specific primers or VP7-specific primers were used, together with 250 ng double-stranded template, 8 μl of the Terminator Ready Reaction mix and the reaction volume made up to 20 μl with ddH_2O. Half reactions with the same amount of template and primer were also successfully used. All thermal cycle reactions were done in an ABI termal cycler 9600 with heated lid, obviating the need for light mineral oil overlays. A rapid thermal ramp to 96°C was followed by incubation at 96°C for 10 sec, rapid cooling ramp to 50°C for annealing, rapid thermal ramp to 60°C and continued incubation at 60°C for 4 min to enable primer extension. This cycle was repeated 25 times, followed by rapid cooling to 4°C. Excess dye terminators were removed through simplified ethanol precipitation as follows: the 20 μl PCR reaction was added to 16 μl ddH_2O and 64 μl 98% ethanol in a clean tube, with the solution containing no salts. The DNA fragments were precipitated for 10 min at room temperature and centrifuged for 25 min in a microfuge. The pellet was rinsed with 70% ethanol, repelleted and air-dried.

4.2.5.3. ABI PRISM^{TM} Sequencing

All sequencing reactions were analysed using an ABI PRISM 377 sequencer. Dried samples were resuspended in 3.0 μl sequencing loading buffer (5:1 ratio of deionized formamide to 25 mM EDTA pH 8.0 containing 50 mg/ml dextran blue) prior to loading. The samples were denatured by heating to 95°C for 2 min. Samples were placed on ice and 1.5 μl were loaded on a 4% denaturing polyacrylamide gel and run for 7 h at

1.6 kV. Sequences were analysed using the ABI PRISM Sequencing Analysis™ program, as well as the ABI PRISM Navigator™ program and aligned using Clustal X (Thompson *et al.*, 1994). Translated sequences were submitted to the National Centre for Biotechnology Information (NCBI) using the BLAST network server and the SwissProt database (Altschul *et al.*, 1990). Hydropathy plots of VP7, mt177 and mt200 were prepared using the ANTHEPROT package (Geourjon *et al.*, 1991; Geourjon & Deleage, 1995) and the Hopp and Woods predictive method (Hopp & Woods, 1981 & 1983).

4.2.5.4. Structural modelling

A three-dimensional model of the insertion mutant proteins was constructed using the MODELLER 4 package and a Silicon Graphics Power Indigo Extreme workstation (Sali & Blundell, 1993). The X-ray crystallographic structure of AHSV-4 VP7, obtained from Brookhaven Protein Database, was used as an initial template for model building. The models were based on an optimal alignment of the insertion mutants to the VP7 template. The homology structure was calculated by the satisfaction of spatial restraints as described by empirical databases. Structures were visualised with Rasmol (Massachusetts University).

4.2.6. Production of recombinant single and dual baculoviruses

The construction and isolation of composite bacmid DNA was done as described in sections 3.2.2 and 3.2.3, using the recombinant transfer vectors pFB-mt177, pFB-mt200, pFB177/TrVP2, pFB200/TrVP2, pFBD-S3.177, pFBD-S3.200, pFBD-S3.177/TrVP2 and pFBD-S3.200/TrVP2. Transfection was performed as in section 3.2.4 using cellfectin, recombinant viruses were plaque purified and high titered stocks prepared. Recombinant baculoviruses were designated Bac7mt177, Bac7mt200, Bac177/VP2tr and Bac200/VP2tr and dual recombinant baculoviruses Dual-VP3.177, Dual-VP3.200.

4.2.7. Synthesis and purification of the VP7 and recombinant protein complexes

S. frugiperda cells in 75 cm^3 tissue culture flasks (1 x 10^7 cells/flask) were infected with the recombinant baculoviruses BacVP7, Bac7mt177, Bac7mt200, Bac177/VP2tr or Bac200/VP2tr at a MOI of 5-10 pfu/cell. The infected cells were harvested after an incubation period of 72 h at 28°C. Subcellular fractions were then prepared essentially according to the procedures described by Chuma *et al.* (1992), Burroughs *et al.* (1994) and Basak *et al.* (1996). The infected cells were concentrated by centrifugation at 2000 rpm for 5 min at 4°C and washed twice with 1 x PBS. The cell pellets were resuspended in TNN lysis buffer (10 mM Tris-HCl pH 8.0, 150 mM NaCl containing 0.25% Nonidet P-40) at 2 x 10^7 cells per ml and incubated on ice for 15-30 min. Following homogenisation of the cell suspension by 15 strokes with a dounce homogeniser, the nuclei were removed from the cell lysate by centrifugation at 1000 rpm (160 x g) for 10 min. In order to recover the maximum amount of crude protein, the process of cell lysis and extraction of cytoplasmic fraction was repeated three times. The supernatant was then loaded onto a 40% to 70% (w/v) discontinuous sucrose gradient in 0.2 M Tris-HCl (pH 7.5-8.0). The gradients were centrifuged at 20 000 rpm for 1 h at 4°C in a SW50.1 Beckman rotor. The particulate fraction (pellet) was resuspended in 1/10 of the original fraction volume in 10 mM Tris-HCl (pH 8.0) and re-centrifuged on a self-forming CsCl gradient (density 1.32 g/ml CsCl) for >16 h at 38 000 rpm in a Beckman SW50.1 rotor. The material formed a sharp white band and was

recovered and dialysed against Tris-HCl buffer or diluted (1:4) with 0.2 M Tris-HCl (pH 8.0) and re-centrifuged at 20 000 rpm for 1 h in a Beckman SW50.1 rotor. Alternatively, the cytoplasmic fraction was loaded onto a 40% to 70% (w/v) continuous sucrose gradient and centrifuged at 12 000 rpm (13 000g) for 1h at 4°C in a SW41 Beckman rotor. The gradients were fractionated from the bottom in 12x 1 ml fractions. The fractions containing the AHSV-9 VP7, VP7 insertion mutants and VP7/VP2 chimeric proteins were pooled, diluted 4x in 10 mM Tris-HCl (pH 8.0) and the proteins recovered by centrifugation at 20 000 rpm in a SW50.1 rotor. The purity of the protein was finally checked using SDS-PAGE analysis.

4.2.8. Solubility assays and purification of recombinant VP7 proteins

Infected Sf9 cells were harvested 72 h post-infection, washed in 1 x PBS, resuspended in cold TNN lysis buffer and homogenised at 4°C. Cell debris and nuclei were then pelleted by low speed centrifugation as described above. The nuclei were then washed at least three times with TNN lysis buffer and all the cytoplasmic fractions were pooled. The cytoplasmic extract was separated into a soluble fraction and a particulate fraction by centrifugation at 5 000 rpm for 30 min at 4 °C in a Beckman J21 supercentrifuge. The VP7 protein remaining in the soluble fractions was precipitated by adding the required amount of ice-cold, saturated ammonium sulphate (in 100 mM Tris-HCL, pH 7.5) to the soluble extract to provide a final concentration of 20% (v/v). The precipitated protein was pelleted by centrifugation and resuspended in TNN buffer at 1/10 of the original volume. The particulate fraction was resuspended in TNN buffer in 1/10 of the original fraction volume and banded on a 40% to 70% continuous sucrose gradient as described above. All fractions were analysed by SDS-PAGE.

4.2.9. Analysis by scanning electron microscopy

Samples of purified VP7 specific protein were fixed in phosphate buffered 2.5% formaldehyde/0.1% glutaraldehyde at room temperature for 30 min. The fixed particulate protein samples were filtered onto a 0.2 μm nylon filter, washed three times in 0.075 M NaH_2PO_4/Na_2HPO_4 and then dehydrated by successive treatment of 30%, 50%, 70%, 90% and 100% ethanol. The treatment with 100% ethanol was repeated three times after which the filters were air-dried, mounted onto a stub and spatter coated with gold-beladium, a few atoms thick followed by a layer carbon. The stub was viewed at 5.0 kV in a Jeol scanning electron microscope.

4.2.10. Purification and analysis of CLP formation

Sf9 cells were infected at a M.O.I. of 5-10 pfu per cell with dual recombinant baculoviruses expressing AHSV-9 VP3 and the VP7 insertion mutant proteins or VP7/VP2 chimeric proteins. Cells were harvested 48 h p.i., rinsed with 1x PBS and lysed at 4°C in TNN buffer. Particles were purified by sucrose gradient centrifugation as described in section 3.2.5.2. CLPs were analysed by SDS-PAGE and examined by electron microscopy after resuspension in 150 mM NaCl, 0.1 M Tris-HCL pH 8.0.

4.3. RESULTS

4.3.1. Molecular structure modelling of the VP7 protein

Hydropathic profile analysis of VP7 (*Figure 4.1*) indicates that the amino-terminal region of VP7 is considerably less hydrophobic than the carboxy terminus, while the central region of the VP7 amino acid sequence (residues 120 - 249), which represents the top domain of VP7, displayed alternating hydrophilic and hydrophobic stretches. Mapping the hydrophobicity plots to the solvent-accessible surface of AHSV VP7, has shown the presence of at least one large and three smaller hydrophilic regions, of four to eight amino acids, which are prominent in the middle domain of the VP7 amino acid sequence. The four linear hydrophilic domains most accessible to the aqueous environment of the VP7 protein are amino acids 141 to 146, 167 to 178, 196 to 201 and amino acids 237 to 242 (*Figure 4.1*). Secondary structure predictions of VP7 indicated that these hydrophilic domains are located in β-turns between the β-sheet structures, characteristic of the amino acid region 120 and 250. These domains could be suitable targets for the insertion of short, foreign, immunogenic peptides. A model of the three-dimensional structure of VP7 was obtained with the RASMOL computer program to identify amino acids located on the surface of the VP7 trimer (*Figure 4.2*). From the available crystallographic data, the four linear hydrophilic regions are located on the surface of the trimeric VP7 molecule when the hydrophobicity plots are compared to the surface structure of the VP7 trimers. Three of the four hydrophilic regions, which are optimally located and accessible on the surface of the top domain of AHSV VP7 trimeric molecule, are indicated (*Figure 4.2*). The first hydrophilic region is located between amino acids 141 to 146 (144 to 145 best possible position), the second between amino acids 163 to 180 (best location 177 to 178) and the third between 196 and 201 (best location between 200 to 201) and the last site at position 237 to 242. The last site is not very accessible on the surface. The two most promising sites were found to be 177 - 178 and 200 - 201. The arginine at position 178 forms part of a RGD motif, which is located on a highly flexible loop which stretches from amino acid 175 to 180 and represents an ideal site for the insertion of peptides, since it loops out and is exposed on the surface of VP7. These two sites were therefore targeted for modification to facilitate the insertion of antigenic determinants.

In order to enable the insertion of small peptides into these target sites, it was necessary to introduce unique restriction enzyme sites in the VP7 nucleotide sequence corresponding to the two hydrophilic regions. As a first step the sites were modified by the insertion of three restriction enzyme sites, *Hind*III, *Xba*I and *Sal*I that are absent in the VP7 gene of AHSV-9. *Hind*III, *Xba*I and *Sal*I, encode lys-leu (AAGCTT), ser-arg (TCTAGA) and val-asp (GTCGAC), respectively. The amino acids encoded by the 18 nucleotides are either hydrophilic (positive, e.g. K and R, or negatively, e.g. D, charge) or neutral (e.g. L, S and V), which it is assumed will have little or no influence on the structure of VP7. The effect of the six inserted amino acids on the solubility, trimer formation and the structure of the VP7 crystals were investigated.

Figure 4.1: Hydrophilicity (a) and antigenicity profiles (b) of AHSV-9 VP7 in comparison with the predicted solvent-accessiblity (c). Hydrophilicity and antigenicity was predicted according to Hopp & Woods (1981) and Welling *et al.* (1989), respectively. Areas with positive values have a nett hydrophilicity while areas with negative values have a nett hydrophobicity.

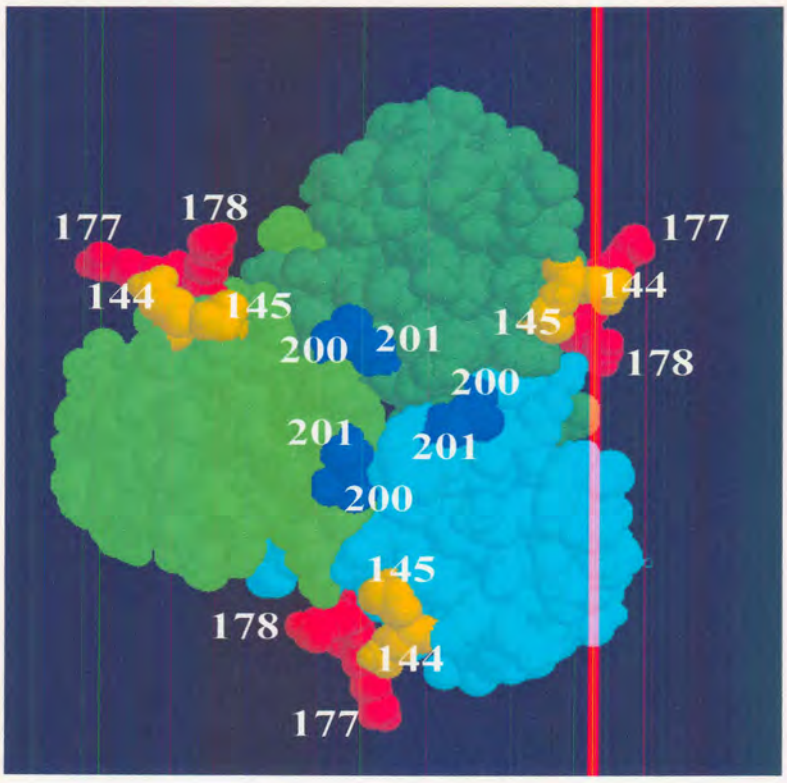

Figure 4.2: A schematic representation of the three-dimensional structure of AHSV VP7 trimer, looking vertically into the top of the trimer. The three VP7 monomers are highlighted in light blue, light green and dark green. The tripeptide RGD (residues 177-179) is highlighted in red. Two other hydrophilic regions, exposed to the surface of the trimer are amino acid residues 199 - 201 (dark blue) and 143 - 145 (orange). The red and dark blue sites were targeted for modifications and insertions.

4.3.2. Construction of recombinant baculovirus transfer vectors containing the mutagenised DNA copies of the VP7 gene

An insertion of the 6 amino acids encoded by the 18 nucleotides of the three unique restriction enzyme sites was introduced in the correct reading frame between nucleotides 548 to 549 (codons 177 to 178) and nucleotides 617 to 618 (codons 200 to 201), respectively, using two different PCR methods. In one of these methods (*Figure 4.3*) two synthetic oligonucleotide primers were designed in inverted tail-to-tail directions and used in combination with the 5' and 3' external VP7 specific primers (table 4.1). The two sets of mutagenic primers contained nucleotides at their 3' ends, which were identical or complementary to the coding sequence of the VP7 gene, which flanked the sequence where the insertion was to be introduced. In addition, the 14 nucleotide extended 5' ends of the primers specified two unique restriction enzyme sites, namely *Hind*III and *Xba*I for the reverse primers and *Sal*I and *Xba*I for the forward primers, along with two clamp bases. The choice of the three sites was motivated by the observation that the AHSV-9 VP7 gene does not contain these restriction enzyme sites. This allows for the rapid and cost-effective insertion of sequences encoding for foreign epitopes, as well as for easy screening of the resulting recombinant plasmids.

Amplification with the two sets of primers resulted in DNA fragments of expected sizes of 590 bp and 550 bp in the case of the mt177 mutagenic primers and 620 bp and 520 bp using the mt200

mutagenic primers (*Figure 4.4 A*). The sizes of the amplified PCR products were in agreement with the size predicted from the VP7 sequence. The PCR products were cloned into the pMosBlue T-vector. Restriction of recombinants with *Bgl*II and *Xba*I, which cut at opposite ends of the PCR products, excised fragments of the same size as the amplified fragments described above, and the orientation of the insert was determined by *Sac*I digestion followed by agarose gel electrophoresis of the restriction fragments (data not shown). The 177/5', 177/3' and 200/5' fragments were in the T7 orientation while 200/3' were in the SP6 orientation in the recombinant pMosBlue vectors. The full-length mutagenised VP7 genes were constructed in pFastbacI transfer vector by a two step cloning procedure. In the first step the 5' fragment of each VP7 insertion mutant (177/5' and 200/5') were recovered by *Bgl*II and *Xba*I digestion and cloned directionally into the *Bam*H1 and *Xba*I sites of the bacmid transfer vector, pFastbac1, to create the pFB-177/5' and pFB-200/5' intermediates (*Figure 4.3*). Recombinant plasmids were selected from which ca. 490 bp or 520 bp fragments were excised with *Bam*H1 and *Xba*I digestion, in the case of insertion mutant 177 and 200, respectively. In the second step the 3' end of the insertion mutant 177 was recovered by *Xba*I and *Kpn*I digestion, while the 3' end in the case of mutant 200 was recovered by only *Xba*I digestion because of difference in orientation. The 3' end of insertion mutant 177 was cloned by directional cloning into the *Xba*I and *Kpn*I site of the recombinant pFB-177/5' intermediate, which resulted in the loss of the largest part of the multiple cloning site of pFastbac1 except for the *Kpn*I and *Hind*III sites. Recombinant plasmids that displayed the full-length VP7 gene, containing the three restriction enzyme sites, were selected following restriction enzyme mapping with *Bam*H1, *Sal*I, *Sac*I and *Hind*III individually or in combinations. One such clone was selected, designated pFB-mt177 (*Figure 4.4 B*). Since the *Hind*III site present in the vector would complicate future cloning into the mutant 177 gene, the *Hind*III site in the vector was deleted by partial digestion with *Hind*III, filling up of the overhangs with Klenow, self-ligation and restriction enzyme mapping as described above. The 3' end of insertion mutant 200 was cloned into the dephosphorylated *Xba*I site of pFB-200/5' intermediate. Recombinant plasmids with the 3' end in the correct orientation were identified by restriction enzyme mapping with *Sac*I and *Sal*1-*Sma*I combination. A recombinant which yielded fragments of the expected sizes was selected and designated pFB-mt200 (*Figure 4.4 C*). The *Xba*I and *Hind*III sites, still present in the multiple cloning site of the vector, were deleted by means of partial digestions and self-ligation of the vector. In order to verify the integrity of the desired insertions the nucleotide sequence of both VP7 specific insertion mutants were analysed by automated dideoxynucleotide sequencing.

In the second method (*Figure 4.5*) the site-directed insertion mutagenesis was performed in a one step PCR process, in which the amplification was carried out using the two synthetic mutagenic primers which were designed in an inverted tail-to-tail direction (table 4.1). Using the cloned copy of the full-length VP7 gene in pBS322 (pBS-S7PCR) as template and the primers and PCR reaction conditions described in section 4.2.2, a major DNA band of approximately 4.3 kb was synthesised for each insertion mutant. The size of the amplified PCR product was in agreement with the size

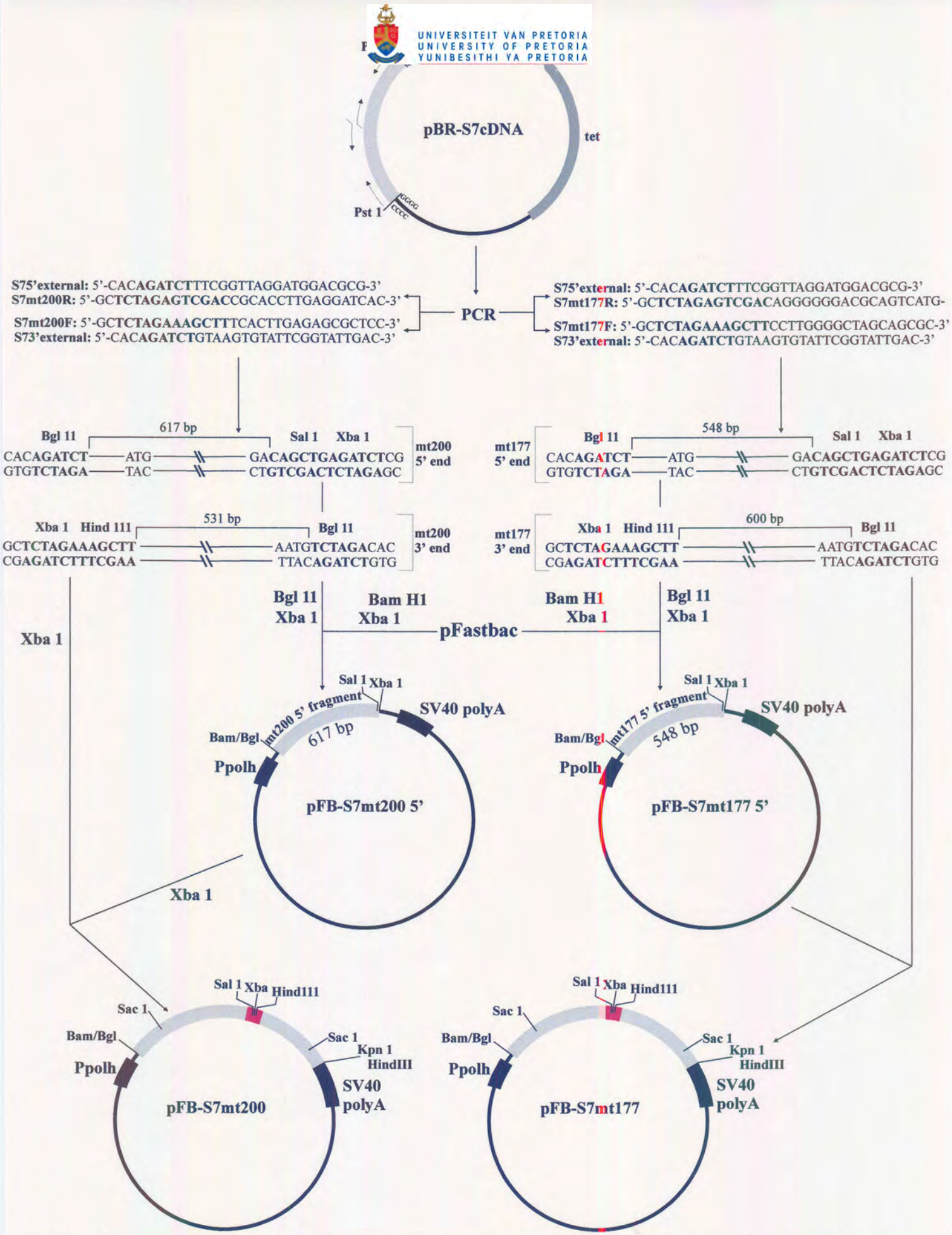

Figure 4.3 Schematic representation of the first PCR method used to construct the recombinant transfer vectors containing the mutagenised DNA copies of the VP7 gene. In this method two oligonucleotide primers were designed in inverted tail-to-tail directions and used in combination of the 5' and 3' external VP7 specific primers.

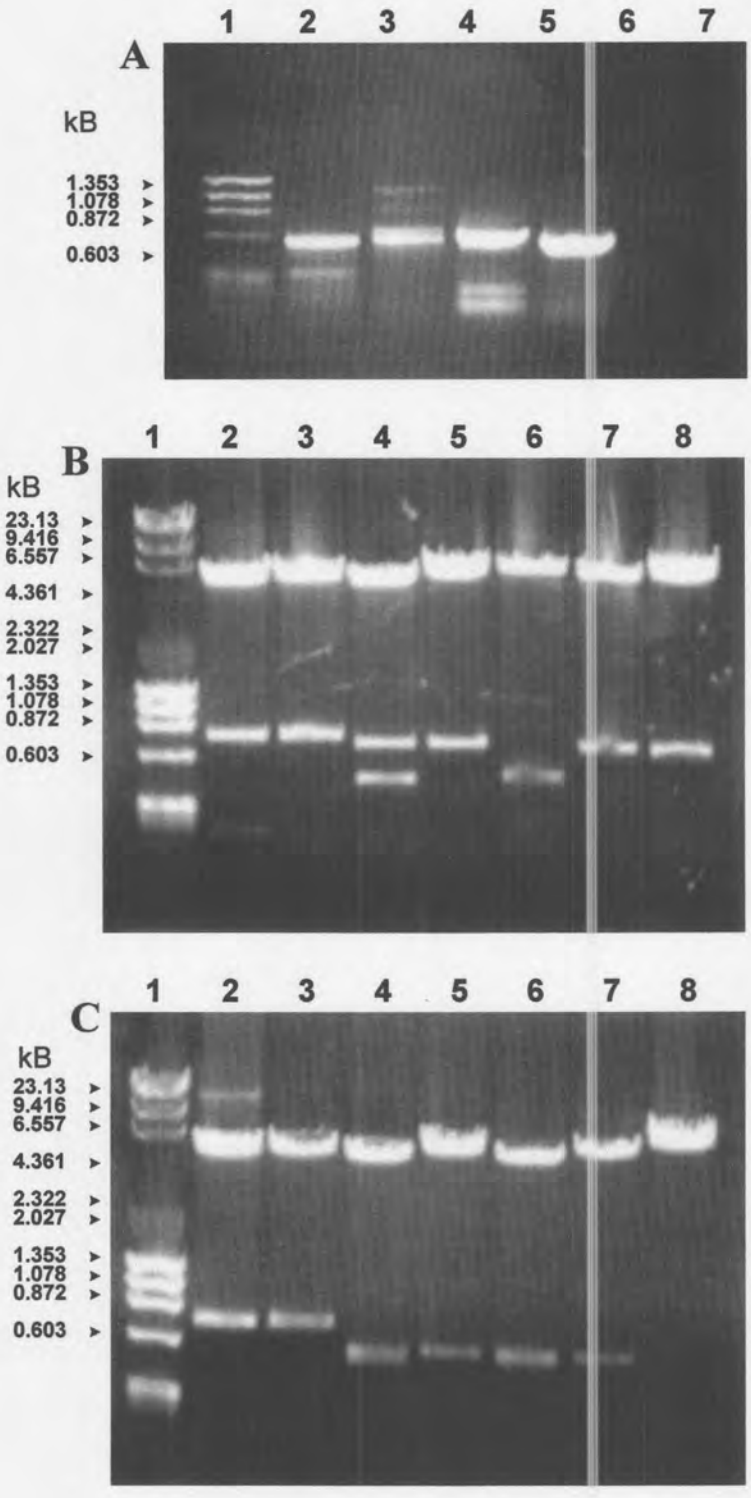

Figure 4.4: (A) Agarose gel electrophoretic analysis of the DNA products obtained by PCR amplification of the AHSV-9 VP7 gene (pBR-S7cDNA), using two inverted tail-to-tail mutagenic primers in combination with VP7 5' and 3' end specific primers. Lane 1 represents HaeIII digested ϕx174 DNA and the relevant sizes are indicated to the left of the figure. Lanes 2 and 3 shows the PCR amplified products of the 5' end and 3' end of VP7 using the primers for insertion mutant 177. Lanes 4 and 5 contain the products of the 5' and 3' ends of VP7 using insertion mutant 200 reverse and forward primers, respectively. Lanes 6 and 7 represents negative controls, containing primers but no template. (B and C) Agarose gel electrophoretic analysis of the recombinant pFastbac plasmids constructed by the cloning of the two PCR DNA fragments of each insertion mutant to generate two full length mutagenised VP7 genes. The derived recombinant plasmids pFB-mt177 (B) and pFB-mt200 (C) were restricted with *Sac*I (lane 3), *Hind*III/*Bam*H1 (lane 4), *Hind*III (lane 5), *Bam*H1/*Sal*I (lane 6), *Sal*I/*Kpn*I (lane 7) and *Xba*I (lane 8). Lane 1 include molecular weight markers MWII and ϕx174 DNA. *Sac*I digested pBS-S7PCR (lane 2) was included as an additional size marker.

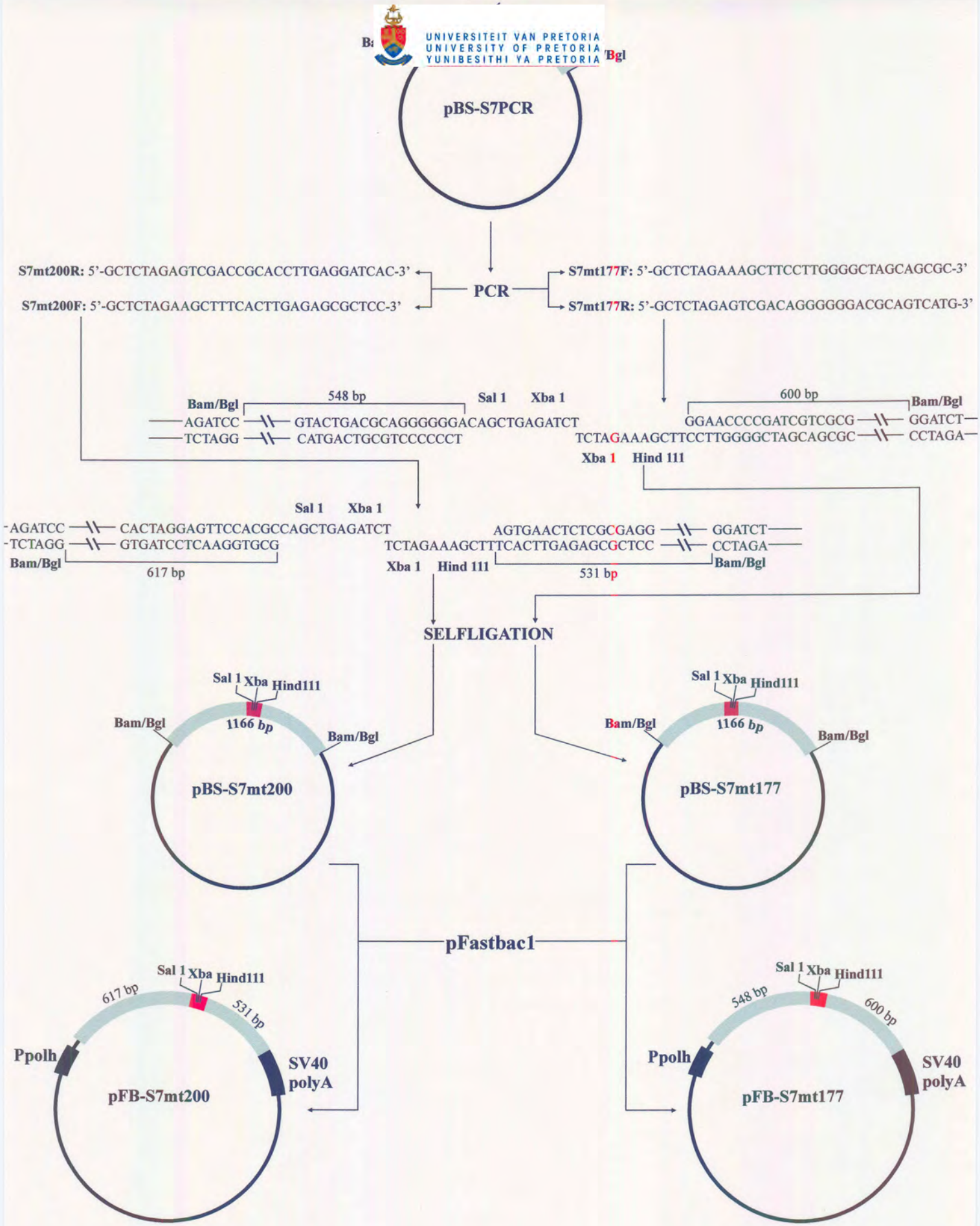

Figure 4.5 In the second method used for insertion mutagenesis the insertion was performed in a one step PCR process. The amplification was carried out using two primers designed in an inverted tail-to-tail direction, tagged at their 5' ends with the chosen R.E. sites.

predicted for the cloning vector (3.2 kb) together with the mutagenised VP7 gene (ca. 1.15 kb). The identity of the purified 4.3 kb PCR product was confirmed by restriction with *Sac*I, which is known to cut twice in VP7 at nucleotide position 200 and 1045. Three fragments of 350 bp, 500 bp and 3.4 kb for mt177 and 410 bp, 440 bp and 3.4 kb for mt200, characteristic of VP7, were generated for each insertion mutant PCR product. Since each of the mutagenic flanking primers contained *Xba*I linker sequences, the purified PCR products were digested with *Xba*I and subsequently self-ligated. Restriction of both insertion mutants (pMt177 and pMt200) with *Bam*H1 (ca. 100 bp from 5' end of VP7) and *Eco*R1 (only cut in MCS) excised a fragment approximately 100 bp smaller than that of the wild-type VP7 gene copy. Restriction with *Hind*III, and *Sal*I generated fragments of approximately 600 bp and 520 bp for mutants 177 and 200 respectively. These results indicate that insertion of the three unique restriction enzyme sites into the VP7 gene was successful at both domains selected. The integrity of the two insertion mutations was subsequently verified by automated dye terminator cycle sequencing.

The mutagenised VP7 genes were excised from pMt177 and pMt200 and directionally cloned into the *Eco*R1/*Kpn*I site of the pFastbac vector, which resulted in the removal of the largest part of the MCS of the vector. Recombinant plasmids from which ca. 850 bp fragments were excised by *Sac*I digestion, were selected for further restriction enzyme analysis. Clones that displayed the correct transcriptional orientation were selected following restriction enzyme mapping with *Hind*III, which recognises a site in the MCS of the vector and cuts asymmetrically in both insertion mutants 550 bp and 620 bp from the 5' end of InM177 and InM200, respectively. One representative clone was selected for each insertion mutant and designated pFB-Mt177 and pFB-Mt200.

4.3.3. Sequence verification and molecular modelling of the modified VP7 proteins

The sequences of the recombinant VP7 clones in pFastbac1 were confirmed by automated nucleotide sequencing. No nucleotide alterations other than the specified insertions were observed in the VP7 mutant genes, constructed using both strategies (*Figure 4.6*). Therefore, pFB-mt177 and pFB-mt200 were utilised in subsequent cloning procedures and for expression. Analysis of the electropherograms indicated that the 18 nucleotides, encoding the 6 amino acids K L S R V D were inserted. The correct reading frame of the insertional genes was verified by translation of the sequences and comparing them with the original VP7 amino acid sequence (*Figure 4.7*).

The hydropathic profiles of VP7mt177 and VP7mt200 deduced amino acid sequences were compared to that of AHSV-9 VP7. Although the profiles were identical in the unmodified regions of the three proteins as will be expected, the regions of the insertional mutants, which were targeted during mutagenesis, showed an increase in hydrophilicity (*Figure 4.8*), which also differed between the two insertion mutants. The insertion of the six amino acids between amino acids 177 and 178 of

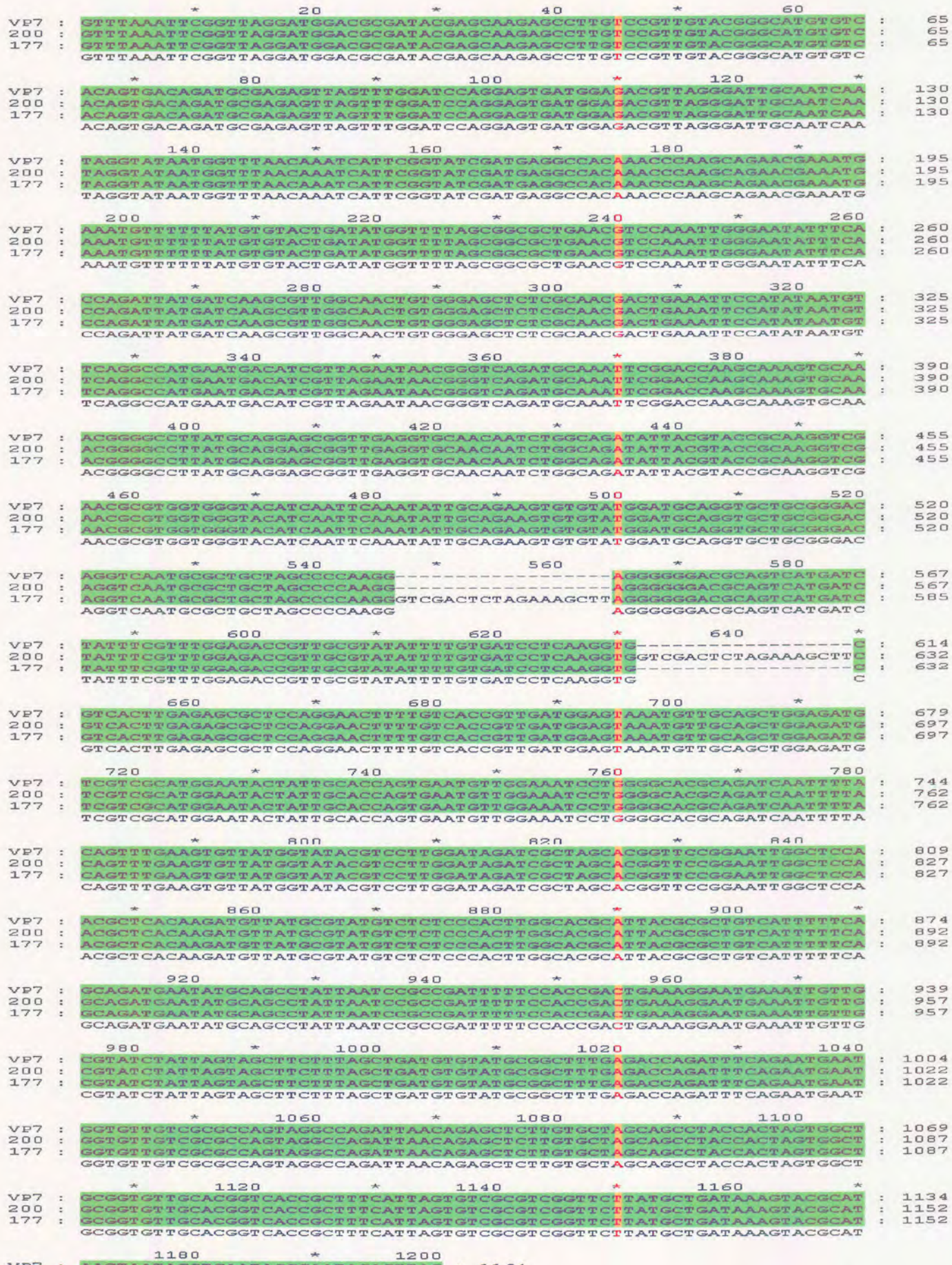
VP7 : GTTTAAATTCGGTTAGGATGGACGCGATACGAGCAAGAGCCTTGTCCGTTGTACGGGCATGTGTC : 65
200 : GTTTAAATTCGGTTAGGATGGACGCGATACGAGCAAGAGCCTTGTCCGTTGTACGGGCATGTGTC : 65
177 : GTTTAAATTCGGTTAGGATGGACGCGATACGAGCAAGAGCCTTGTCCGTTGTACGGGCATGTGTC : 65
VP7 : ACAGTGACAGATGCGAGAGTTAGTTTGGATCCAGGAGTGATGGAGACGTTAGGGATTGCAATCAA : 130
200 : ACAGTGACAGATGCGAGAGTTAGTTTGGATCCAGGAGTGATGGAGACGTTAGGGATTGCAATCAA : 130
177 : ACAGTGACAGATGCGAGAGTTAGTTTGGATCCAGGAGTGATGGAGACGTTAGGGATTGCAATCAA : 130
VP7 : TAGGTATAATGGTTTAACAAATCATTCGGTATCGATGAGGCCACAAACCCAAGCAGAACGAAATG : 195
200 : TAGGTATAATGGTTTAACAAATCATTCGGTATCGATGAGGCCACAAACCCAAGCAGAACGAAATG : 195
177 : TAGGTATAATGGTTTAACAAATCATTCGGTATCGATGAGGCCACAAACCCAAGCAGAACGAAATG : 195
VP7 : AAATGTTTTTTTATGTGTACTGATATGGTTTTAGCGGCGCTGAACGTCCAAATTGGGAATATTTCA : 260
200 : AAATGTTTTTTTATGTGTACTGATATGGTTTTAGCGGCGCTGAACGTCCAAATTGGGAATATTTCA : 260
177 : AAATGTTTTTTTATGTGTACTGATATGGTTTTAGCGGCGCTGAACGTCCAAATTGGGAATATTTCA : 260
VP7 : CCAGATTATGATCAAGCGTTGGCAACTGTGGGAGCTCTCGCAACGACTGAAATTCCATATAATGT : 325
200 : CCAGATTATGATCAAGCGTTGGCAACTGTGGGAGCTCTCGCAACGACTGAAATTCCATATAATGT : 325
177 : CCAGATTATGATCAAGCGTTGGCAACTGTGGGAGCTCTCGCAACGACTGAAATTCCATATAATGT : 325
VP7 : TCAGGCCATGAATGACATCGTTAGAATAACGGGTCAGATGCAAATTCGGACCAAGCAAAGTGCAA : 390
200 : TCAGGCCATGAATGACATCGTTAGAATAACGGGTCAGATGCAAATTCGGACCAAGCAAAGTGCAA : 390
177 : TCAGGCCATGAATGACATCGTTAGAATAACGGGTCAGATGCAAATTCGGACCAAGCAAAGTGCAA : 390
VP7 : ACGGGGCCTTATGCAGGAGCGGTTGAGGTGCAACAATCTGGCAGATATTACGTACCGCAAGGTCG : 455
200 : ACGGGGCCTTATGCAGGAGCGGTTGAGGTGCAACAATCTGGCAGATATTACGTACCGCAAGGTCG : 455
177 : ACGGGGCCTTATGCAGGAGCGGTTGAGGTGCAACAATCTGGCAGATATTACGTACCGCAAGGTCG : 455
VP7 : AACGCGTGGTGGGTACATCAATTCAAATATTGCAGAAGTGTGTATGGATGCAGGTGCTGCGGGAC : 520
200 : AACGCGTGGTGGGTACATCAATTCAAATATTGCAGAAGTGTGTATGGATGCAGGTGCTGCGGGAC : 520
177 : AACGCGTGGTGGGTACATCAATTCAAATATTGCAGAAGTGTGTATGGATGCAGGTGCTGCGGGAC : 520
VP7 : AGGTCAATGCGCTGCTAGCCCCAAGG----------AGGGGGGACGCAGTCATGATC : 567
200 : AGGTCAATGCGCTGCTAGCCCCAAGG----------AGGGGGGACGCAGTCATGATC : 567
177 : AGGTCAATGCGCTGCTAGCCCCAAGGGTCGACTCTAGAAAGCTTAGGGGGGGACGCAGTCATGATC : 585
VP7 : TATTTCGTTTGGAGACCGTTGCGTATATTTTGTGATCCTCAAGGTC----------C : 614
200 : TATTTCGTTTGGAGACCGTTGCGTATATTTTGTGATCCTCAAGGTGGTCGACTCTAGAAAGCTTC : 632
177 : TATTTCGTTTGGAGACCGTTGCGTATATTTTGTGATCCTCAAGGTG----------C : 632
VP7 : GTCACTTGAGAGCGCTCCAGGAACTTTTGTCACCGTTGATGGAGTAAATGTTGCAGCTGGAGATG : 679
200 : GTCACTTGAGAGCGCTCCAGGAACTTTTGTCACCGTTGATGGAGTAAATGTTGCAGCTGGAGATG : 697
177 : GTCACTTGAGAGCGCTCCAGGAACTTTTGTCACCGTTGATGGAGTAAATGTTGCAGCTGGAGATG : 697
VP7 : TCGTCGCATGGAATACTATTGCACCAGTGAATGTTGGAAATCCTGGGGCACGCAGATCAATTTTA : 744
200 : TCGTCGCATGGAATACTATTGCACCAGTGAATGTTGGAAATCCTGGGGCACGCAGATCAATTTTA : 762
177 : TCGTCGCATGGAATACTATTGCACCAGTGAATGTTGGAAATCCTGGGGCACGCAGATCAATTTTA : 762
VP7 : CAGTTTGAAGTGTTATGGTATACGTCCTTGGATAGATCGCTAGCACGGTTCCGGAATTGGCTCCA : 809
200 : CAGTTTGAAGTGTTATGGTATACGTCCTTGGATAGATCGCTAGCACGGTTCCGGAATTGGCTCCA : 827
177 : CAGTTTGAAGTGTTATGGTATACGTCCTTGGATAGATCGCTAGCACGGTTCCGGAATTGGCTCCA : 827
VP7 : ACGCTCACAAGATGTTATGCGTATGTCTCTCCCACTTGGCACGCATTACGCGCTGTCATTTTTCA : 874
200 : ACGCTCACAAGATGTTATGCGTATGTCTCTCCCACTTGGCACGCATTACGCGCTGTCATTTTTCA : 892
177 : ACGCTCACAAGATGTTATGCGTATGTCTCTCCCACTTGGCACGCATTACGCGCTGTCATTTTTCA : 892
VP7 : GCAGATGAATATGCAGCCTATTAATCCGCCGATTTTTCCACCGACTGAAAGGAATGAAATTGTTG : 939
200 : GCAGATGAATATGCAGCCTATTAATCCGCCGATTTTTCCACCGACTGAAAGGAATGAAATTGTTG : 957
177 : GCAGATGAATATGCAGCCTATTAATCCGCCGATTTTTCCACCGACTGAAAGGAATGAAATTGTTG : 957
VP7 : CGTATCTATTAGTAGCTTCTTTAGCTGATGTGTATGCGGCTTTGAGACCAGATTTCAGAATGAAT : 1004
200 : CGTATCTATTAGTAGCTTCTTTAGCTGATGTGTATGCGGCTTTGAGACCAGATTTCAGAATGAAT : 1022
177 : CGTATCTATTAGTAGCTTCTTTAGCTGATGTGTATGCGGCTTTGAGACCAGATTTCAGAATGAAT : 1022
VP7 : GGTGTTGTCGCGCCAGTAGGCCAGATTAACAGAGCTCTTGTGCTAGCAGCCTACCACTAGTGGCT : 1069
200 : GGTGTTGTCGCGCCAGTAGGCCAGATTAACAGAGCTCTTGTGCTAGCAGCCTACCACTAGTGGCT : 1087
177 : GGTGTTGTCGCGCCAGTAGGCCAGATTAACAGAGCTCTTGTGCTAGCAGCCTACCACTAGTGGCT : 1087
VP7 : GCGGTGTTGCACGGTCACCGCTTTCATTAGTGTCGCGTCGGTTCTTATGCTGATAAAGTACGCAT : 1134
200 : GCGGTGTTGCACGGTCACCGCTTTCATTAGTGTCGCGTCGGTTCTTATGCTGATAAAGTACGCAT : 1152
177 : GCGGTGTTGCACGGTCACCGCTTTCATTAGTGTCGCGTCGGTTCTTATGCTGATAAAGTACGCAT : 1152
VP7 : AAGTAATACGTCAATACCGAATACACTTAC : 1164
200 : AAGTAATACGTCAATACCGAATACACTTAC : 1182
177 : AAGTAATACGTCAATACCGAATACACTTAC : 1182

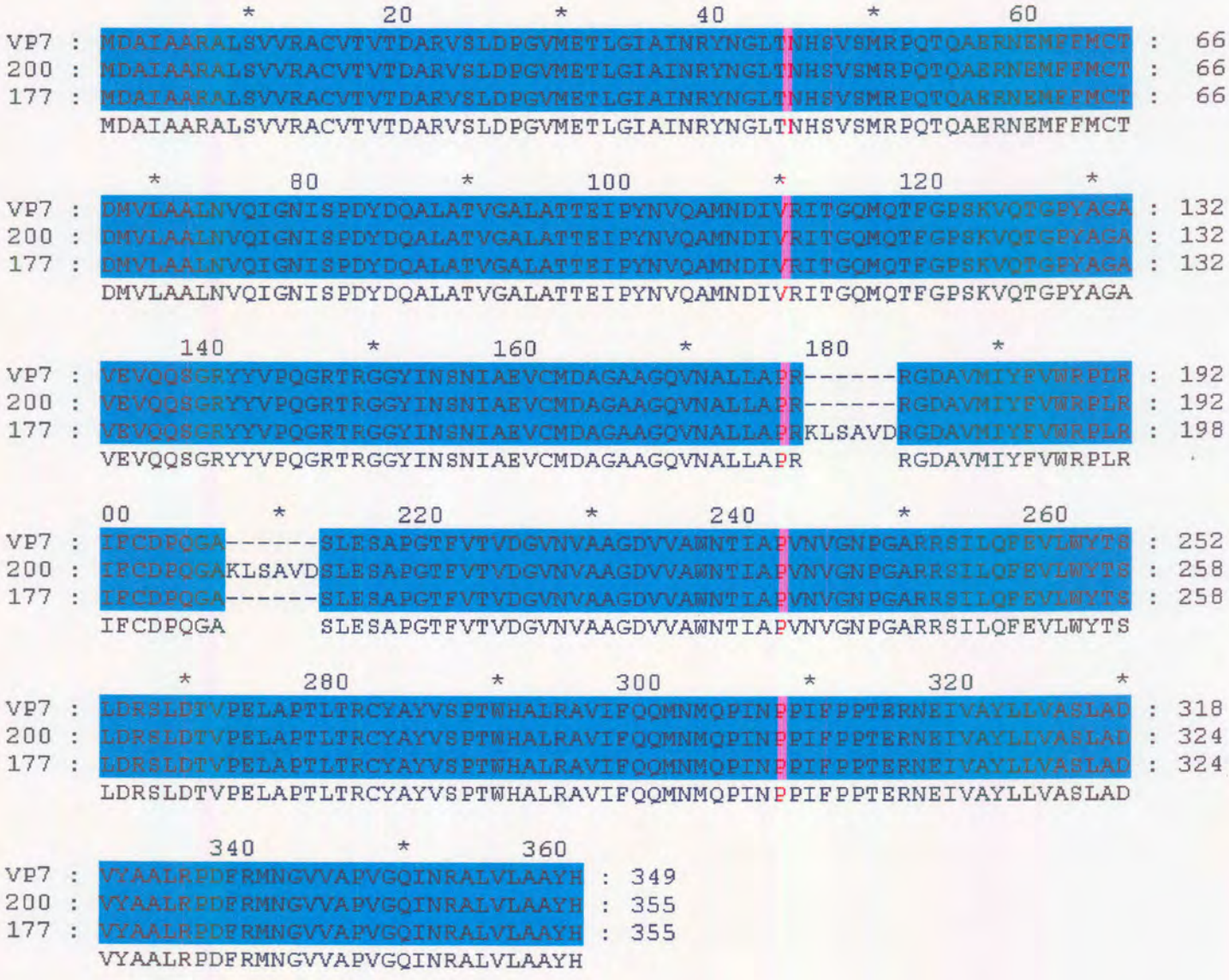

Figure 4.6: (Previous page) Alignment of the nucleotide sequences of the two insertion mutants mt177 and mt200 with the VP7 gene. No nucleotide alterations were found other than the 18 nucleotides inserted by means of PCR-directed site-directional insertional mutation.

Figure 4.7: Comparison of the deduced amino acid sequences of VP7 and insertion mutants 177 and 200. The extra six amino acids, as a result of the insertion of the three restriction enzyme sites, in the two chosen hydrophilic sites in the top domain of VP7 are visible. The rest of the amino acid sequences are identical.

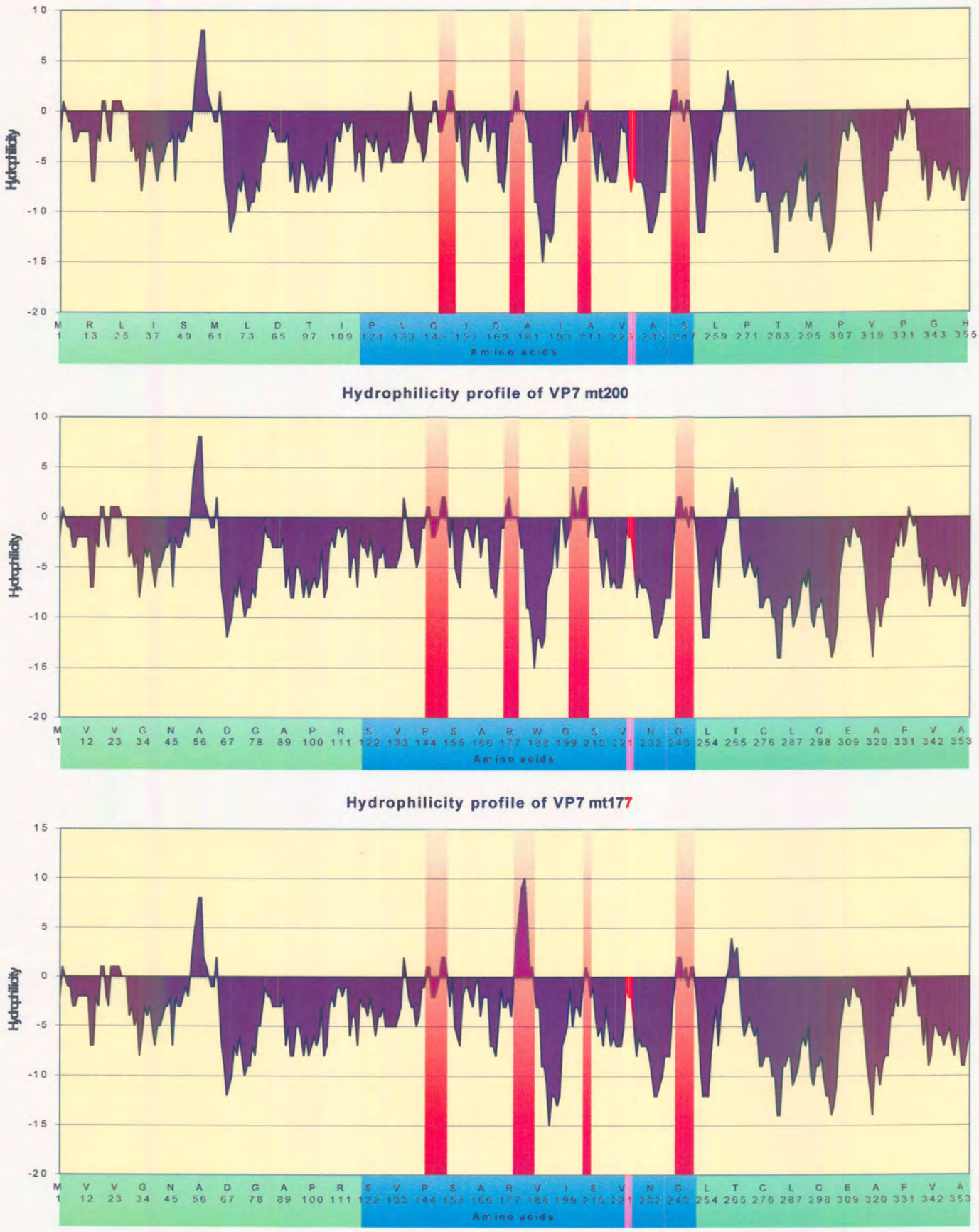

Figure 4.8: Comparison of the hydrophilicity profiles of AHSV-9 VP7 with that of the two insertion mutants mt177 and mt200. Hydrophilicity was predicted according to Hopp & Woods (1981) utilising the ATHEPROT computer program. Areas with positive values have a nett hydrophilicity while areas with negative values have a nett hydrophobicity.

VP7 resulted in a large increase in hydrophilicity of at least 5 times that of normal VP7 (from 2 to 10), in that area. The insertion of the same six amino acids between amino acid 200 and 201 resulted in a mild increase in hydrophilicity from 2 to 4.

A model of the three-dimensional structure of VP7mt177 and VP7mt200 was prepared using a homology-based method incorporating the satisfaction of spatial restraints. The MODELLER package generates a model of the new protein using a known three-dimensional structure together with a sequence alignment, in this case with AHSV-4 VP7 (*Figure 4.9*). The modelled structure of both VP7mt177 and VP7mt200 monomers shows a backbone conformation (green and red respectively) identical to VP7. The six extra amino acids in position 177-178 and 200-201 looped out of the VP7 backbone, facing the aqueous environment. This indicated that the extra amino acids would probably not influence the structure of the modified VP7 proteins, by preventing the hydrophobic associations necessary to form the VP7 3-D structure (represented in *Figure 4.9*).

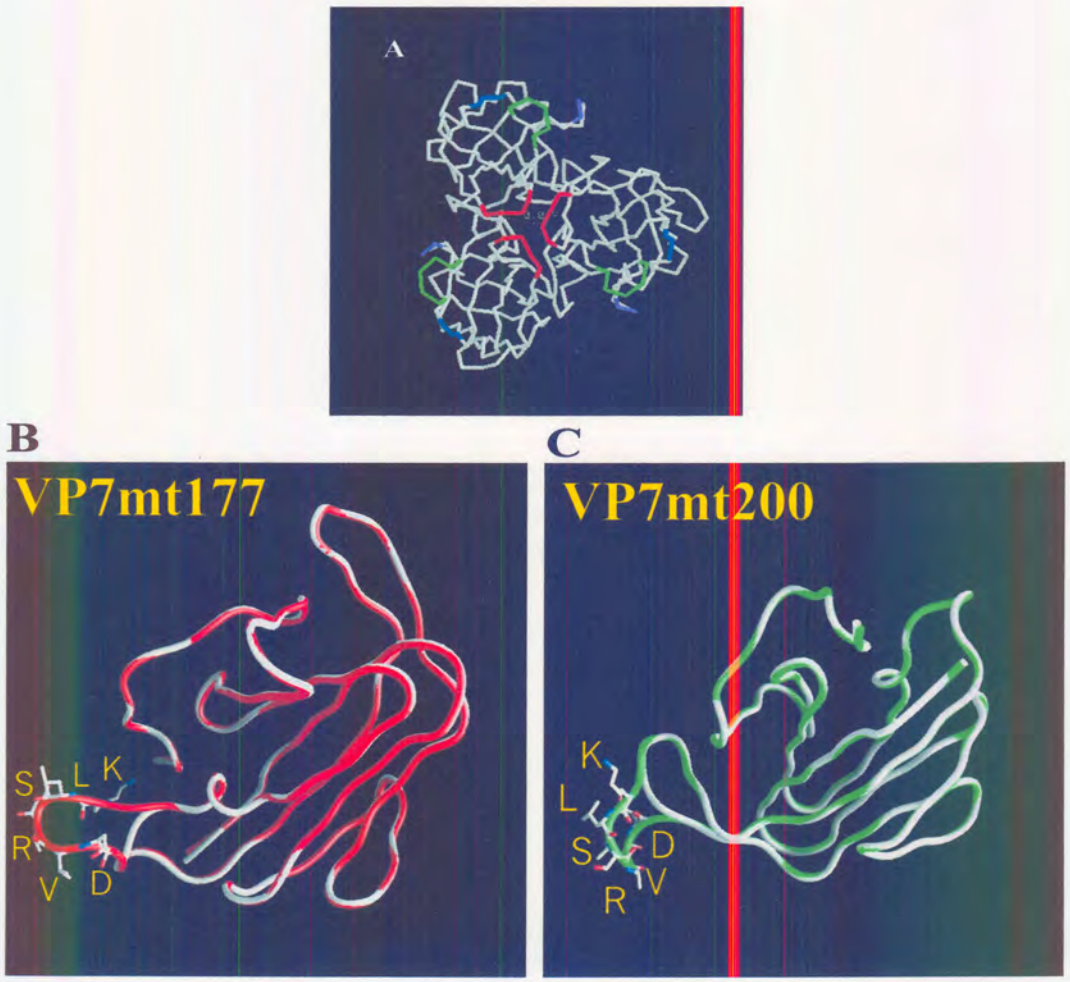

Figure 4.9: A schematic representation of the structure of the insertion mutants mt177 (B) and mt200 (C) monomers as predicted by the MODELLER package. The carbon-a traces of mt177(red) and mt200 (green) in comparison with VP7 (white) is shown. The side chains of the six inserted amino acids are indicated by fine lines and are shown to loop out of the surface of the two proteins. The assembly of the mutagenised VP7 monomers into trimers is shown in (A) with the 177 insertion indicated in green and the 200 insertion in red.

4.3.4. The construction of dual recombinant baculovirus transfer vectors containing AHSV-9 VP3 in combination with VP7mt177 and VP7mt200

The VP3-VP7 dual recombinant transfer vector constructed in chapter 3 (3.2.2.1), pFBd-S3.9-S7.9, was utilised for the cloning of the modified VP7 genes with VP3. The pFBd-S3.9-S7.9 vector was partially digested with *Bam*H1, to obtain restriction at the *Bam*H1 site located 100 bp from the 5' end of the VP7 gene, but not at the second *Bam*H1 site within the VP3 gene. After linearisation, the *Bam*H1 was removed by column purification and the plasmid was completely digested with *Pst*I, which cuts once in the vector downstream of the VP7 gene. The 8.1 kb fragment, containing the vector, the complete VP3 gene and 100 bp from the VP7 gene, was recovered through gel purification. The plasmids, pFB-mt177 and pFB-mt200 were completely digested with *Bam*H1 (cuts at ca.100 bp from 5' end) and *Pst*I (cuts in MCS) and the 1.0 kb and 1.9 kb fragments, respectively, recovered after gel purification. The recombinant VP7 *Bam*H1-*Pst*I fragments were directionally cloned into the corresponding sites of pFBd-S3.9-S7.9. Plasmids yielding 850 bp and 8.3 kb fragments after *Sac*I digestion contained the full-length VP7 insertion mutant genes (*Figure 4.10*). Recombinant plasmids were selected and called pFBd-S3.9-177 and pFBd-S3.9-200.

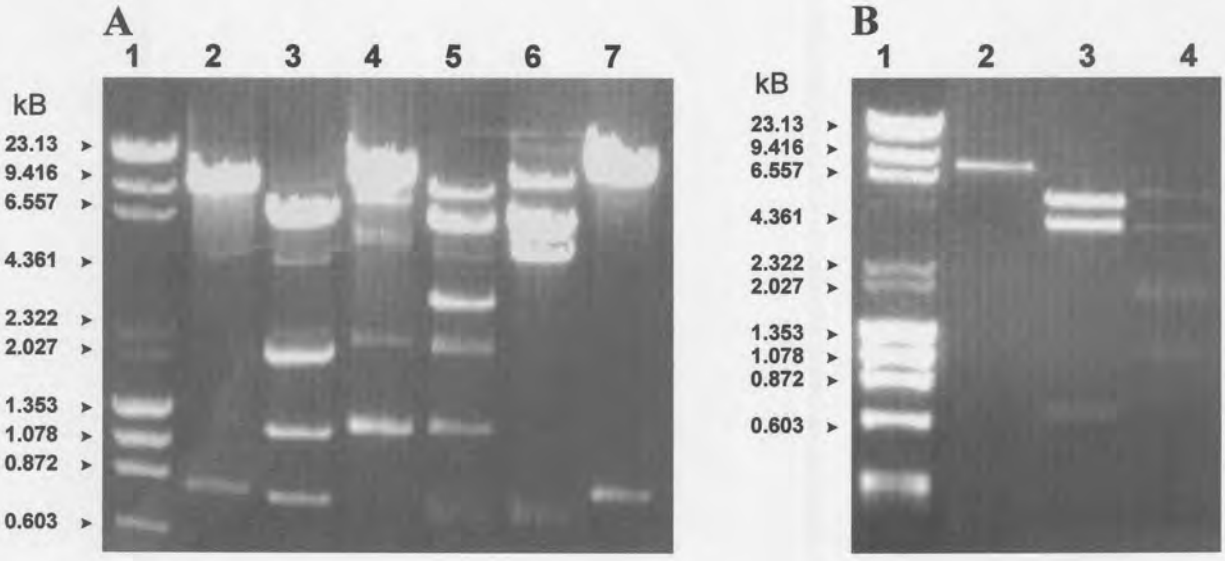

Figure 4.10: Agarose electrophoretic analysis of pFBd-S3.9-mt177 and pFBd-S3.9-mt200. (A) pFBd-S3.9-mt177, containing the AHSV-9 VP3 gene under control of the p10 promoter and VP7mt177 under control of the polyhedrin promoter, was digested with *Sac*I (lane 2), *Hind*III/*Eco*R1 (lane 3), *Eco*R1/*Sal*I (lane 4), *Eco*R1/*Xba*I (lane 5) and *Bam*H1 (lane 7). (B) pFBd-S3.9-mt200 was restricted with *Sac*I (lane 2), *Xba*I (lane 3) and *Hind*III/*Eco*R1 (lane 4).

4.3.5. Baculovirus expression of the VP7 insertion mutants

4.3.5.1. Construction and selection of recombinant baculoviruses

Infectious recombinant baculoviral DNA, containing either the mt177 or the mt200 insertion mutations under control of the polyhedrin promoter, was constructed. The recombinant transfer plasmids, pFBmt177 and pFBmt200, were transposed into the bacmid genome and each transposition was verified by means of PCR. The bacmid DNA was amplified using VP7 specific 5'-terminal primer and M13 reverse primer. The presence of amplified product of the correct size of 1.6 kb for the VP7 insertion mutants (mt177 and mt200) was determined by agarose gel electrophoresis (results not shown). The best efficiency of transfection was obtained when cellfectin was used. High titre recombinant virus stocks (10^8 - 10^9 pfu/ml) were prepared from plaque purified recombinant baculoviruses. Dual recombinant baculoviruses were generated in the same manner from the transfer plasmids pFBd-S3.9-177 and pFBd-S3.9-200.

4.3.5.2. Expression of the modified VP7 proteins in Sf9 cells

Monolayers of Sf9 cells were infected with Bac-mt177, Bac-mt200 and Bac-AH9VP7, which expresses the full-length VP7 gene (constructed by S. Maree). Proteins from infected cell lysates were resolved by SDS-PAGE (*Figure 4.11*). A unique protein band corresponding approximately to the expected size of 39 kDa was synthesised for each of the mutagenised VP7 proteins. The two insertion mutants of VP7 migrated slower through the gel compared to that of wild-type AHSV VP7. The sizes of these two proteins correspond to that of VP7 plus the six extra amino acids (± 1 kDa; total M_r = 39 kDa) and the size difference is visible on a 12% SDS-PAGE gel, which has a resolution of approximately 1 kDa. The insertion mutants of VP7 were synthesised approximately at the same level as wild-type VP7, which indicated that the insertion of extra amino acids did not significantly affect the expression levels (*Figure 4.11*). Maximum expression of VP7 and mt200 was obtained 4 days post-infection, while mt177 gave the highest levels at 3 days p.i. The levels of expression of AHSV-9 VP7, mt200 and mt177 were estimated to be approximately 1-2 mg/2 x 10^7 infected Sf9 cells. Further analysis of the putative VP7, mt177 and mt200 proteins was deemed unnecessary on the basis of the high level expression and visibility on Coomassie blue stained gels.

4.3.6. Solubility and sedimentation analysis of the VP7 insertion mutants

The baculovirus expressed VP7 spontaneously assembles into trimers, which interact to form hexagonal crystals, and as a result is highly insoluble. To determine whether the incorporation of six amino acids, in the top domain of VP7 will have an effect on the solubility of VP7 trimers, the different recombinant VP7 proteins were analysed using simple centrifugation, as well as sedimentation analysis. Cytoplasmic extracts containing the recombinant VP7 proteins were

prepared and separated into soluble and particulate fractions by means of low speed centrifugation (section 4.2.8) followed by SDS-PAGE analysis (*Figure 4.12*). Similar to wild-type VP7, the insertion mutant mt200 protein was predominantly found in a particulate form (>90%), although the amount of soluble mt200 is consistently more than VP7. In contrast to VP7 and mt200, insertion mutant mt177 was separated into approximately equal amounts of a particulate fraction and a soluble fraction. This result indicated that the insertion of six amino acids into the top domain of AHSV VP7 does increase the solubility of VP7 trimers. This is especially true when the incorporation occur in the RGD loop of AHSV VP7, which had a strong positive effect on the solubility of the protein, since approximately 50% of the protein was recovered from the soluble fraction followed low speed centrifugation.

To determine if the ratio of soluble VP7 trimers to particulate VP7 remains the same during the different stages of protein expression, the ratio was determined over a period of time starting at the earliest time of expression where the levels of expression are still low. Synchronised infected Sf9 cells were pulse labelled with ^{35}S-methionine from 18 h post-infection at 6 hourly intervals up to 40 h p.i. For each time interval the solubility of the proteins was analysed as described before. It was evident from this experiment (results not shown) that as soon as the VP7 and mt200 proteins are synthesised, they aggregate into large structures, which subsequently are recovered predominantly in the particulate form. The soluble form of mt200 was always more than that of VP7. For mt177, more protein was recovered from the soluble fraction early on in the infection. As the infection progressed and the expression levels of mt177 increased, more protein was visible in the particulate form. These results indicate that although mt177 is more soluble than either VP7 or mt200, it still aggregates into large particulate structures when synthesised at high levels.

The cytoplasmic extracts from cells infected with the modified VP7 recombinant baculoviruses were also fractionated on sucrose gradients and compared after SDS-PAGE analysis (*Figure 4.13*). Like wild-type VP7 the insertion mutant mt200, sedimented as a large homogeneous complex near the bottom of the gradient. The sedimentation value of VP7 and mt200 was estimated to be >900 S and almost all the protein was recovered from the bottom fractions of the gradient (fractions 1-5; *Figure 4.14*). This indicates that the VP7 and mt200 proteins are present as large structures in the infected cells. The mt177 protein on the other hand was present as a complex mostly found at the top of the gradient (fractions 9-11) with an S value of 75 (*Figure 4.13*). Only a small amount of mt177 protein (approximately 30%; *Figure 4.14*) was present in the bottom of the gradient (fractions 1-4) at the same position as VP7.

From these results there was no indication that the trimeric structures formed by VP7 were disrupted by the introduction of six amino acids. It appears that the VP7 protein still folds in the

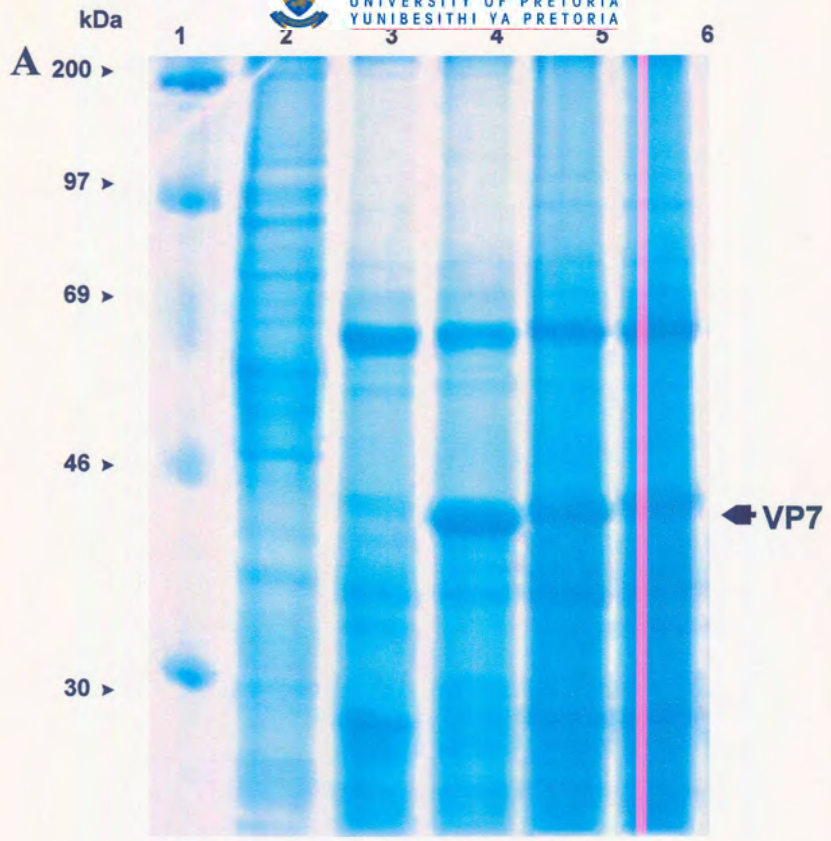

Figure 4.11: SDS-PAGE analysis of the recombinant VP7 protein expression in insect cells. Lane 1 contains rainbow molecular weight marker. Lanes 2 and 3 contain extracts of cells mock-infected or infected with wild-type baculovirus. Lane 4 contains extracts of cells infected with VP7 recombinant baculovirus. Lanes 5 and 6 contain cell lysates of cells infected with recombinant baculoviruses Bac-mt177 and Bac-mt200, respectively.

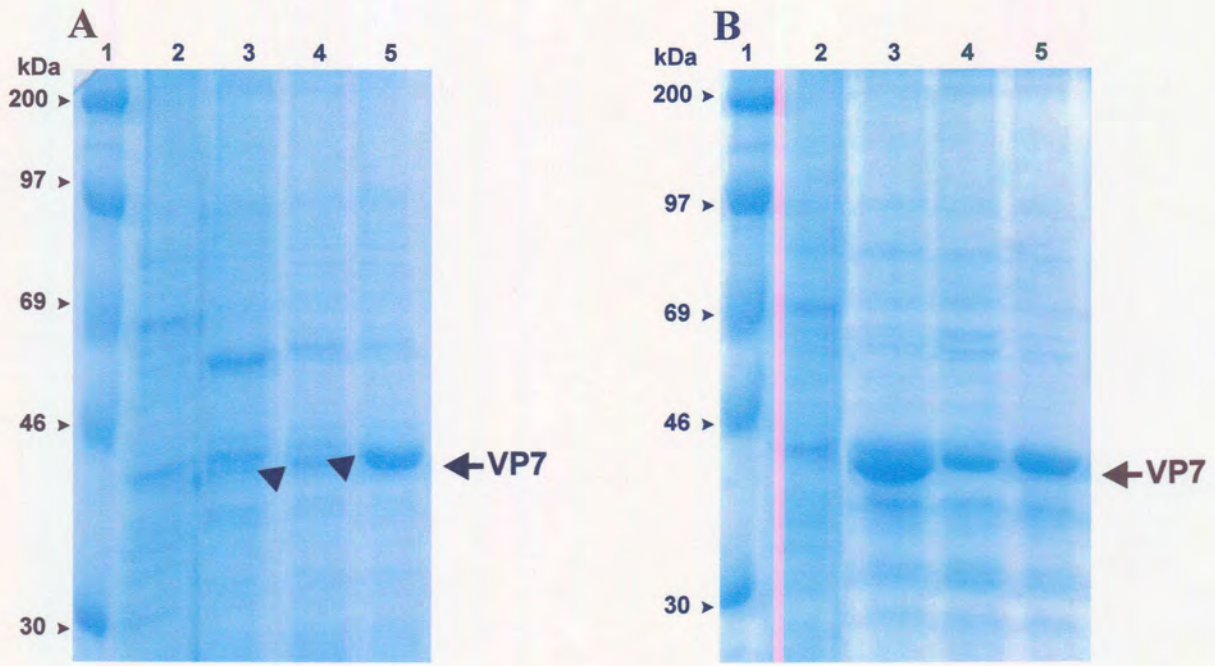

Figure 4.12: Differential centrifugation of the cytoplasmic extracts from Bac-AH9VP7, Bac-mt200 and Bac-mt177 infected cells. The cytoplasmic extracts were separated into a soluble (A) and particulate (B) fractions using low speed centrifugation at 5000 rpm for 30 min. For A and B: lane 2 represent cell lysate from wild-type infected Sf9 cells, lane 3 VP7 soluble/particulate fractions, lane 4 insertion mutant 200 soluble/particulate fraction and lane 5 insertion mutant 177 soluble/particulate fraction. Sizes of protein markers (lane 1) are indicated in kDa at the left of the figure.

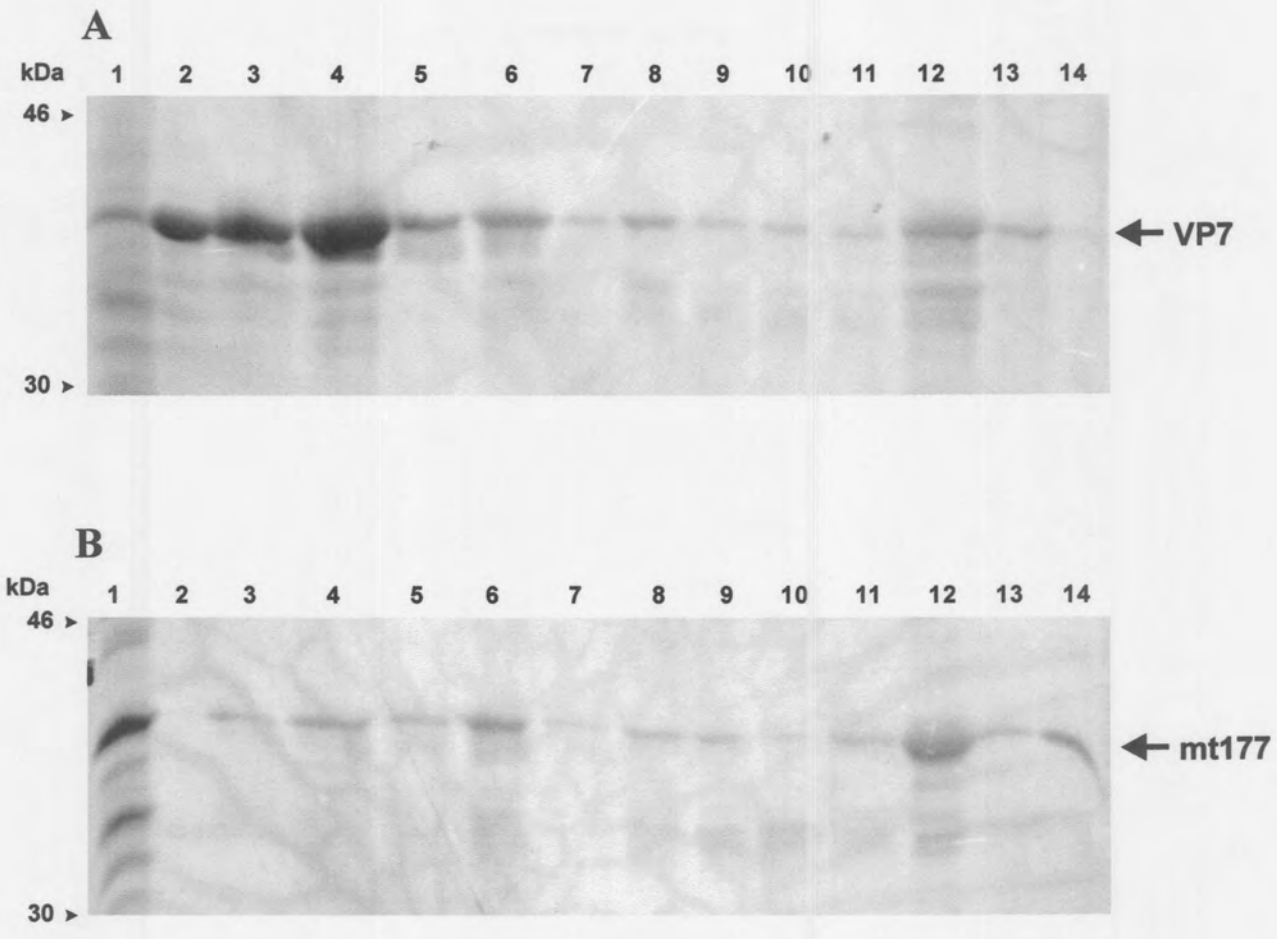

Figure 4.13: Sedimentation analysis of the cytoplasmic extracts from Bac-AH9VP7 (A) and Bac-mt177 (B) infected cells by sucrose density centrifugation. The cells were radioactively labelled 48 h p.i. Prior to sucrose gradient centrifugation the cytoplasmic extracts were separated in a soluble and particulate fractions by differential centrifugation. The particulate fractions were collected and used for the sedimentation analysis. A sample (1/100) of the soluble fractions were loaded in lane 1. Fractions were collected from the bottom (lane 2) to the top (lane 14) of each gradient and a 1/10 of each fraction analysed by autoradiography after resolution by SDS-PAGE.

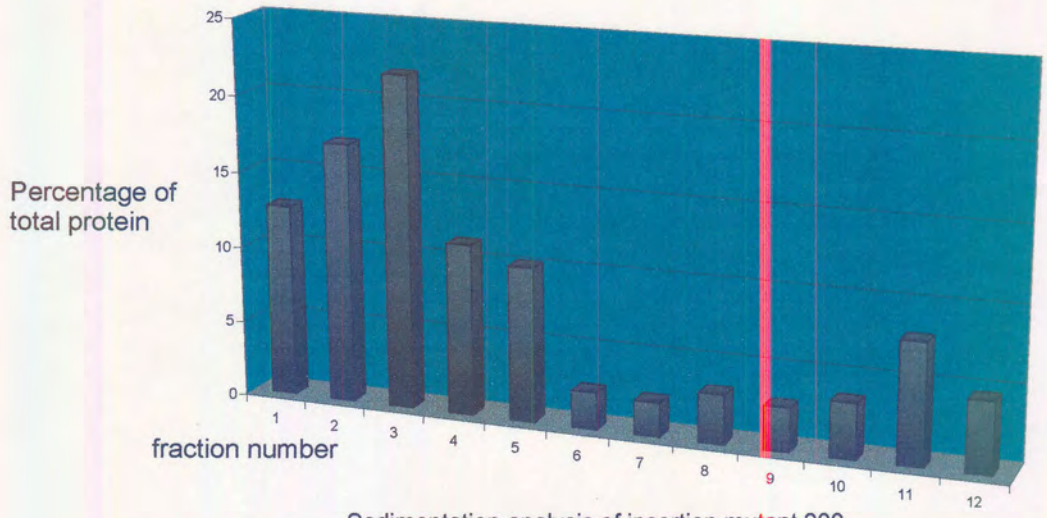

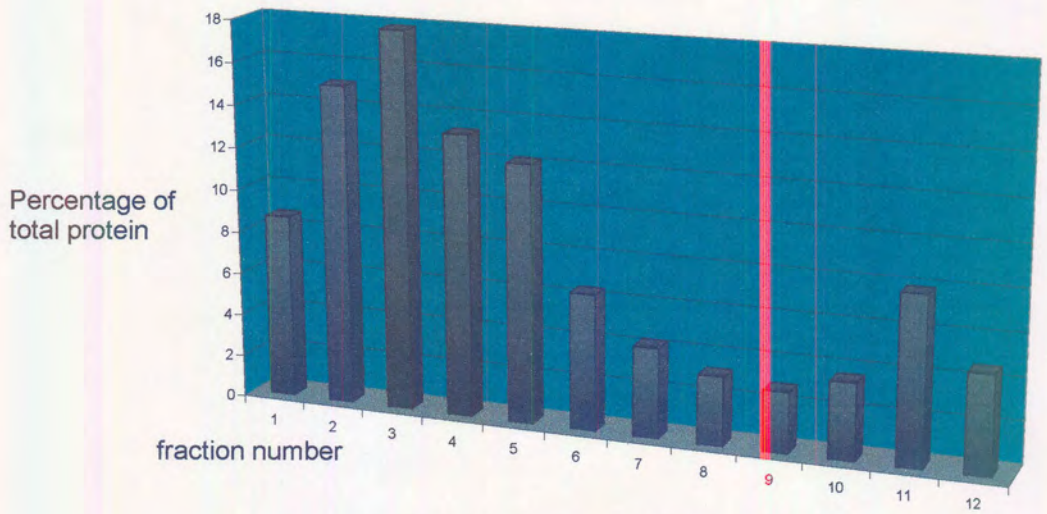

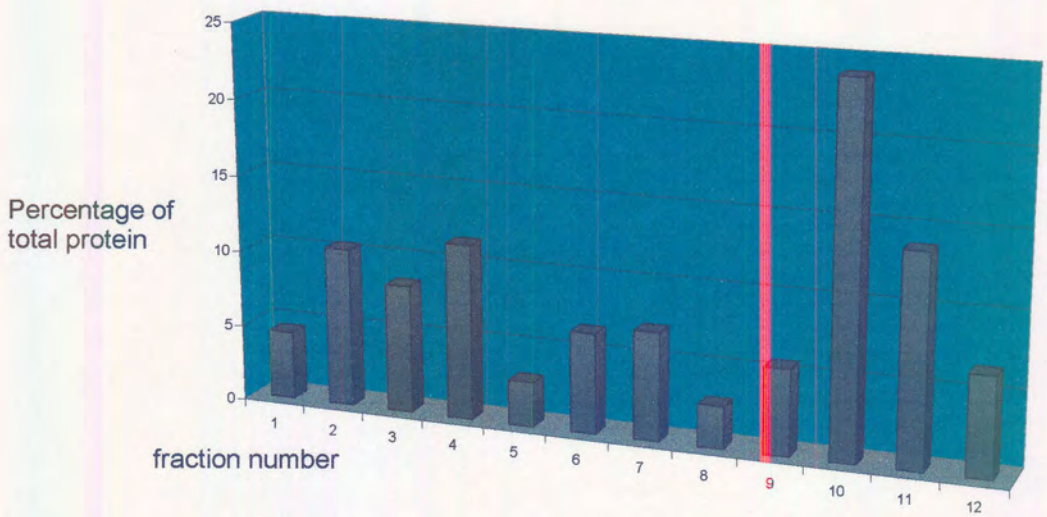

Figure 4.14: Sedimentation analysis of the cytoplasmic extracts from Bac-AH9VP7 and Bac-mt177 infected cells by sucrose density centrifugation. The cells were radioactively labelled 48 h p.i. Prior to sucrose gradient centrifugation the cytoplasmic extracts were separated in a soluble and particulate fractions by differential centrifugation. The particulate fractions were collected and used for the sedimentation analysis. A sample (1/100) of the soluble fractions were loaded in lane 1. Fractions were collected from the bottom (lane 2) to the top (lane 14) of each gradient and a 1/10 of each fraction analysed by autoradiography after resolution by SDS-PAGE. The fraction of the total amount of protein in each fraction is indicated as a percentage (y axis).

correct 3-D orientation and also forms its trimeric structure. Although the VP7 particulate structures are relatively stable under a wide variety of ionic strength and pH conditions, it was found that the crystal structure was partially disrupted with the use of high concentration of Nonidet-P40 (>0.5%) during cell lysis. This caused the VP7 structures to be present as a more heterogeneous complex on the sucrose gradient. On the other hand too little Nonidet-P40 (<0.1%) resulted in inefficient cell lysis. The optimum concentration of the non-ionic detergent was found to be approximately 0.25%, which resulted in minimum disturbance of the crystal structures.

4.3.7. Purification and electron microscopy analysis of modified VP7 complexes

The identity of the modified VP7 proteins was confirmed by their ability to form crystals or CLPs (next section). Crystal formation was analysed by means of light microscopy and scanning electron microscopy. Approximately 2 days following infection, the cellular cytopathic effects of a baculovirus infection became apparent. In addition, cells infected with Bac-mt200 exhibited distinct disc-shaped crystals as in cells infected with the recombinant baculovirus containing the unmodified VP7 gene. Cells infected with Bac-mt177 lacked any such crystals, although structures that appear more round were visible after 3 to 4 days p.i. (results not shown). Insect cells infected with other types of recombinant or wild type baculoviruses lacked any such structures. These structures exhibited variation in both size and number per cell, usually containing between one and three crystals. The ability of AHSV VP7 insertion mutants to form morphological structures was utilised to subsequently purify the proteins by one step linear sucrose gradient centrifugation. Sucrose gradient peak fractions, containing the protein of interest, were pooled and the protein recovered by high-speed centrifugation. The gradient purified VP7 proteins were then examined with SEM.

The results obtained in the sucrose gradient assay indicated that the baculovirus expressed modified VP7 proteins differ in their ability to form crystals. Hexagonal crystals, similar to that formed by wild-type AHSV VP7, were observed in the case of the insertion mutant mt200. A typical preparation of mt200 crystals examined at low magnification in a SEM revealed large numbers of intact and fragmented flat, hexagonal structures with a maximum diameter of 6 μm (*Figure 4.15*). When examined at higher magnification by TEM, it was found that these structures were composed of a highly ordered two-dimensional crystalline lattice. SEM analysis of purified mt177 protein from the bottom fractions of the gradient revealed the presence of a large number of rounded particulate structures. No recognisable hexagonal crystals were observed. These structures were essentially homogeneous with a diameter of up to 5 μm (*Figure 4.16*). Since the mt177 protein in the bottom fractions was more than 95% purified as determined by SDS-PAGE (*Figure 4.13*) it is assumed that these ball-like structures are composed of the mt177 protein. There was no indication of any recognisable structure in the top fractions of the mt177 gradient. The mt177 protein in these

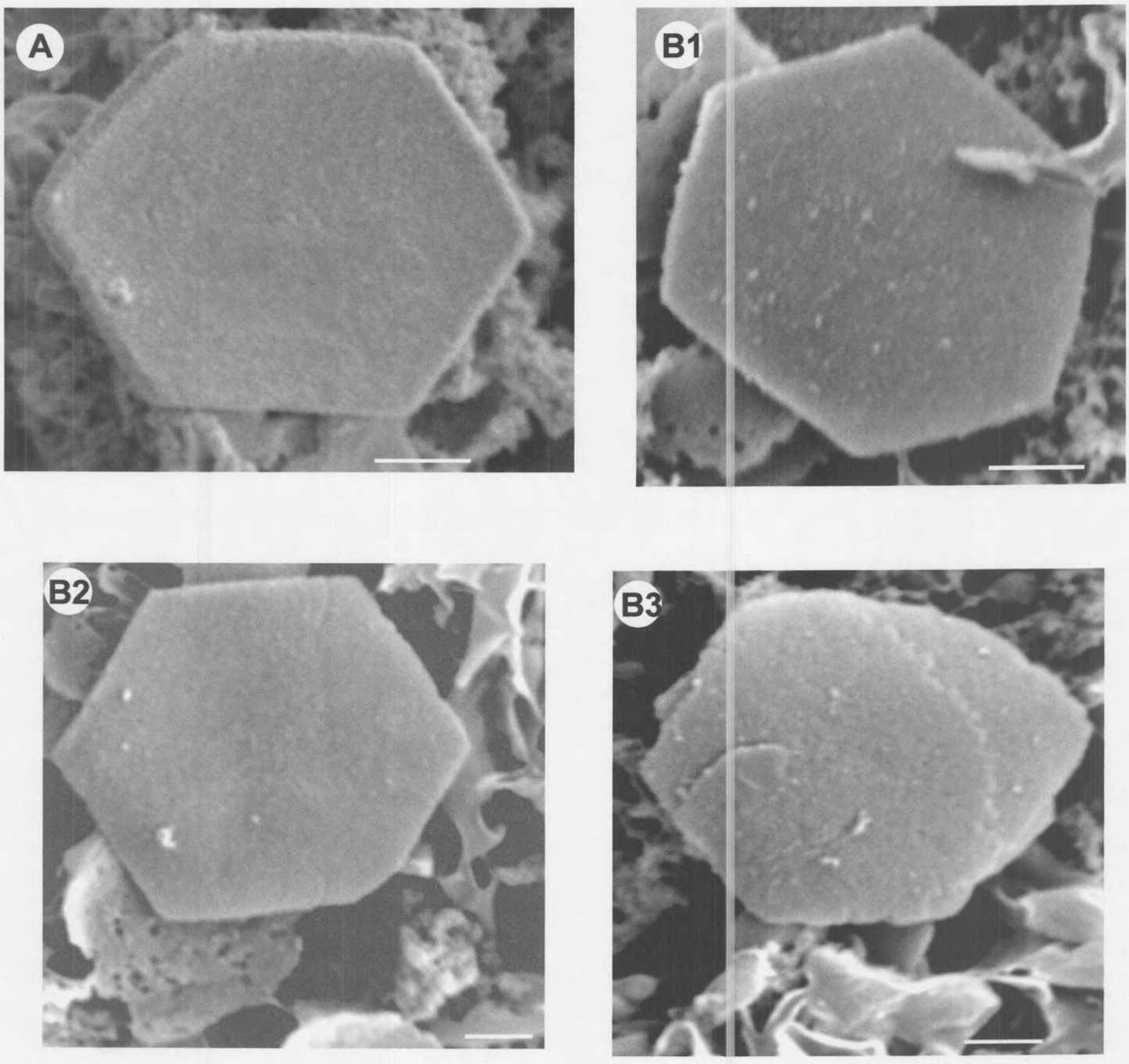

Figure 4.15: Scanning electron micrographs of sucrose gradient purified VP7 (A) and mt200 (B1-3) crystals, spatter coated with gold-beladium. Mt200, like VP7, aggregate into crystals with an intact haxagonal profile, with the same lattice detail as described by Buroughs *et al.* (1994). The bar markers represent 1 um.

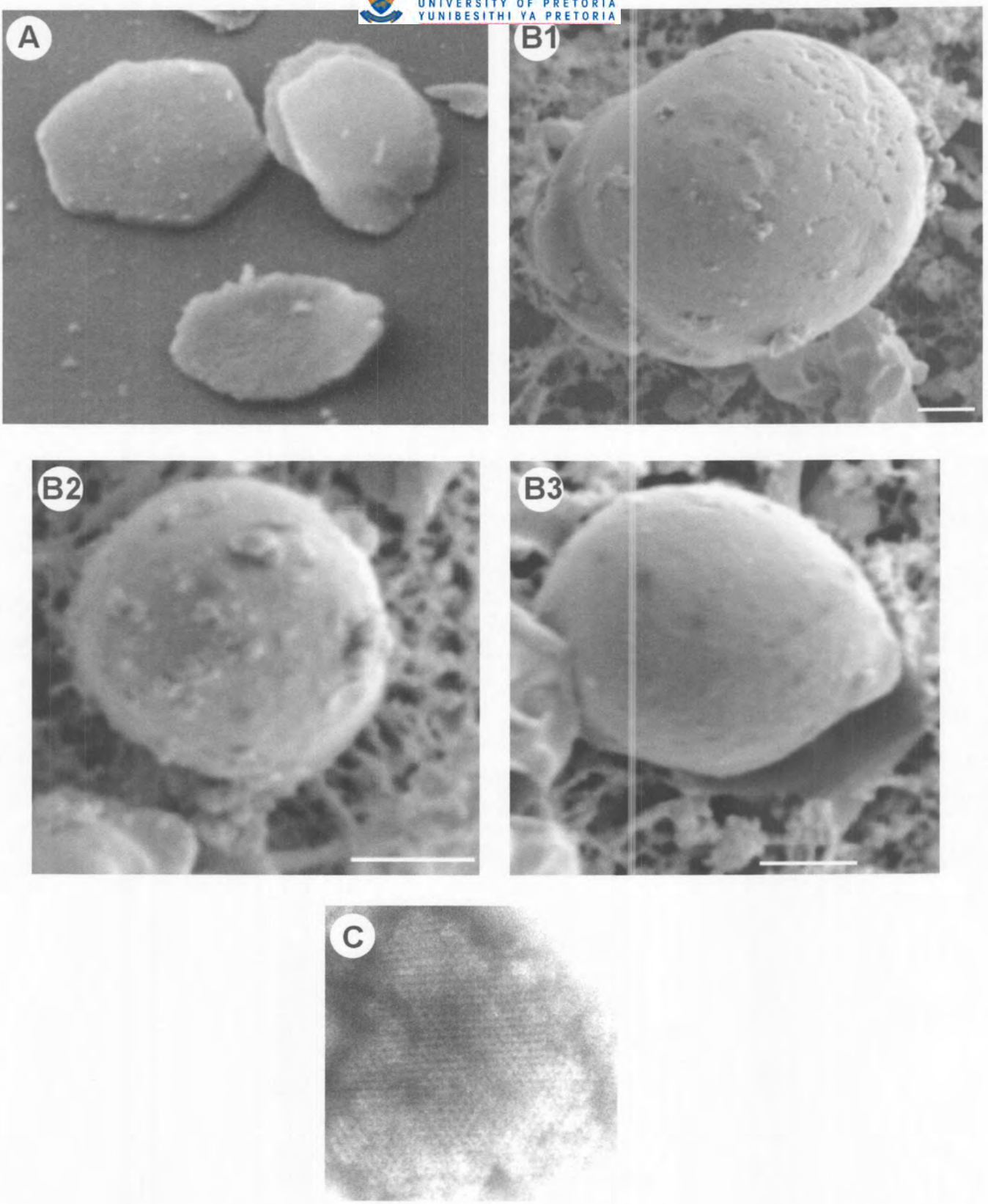

Figure 4.16: Scanning electron micrographs of purified VP7 crystals (A) and mt177 ball-like structures (B1-3). Mt177 did not show the same intact hexagonal outline as VP7. The bar markers represent 1 um.

fractions may represent soluble trimeric form of the insertion mutant mt177 protein. When examined with TEM the mt177 proteins also assemble into the highly ordered two-dimensional crystalline lattice seen with VP7 and mt200 (*Figure 4.16*).

4.3.8. CLP formation using VP7 insertion mutants

The integrity of the three-dimensional structure of the VP7 insertional mutants and chimeras was analysed according to their ability to form CLPs when co-expressed with VP3. Recombinant baculoviruses containing the VP3 gene and either the mt177 or mt200 gene, was constructed (Bac-VP3.9-mt177 and Bac-VP3.9-mt200). To verify expression, proteins from insect cells infected with Bac-VP3.9-mt177 and Bac-VP3.9-mt200 were analysed by SDS-PAGE. For comparison, cells were either mock infected or infected with the wild type virus or Bac-S3.9-S7.9. By comparison with mock infected or wild type baculovirus infected cell lysates, each of the dual recombinant baculovirus clones synthesised two unique protein bands which corresponded with VP3 and VP7 in Bac-S3.9-S7.9 infected cells (*Figure 4.17*). One band was approximately 90 kDa, the estimated size of AHSV-9 VP3, while the other displayed a somewhat slower mobility than VP7, at approximately 39 kDa. This was expected, since the two insertion mutants contained six extra amino acids with an estimated molecular mass of ±1 kDa as explained in section 4.3.5.2.

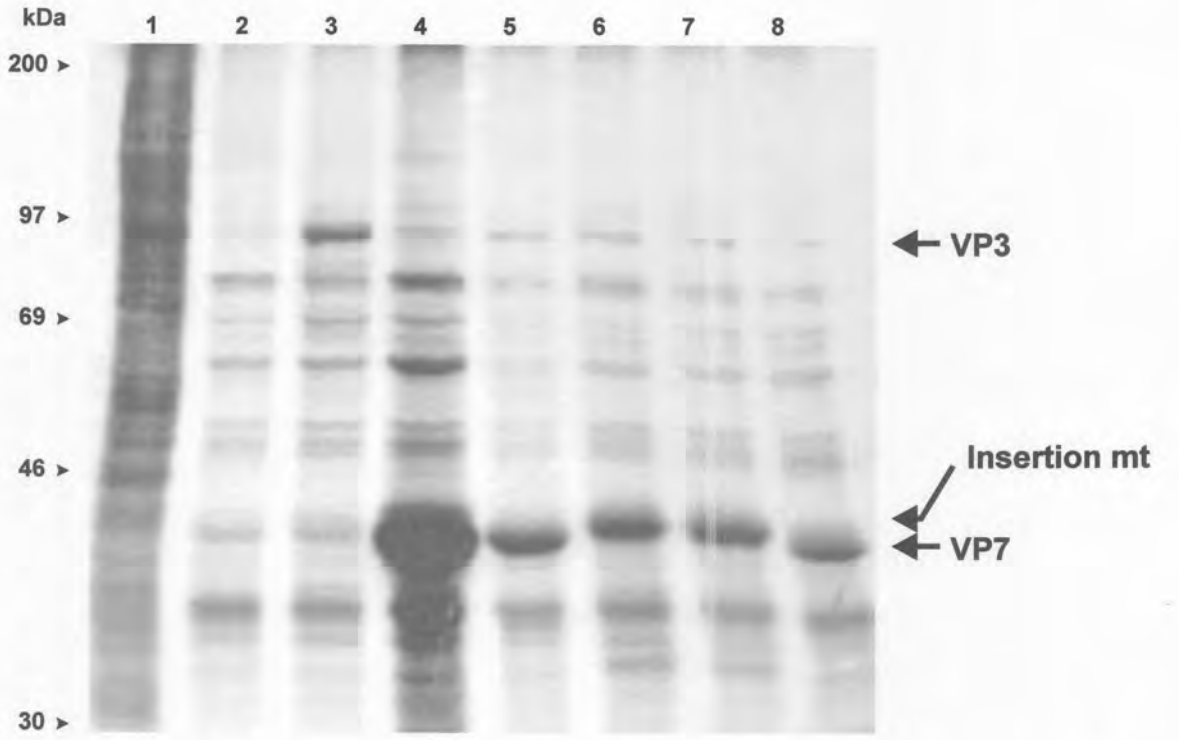

Figure 4.17: Autoradiograph of ^{35}S-methionine labelled proteins resolved by SDS-PAGE to evaluate co-expression of AHSV-9 VP3 and the VP7 insertion mutants in insect cells by dual recombinant baculoviruses. Sf9 cells were mock-infected (lane 1), infected with wild-type baculovirus (lane 2), Bac-VP3 (lane 3), Bac-VP7 (lane 4), DBac-S3.9-S7.9 (lane 5 and 8), Bac-S3.9-mt177 (lane 6) and Bac-S3.9-mt200 (lane 7). The positions of VP3, VP7 and mutagenised VP7 are indicated by arrows.

To investigate whether the two VP7 insertion mutants are capable of forming CLPs in the presence of AHSV-9 VP3, insect cells were infected with the dual recombinant baculoviruses and lysates of infected cells fractionated on sucrose or CsCl gradients. When the protein components of the gradient fractions were analysed by SDS-PAGE, both the VP3 and the insertion mutants of VP7 were identified. It was found that the insertion mutants of VP7 formed a complex with VP3, which sedimented with the same sedimentation rate as particles formed by unmodified VP7 and VP3. Particles were also recovered from CsCl gradient, indicating that the particles are as stable as CLPs derived from unmodified VP7 under high-salt conditions. The protein complexes were recovered from the gradients by high-speed centrifugation and analysed by electron microscopy after negative staining with uranyl acetate.

The yield of protein complexes recovered from the VP3 and VP7mt177 gradient was much higher than that generated by expression of VP3 with either an unmodified VP7 or with VP7mt200. Since both VP3 and VP7mt177 were present in the particulate fractions, it was the first indication that these proteins could assemble to form CLPs. The results suggest that the modification in the amino acid position 177 to 178 may have an influence in the solubility of the VP7 protein, but not on the 3-D structure or trimerisation of VP7. The increase in solubility may result in an increase in the number of VP7 trimers that are available for attachment to subcores, composed of VP3. As a result, conditions for the formation of CLPs were more favourable than with unmodified VP7, which by preference aggregate into crystals.

Electron micrographs of purified CLPs derived from co-expression of AHSV-9 VP3 and either of the two VP7 insertion mutants, revealed morphological structures similar to authentic AHSV cores and CLPs assembled from wild-type AHSV VP3 and VP7 proteins (*Figure 4.18*). Like unmodified CLPs, the 177CLPs and 200CLPs were empty, with the typical icosahedral symmetry. The knobby morphological protrusions, representing VP7 trimers, extended outwards. High salt, pH fluctuation between 6.0 and 8.5 and storage at 4°C of the CLPs composed of VP7mt177 or VP7mt200 and VP3 had no influence on the surface knob-like structures. This indicated that the modifications to VP7 did not influence the stability of CLPs. In addition, treatment of the VP7 insertion mutant CLPs with a low salt buffer led to the loss of the surface capsid structures and derivation of subcore-like particle similar to those found by Burroughs *et al.* (1994) and Oellerman (1969). The identity of the CLPs was verified by antibody decorating of the particles using monoclonal VP7 antibodies (Van Wyngaard *et al.*, 1992). Each particle was masked by a dark shadow resulting from the specific interaction of monoclonal VP7 antibodies with the VP7 outer shell, which confirmed the VP7 nature of the trimers.

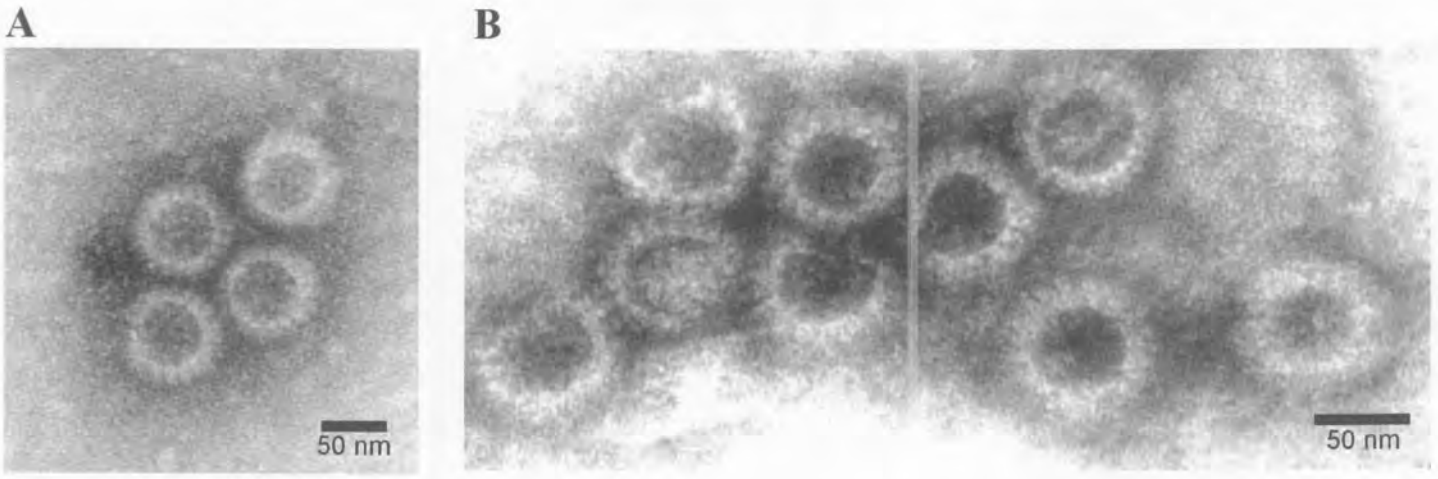

Figure 4.18: Electron microscopy of purified CLPs obtained from the co-expression of the two VP7 insertion mutants mt200 (A) and mt177 (B) with AHSV-9 VP3 in insect cells. The sucrose gradient purified particles were stained with 2% uranyl acetate.

4.3.9. Construction of recombinant baculovirus transfer vectors containing VP7/TrVP2 chimeric genes

In order to determine what the effect insertion of a foreign polypeptide will have on the solubility, and trimerisation of the VP7 protein, two VP7 chimeric genes were constructed which contained a fragment overlapping a previously identified immunogenic region of AHSV-9 VP2 (amino acid 385 - 415). A region of the VP2 gene from *HindIII* (position 957) to *EcoR1* (position 1260), was directionally cloned into the unique introduced restriction sites of mt177 and mt200. The unique restriction sites inserted into VP7 allows the insertion of the AHSV-9 VP2-specific DNA fragment by directional cloning in the correct reading frame of the VP7 sequence. Seeing as the cloning strategy, followed by Samantha Hopkins in producing the two chimeric VP7/TrVP2 proteins, has not been documented elsewhere, it is included in this section for reference purposes. The strategy for the construction of the chimeras is summarised in *Figure 4.19 A*.

A large AHSV-9 VP2 fragment which contained the nucleotide sequence that corresponds to amino acid region 313 to 415 (957 –1260 bp) of VP2 was recovered by *HindIII* digestion from pAHSV9.2 (3.2.2.2). The *Hind*III cuts asymmetrically in the VP2 gene ca. 957 bp from the 5' end and once in the vector downstream of the VP2 gene and excised a 2300 bp fragment that was cloned into the

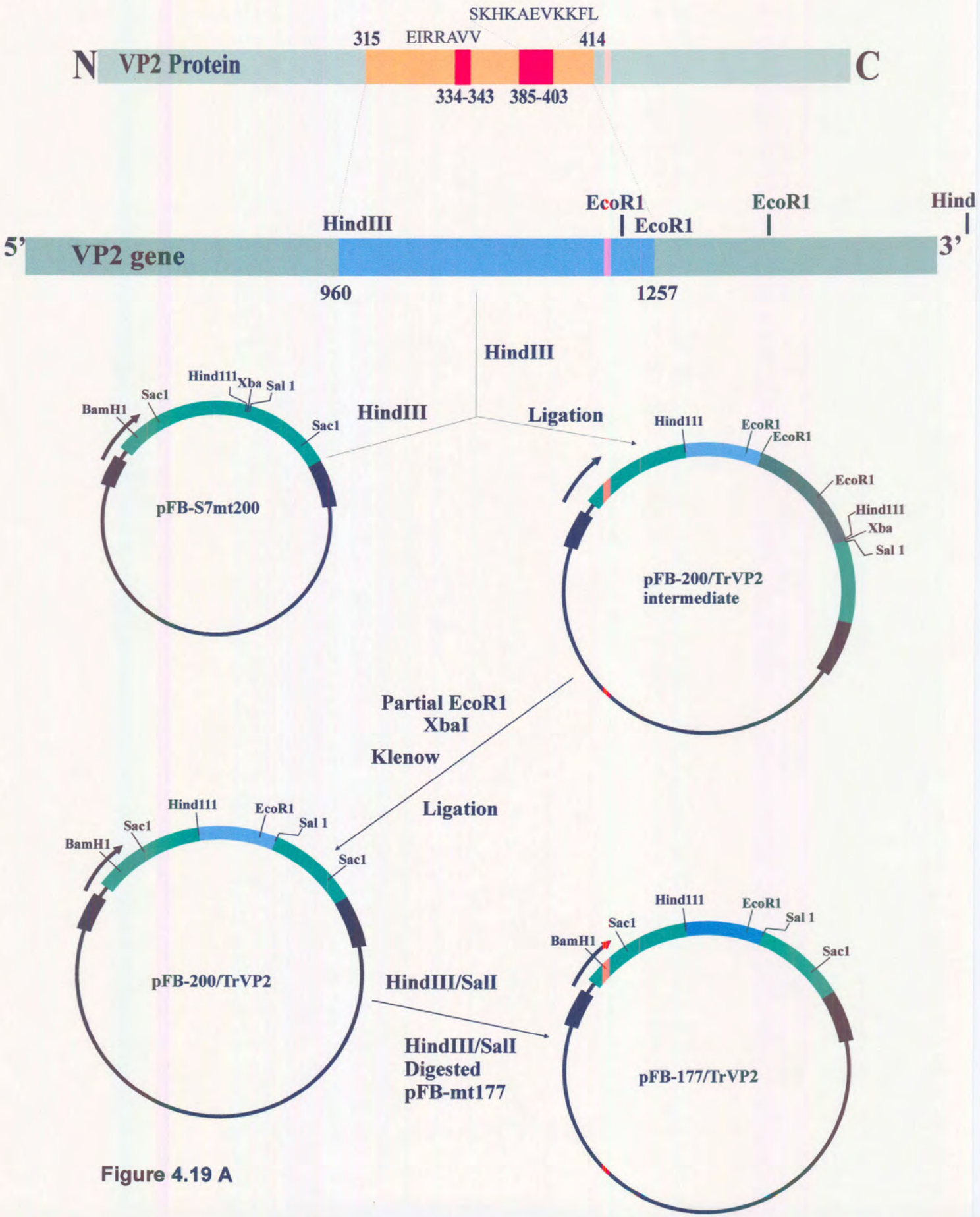
SKHKAEVKKFL
315
EIRRAVV
414
N
VP2 Protein
C
334-343
385-403
HindIII
EcoR1
EcoR1
EcoR1
Hind
5'
VP2 gene
3'
960
1257
HindIII
HindIII
Ligation
Hind111
Xba
Sal 1
Sac1
BamH1
pFB-S7mt200
Hind111
EcoR1
EcoR1
EcoR1
Hind111
Xba
Sal 1
pFB-200/TrVP2
intermediate
Partial EcoR1
XbaI
Klenow
Ligation
Hind111
EcoR1
Sal 1
Sac1
BamH1
Sac1
pFB-200/TrVP2
HindIII/SalI
HindIII/SalI
Digested
pFB-mt177
Hind111
EcoR1
Sal 1
Sac1
BamH1
Sac1
pFB-177/TrVP2

Figure 4.19 A

HindIII site of modified VP7 protein mt200. Recombinants in the correct orientation were selected with simultaneous *EcoR1* and *Sal1* digestions and yielded fragments of ca. 6.1 kb, 1.2 kb and 700 bp. The mt200/VP2-intermediate was partially restricted with *EcoR1*, which cut thrice in the VP2-specific fragment (at positions ca. 1180, 1260 and 2500) and completely digested with *Xba*I, in order to remove the 3' 2.0 kb region of the VP2 gene. A fragment of 6.6 kb was gel purified, the non-complementary overhangs were filled up by Klenow to restore the reading frame and self-ligated. Recombinant plasmids, which were linearised with *Eco*R1, which cuts once in the VP2-specific insert (ca. 1180 of VP2; the other VP2-specific *Eco*R1 sites and the one in the vector was removed; see *Figure 4.19 A* and section 4.3.2), were selected for further restriction enzyme analysis. Clones that contained the VP2 DNA sequence of interest were selected following simultaneous digestion with *Hind*III and *Sal*1 (*Figure 4.19 B*). A final construct containing the 303 bp *Hind*III-*Eco*R1 (957-1260) fragment of AHSV-9 VP2 was selected and named pFB-200/TrVP2. The reading frame was verified by automated sequencing using VP7 specific primers.

The VP2-specific domain was recovered from mt200/VP2 chimera (pFB-200/TrVP2) by *HindIII* and *Sal1* digestion and cloned directionally into the corresponding sites of the modified VP7 protein mt177, in order to construct the mt177/VP2 chimera. This cloning strategy positioned the VP2-specific insert in the correct reading frame of VP7mt177. Restriction of recombinant plasmids with

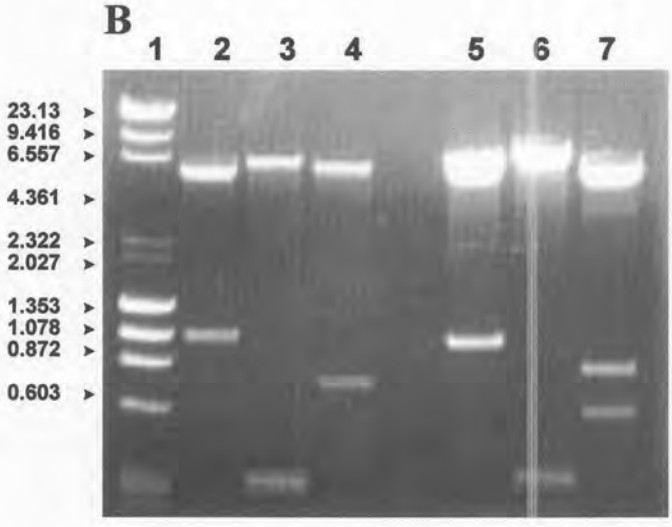

Figure 4.19: (A) A schematic diagram of the cloning strategy for the construction of two VP7/TrVP2 chimeric genes for expression in the Bac-to-Bac baculovirus system. (B) Agarose gel electrophoretic analysis of the two recombinant chimeric VP7 gene cloned into pFastbac transfer vector. The 177/TrVP2 chimera was digested with *Sac*I (lane 2), *Hind*III/*Sal*I (lane 3) and *Bam*H1/*Sal*I (lane 4) to identify the VP2 specific insert. The 200/TrVP2 chimera was restricted with the same enzymes in lanes 5 - 7 respectively. The sizes of the DNA molecular weight markers are indicated to the left of the figure.

*Sac*I indicated the presence of an insert of the expected size (303 bp) between the VP7-specific *Sac*I sites (ca. 200 and 1050). The correct translational orientation was verified by restriction enzyme mapping with *Bam*H1 and *Eco*R1, which recognises one site in the VP7-specific sequence, 100 bp from the 5' end and one site in the VP2-specific fragment, 750 bp from the 5' end of the chimeric gene, respectively. Recombinant chimeras that yielded fragments of sizes (ca. 650 bp) were selected and designated pFB-mt177/TrVP2 and the correct reading frame was confirmed by nucleotide sequencing.

Analysis of the resulting sequences of the two chimeric genes revealed that in each instance there is no divergence between the wild type and chimeric sequence of VP7 or between the inserted VP2 fragment and the original AHSV-9 VP2 sequence. The hydropathy plots of the deduced amino acid sequences of the two chimeras showing profiles similar to VP7 except for the region of the VP2 insertion. The profile in this region (indicated in blue), compare to the corresponding region in the VP2 protein. The hydropathic profiles of the two chimeras showed a profile of a combination between VP7 and VP2. The profiles of the 5' 177 or 200 amino acids and the 3' 171 or 148 amino acids of the 177/TrVP2 and 200/TrVP2 chimeras are identical to that of VP7. The inserted 101 VP2 specific amino acids showed the same profile as the corresponding region in the VP2 protein, which is characterised by four large hydrophilic peaks separated by two large and one small hydrophobic regions (*Figure 4.20*).

4.3.10. Expression of the two VP7/TrVP2 chimeric genes in insect cells

Composite bacmid DNA, containing mt177/Tr9.V2 or mt200/Tr9.V2 chimeric genes, was constructed as described before and used to transfect insect cells. Recombinant baculoviral stocks were prepared directly from the transfection supernatants and used to re-infect cells for protein expression. The VP7/VP2 chimeric proteins, expressed by the baculovirus recombinants, Bac-177/TrVP2 and Bac-200/TrVP2, were analysed by SDS-Page. The two VP7/TrVP2 chimeras with an estimated molecular weight of 52 kDa, as predicted for VP7 plus the 101 amino acids of the VP2-specific insert, separated accordingly on the SDS-PAGE gel. No similar bands were visible in the wild type or mock-infected Sf9 cells (*Figure 4.21*). The expression levels of the two VP7/VP2 chimeric proteins were lower than that of wild-type VP7. This could be due to the fact that Bac-177/TrVP2 and Bac-200/TrVP2 were not plaque purified as in the case of VP7, mt177 and mt200 recombinant baculoviruses. The lower expression results of the Bac-mt177 and Bac-mt200 before plaque purification confirmed this observation (result not shown). Increasing the expression levels of the chimeric proteins was deemed to be unnecessary. Maximum expression of the two chimeric proteins was obtained 4 days post-infection. The yields of expressed mt177/TrVP2 and mt200/TrVP2 were estimated to be roughly 100-150 μg/2 x 10^7 infected Sf9 cells. No crystals, or any other recognisable structure, were visible under the light microscope in insect cells infected with either of the two chimeric VP7/TrVP2 recombinant baculoviruses.

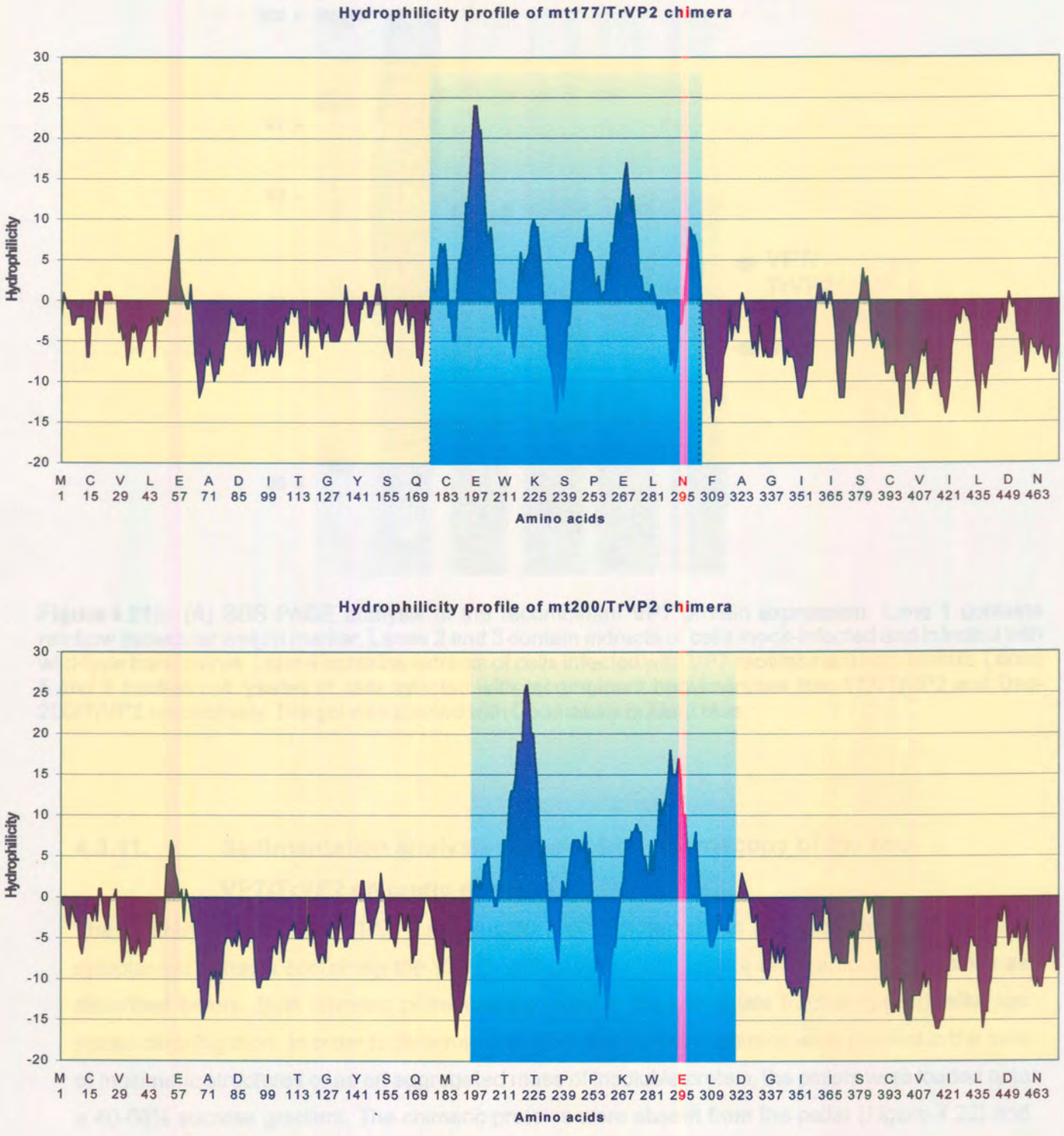

Figure 4.20: Comparison of the hydrophilicity profiles of the two chimeric proteins mt177/TrVP2 and mt200/TrVP2. Hydrophilicity was predicted according to Hopp & Woods (1981) utilising the ATHEPROT computer program. Areas with positive values have a nett hydrophilicity while areas with negative values have a nett hydrophobicity. The hydrophilicity profiles shows the insertion of the VP2 region stretching from amino acids 313 to 415, containing predominantly hydrophilic domains (indicated by blue bar at top of graph).

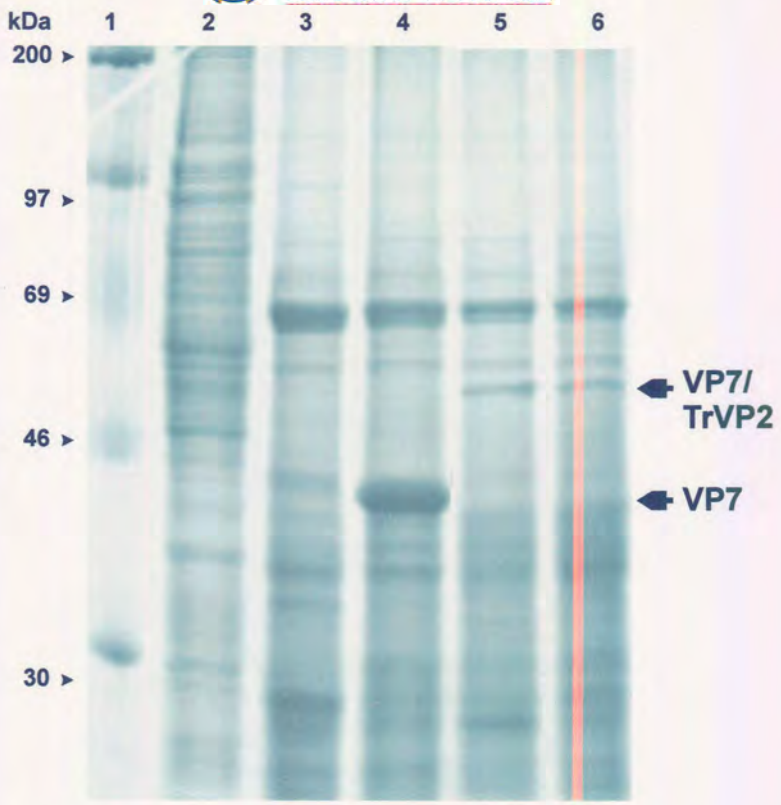

Figure 4.21: (A) SDS-PAGE analysis of the recombinant VP7 protein expression. Lane 1 contains rainbow molecular weight marker. Lanes 2 and 3 contain extracts of cells mock-infected and infected with wild-type baculovirus. Lane 4 contains extracts of cells infected with VP7 recombinant baculovirus. Lanes 5 and 6 contain cell lysates of cells infected with recombinant baculoviruses Bac-177/TrVP2 and Bac-200/TrVP2 respectively. The gel was stained with Coomassie brilliant blue.

4.3.11. Sedimentation analysis and electron microscopy of the two VP7/TrVP2 chimeric proteins

The solubility of the mt177/TrVP2 and mt200/TrVP2 proteins was analysed by separating the cytoplasmic extracts containing the VP7/TrVP2 proteins into soluble and particulate fractions as described before. Both chimeric proteins were found in the particulate fraction (pellet), after low speed centrifugation. In order to determine whether the chimeric proteins were present in the form of multimeric structures or as an aggregated mass of insoluble protein, the pellets were loaded onto a 40-68% sucrose gradient. The chimeric proteins were absent from the pellet (*Figure 4.22*) and therefore not an insoluble mass of protein. It was found that for both chimeric proteins the largest fraction was found as a heterogeneous complex in the gradient. The structures formed by the two chimeric proteins were much smaller than that of the normal VP7 protein (fractions 6-9) as determined by their lower S value. The results obtained in the sucrose gradient assay indicated that the baculovirus expressed chimeric VP7 proteins differ in their ability to form particulate structures. It was thought that these differences might be related to the ability or inability of the chimeras to form trimers or alternatively to increased solubility.

Peak fractions from the sucrose gradient containing either the mt177/TrVP2 or mt200/TrVP2 chimeric proteins were pooled and the recovered protein complexes analysed by SEM. In the case of the two VP7/TrVP2 chimeras no flat hexagonal crystals were found as with VP7. A large number of small ball-like structures, which resemble the structures found with mt177, were visible for each chimera (*Figure 4.23*). These structures were much smaller than those observed in the case of mt177, with a diameter of approximately 0.5 to 0.8 μm. The size difference of the structures may be a result of the lower expression levels of the chimeras, although it may also be due to alterations in the protein-protein contacts between VP7 molecules, leading to a greater distortion of the flat-sheet structure that is required to form the hexagonal crystal lattice and morphology.

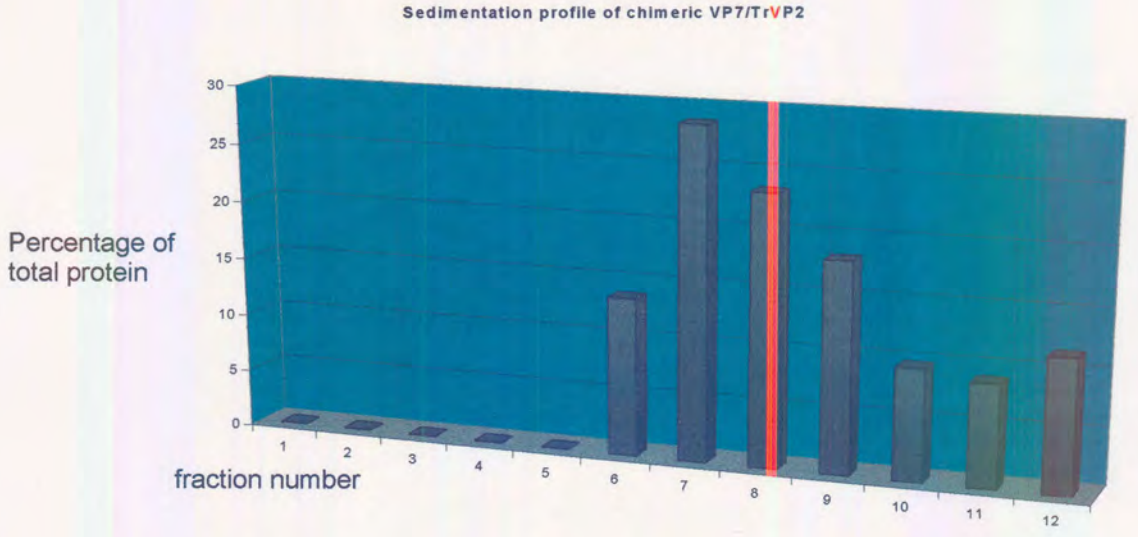

Figure 4.22: A graph representing the sedimentation analysis of the cytoplasmic extracts from Bac-177/TrVP2 infected cells by sucrose density centrifugation. The cells were radioactively labelled 48 h p.i. Prior to centrifugation the cytoplasmic extracts were separated in a soluble and particulate fractions as described in section 4.2.7. The particulate fractions were collected and used for the sedimentation analysis and fractions were collected from the bottom and analysed by autoradiography after resolution by SDS-PAGE. The bands were converted to Boehringer light units (BHU) using the lumi-imager and plotted as a percentage of the total amount of protein in the gradient. A similar profile were acquired from 200/TrVP2.

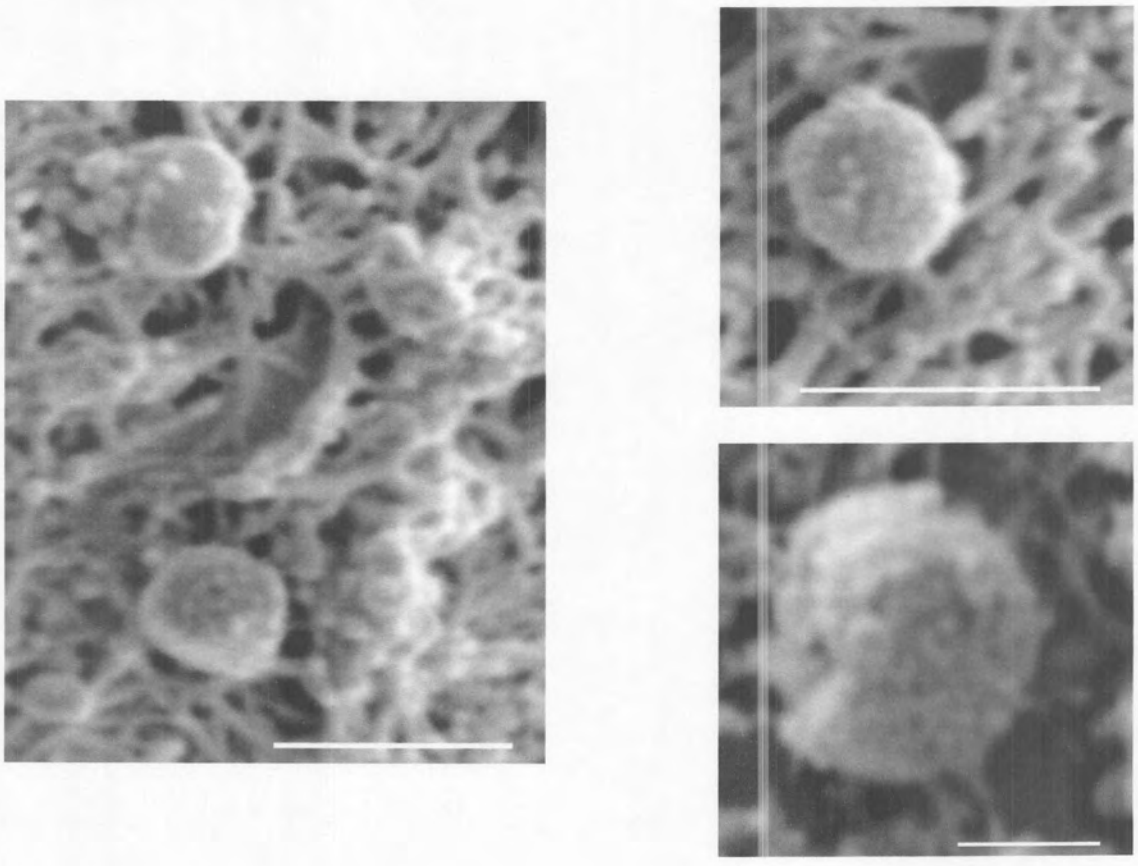

Figure 4.23: Scanning electron micrographs of purified chimeric VP7/TrVP2 ball-like structures. (A) represent structures from 177/TrVP2 and (B) 200/TrVP2. These structures did not show the same intact hexagonal outline as VP7. Bar markers represent 1 um.

4.4. DISCUSSION

In order to evaluate the potential of AHSV VP7 as an antigen delivery system in a subunit vaccine it is necessary to express large quantities of this protein in its native form. The VP7 protein was successfully expressed using an improved baculovirus system. Chuma et al. (1992) reported that AHSV VP7 synthesised in insect cells self-assembled to form disc-shaped crystal structures. When AHSV VP7 is co-expressed with AHSV VP3 in insect cells, it not only aggregate into crystals, but also assembles onto the VP3 scaffold to form CLPs (Maree *et al.*, 1998; chapter 3). The biologically active form of VP7, which is represented by the trimeric molecule, associates with other trimers to form crystals or assembles onto VP3 scaffolds to form CLPs. The availability of the expressed VP7 in its biologically active form will facilitate studies on the immunogenicity of the protein and provide further basis for assessing the suitability of VP7 as a subunit/epitope delivery system.

The large VP7 crystal structures provide an excellent opportunity for presenting antigenic epitopes, since they provide a large surface for epitope display. The disc-shaped crystals are also easily purified. To investigate the use of AHSV-9 VP7 crystals as an antigen delivery system, it was necessary to determine the immune response elicited by these crystals. Semi-purified AHSV-9 VP7 crystals were injected into Macaques and both the antibody and T-cell proliferative responses evaluated. Although a very strong humoral immune response was elicited, only a weak CTL response was detected (personal communication: Wade-Evans, A). This observation confirmed the result that AHSV VP7 crystals, purified from BHK cells infected with AHSV-9, was shown to be highly immunogenic, elicited a strong immune response and is effective as a subunit vaccine in a mouse model (Wade-Evans *et al.*, 1997; Wade-Evans *et al.*, 1998). The passive transfer of antibodies from immunised mice failed to protect syngeneic recipients from AHSV challenge, indicating that an antibody response is unlikely to represent the primary mechanism involved in the protection. Based on this result it was proposed that immunisation with VP7 induces a protective T-cell response in mice. Furthermore, it was found that denatured VP7 crystals resulted in lower levels of protection. The data indicated that the conformation and possibly the assembly of the VP7 into crystals appear to be important in the mechanism of protection against the heterologous serotype challenge. Reports from BTV VP7 indicated that the VP7 protein, contains immunodominant, serotype cross-reactive T-cell epitopes (Angove, 1998). These results imply that VP7 crystals are associated with a strong immune response in animals. The crystals have therefore potential as an antigen presentation system especially if neutralisation relies on a strong humoral immune response.

The use of chimeric AHSV CLPs as vehicles to present immunogenic peptides to the immune system, similar to the chimeric BTV CLPs (Roy *et al.*, 1994) has never been investigated. The main problem with this approach is the low yield of CLPs produced when the two major core proteins of

AHSV, VP3 and VP7, are co-expressed. It is therefore improtant to increase the yield of CLP synthesis in insect cells and secondly to introduce epitope insertion sites into VP7 without disturbing the 3-D structure of VP7. One possible approach to increase the yield of CLP synthesis is to increase VP7 solubility. VP7 crystals are present in insect cells expressing both VP3 and VP7 (chapter 3), which means that VP7 crystal formation compete with the assembly of VP7 trimers onto VP3 scaffolds to form CLPs. In view of this it is therefore possible that an increase in the solubility of VP7 might increase the concentration of free trimers in a cell, which might result in a higher yield of CLPs.

An important component in the development of AHSV VP7 crystals and/or chimeric CLPs as antigen delivery systems is to identify regions in the VP7 molecule, which may act as insertion sites for epitopes. The molecular structure of AHSV VP7, described in chapter 1, formed a basis for deciding which sites were to be exploited for insertion of epitopes, without disrupting the structure. The atomic structure of AHSV VP7 has been found to be very similar to that of the BTV VP7 trimers (described in chapter 1), as expected from the high degree of sequence similarity of the BTV and AHSV VP7 proteins. From the crystallographic data of AHSV VP7 Basak *et al.* (1996) identified properties of the molecular surface of AHSV VP7 which may play a role in the difference in solubilities between AHSV and BTV VP7. These data implicated the upper domain in contributing to the insolubility of AHSV VP7. In other studies it has been reported that single amino acid substitutions can significantly improve protein solubility (Zhao & Sommerville, 1992; Izard *et al.*, 1994). In the AHSV VP7 sequence, amino acid residue 167 is an alanine (A167) while in the comparable sequence of BTV VP7 it is an arginine (Iwata et al., 1992; Basak *et al.*, 1996). At amino acid position 209 in the AHSV VP7 there is a phenylalanine, while in the corresponding sequence of BTV VP7 there is a threonine. The substitution of A167 and F209 by the amino acid residues located in equivalent positions in BTV VP7 (R and T) has been suggested as a means to improve the solubility of AHSV VP7 (Basak *et al.*, 1996). This issue was investigated by Monastyrskaya *et al.* (1997) and it was found that neither mutation improved the solubility of AHSV VP7.

Mapping the hydrophobicity plots to the solvent-accessible surface of AHSV and BTV VP7 trimers has shown the presence of a large hydrophilic area composed of strand βC and η1 (aa 168-178, including the RGD motif of the top domain of one monomer, and the C-terminal helix 9 of the adjoining monomer)(Basak *et al.*, 1996). The A167 forms part of this area. The observation that changing this alanine to arginine did not increase the solubility of AHSV VP7 might reflect the impact of the C-terminal helix 9, as the C-terminus of AHSV VP7 is more hydrophobic with L346 replacing R345 of BTV VP7. Therefore, increasing the solubility of AHSV VP7 may involve mutating a number of amino acids and the factors involved in its solubility may prove to be complicated. The AHSV VP7 crystallographic data also revealed that the N-terminus is situated in the lower domain of VP7, and is likely to be constrained by steric hindrances for the insertion of epitopes. The short C-

terminal arm of VP7 ties the trimers together during capsid or crystal formation and addition of epitopes at the C-terminus may abolish CLP formation as well as aggregation into crystals. The deletion of only 5 amino acids or the in-frame addition of 11 amino acids at the C-terminus of BTV VP7 abolishes CLP formation presumably due to lack of trimer-trimer interaction (Le Blois & Roy, 1993). The absence of trimer-trimer interactions in the case of AHSV VP7 would not only abolish CLP formation but also crystal formation. An extension mutant of BTV VP7 with 11 additional amino acids at the amino terminus of the protein resulted in the assembly of CLPs, which were unstable. The only successful insertion of foreign epitopes in BTV VP7 was at an internal site at position 145 (A145), where 29 amino acids were inserted without inhibiting CLP formation. The site 144-145 is one of the four hydrophilic regions in the top domain of VP7, ideal for the insertion of epitopes.

Accordingly, four internal sites in the top domain of VP7 were identified as hydrophilic regions, located on exposed loops on the surface of the VP7 trimeric molecule. These hydrophilic loops make contact with the surrounding environment in both the VP7 crystals and CLPs. Two of these four hydrophilic sites, Arg177Arg178 and Q200Gly201, were chosen for modification in order to implement the insertion of epitopes. The decision was based on the hydrophilicity and availability of the two sites on the surface of the molecule as analysed by their X-ray crystallographic structure.

Two site-specific insertion mutants of VP7 were prepared through two PCR based strategies. The first is a modification of a strategy reported by Imai *et al.* (1991), while the second, more time consuming method, amplified the gene as two fragments. Both mutational methods, reported in this chapter resulted in the precise introduction of six codons and the creation of three unique restriction sites. The hydrophilicity profile of insertion mutant mt177 demonstrated a significant increase in hydrophilicity for the extended RGD loop. However, the insertion of the same amino acids between amino acids 200-201 resulted in only a small increase in hydrophilicity in that area. This could be explained by the location of the insertions. The exposed region 198-201 is only a small hydrophilic area of 4 amino acids, adjacent to large stretches of hydrophobic residues. The insertion of the extra amino acids adjacent to these hydrophobic regions had a much smaller effect of the hydrophilicity in that region than insertion of the amino acids into the already extensive hydrophilic RGD loop. Computer modelling of the molecular structure of the two insertion mutants indicated that in each case, the extra amino acids would be presented on the surface of the VP7 monomer rather than folding inwards.

For expression in the baculovirus system, the two modified VP7 genes were cloned into the transfer vector pFastbacI. Additional restriction sites, which remained in the multiple cloning site of the vector after the cloning strategy, were also removed to allow easy insertion of foreign sequences at the chosen positions in VP7. One site, *Kpn*I, was retained to enable retrieving of the VP7 gene for future recloning purposes. The recombinant transfer vectors were used to transform *E. coli* cells, containing the bacmid DNA and transposition helper plasmid. Composite bacmid DNA was used to

transfect *S. frugiperda* cells. Both insertion mutants, like unmodified AHSV-9 VP7, were expressed to the same high levels in Sf9 cells infected with the derived baculovirus recombinants. Both modified VP7 proteins migrated as a single distinct band with an electrophoretic mobility slightly slower than wild-type VP7. The distinction in size is approximately 1 kDa and can be accounted for by the six extra amino acids (estimated at approximately 900 daltons) which were introduced into the two modified VP7 proteins. An important question that had to be addressed in the course of this investigation was whether the top domain of VP7 would be flexible enough to allow the insertion of extra amino acids as part of the vector development. Two insertion mutants each containing six extra amino acids between amino acids 177-178 and 200-201 were constructed and expressed. The mutants were analysed for their solubility, crystal formation, antigenic properties and ability to form CLPs with AHSV VP3.

When cytoplasmic extracts of cells infected with either the VP7, mt200 and mt177 recombinant baculoviruses were subjected to low speed centrifugation, almost all the VP7 and mt200 proteins were recovered in the particulate fraction. The mt177 protein was separated into approximate equal amounts of a soluble and a particulate fraction, using differential centrifugation. When the particulate fraction of the three proteins were analysed by sedimentation analysis on sucrose gradients, almost all the VP7 and mt200 proteins migrated at a sedimentation rate of approximately 900 S to the bottom fractions of the gradient. The mt177 protein was present in two different forms on the gradient. Some of the mt177 protein accumulated at the top of the gradient and represents the soluble form of mt177 trimers, while the particulate form of mt177 sedimented at about 900 S to the bottom of the gradient. This indicated that the extra amino acids in the RGD loop of VP7 dramatically increased the solubility of VP7, while no change in solubility was observed when the insertion occurs in Q200G201. The aggregation of VP7 trimers into highly ordered hexagonal lattice of trimeric subunits is an equilibrium process in which the equilibrium is shifted so far to crystal formation that nearly no subunits are present in soluble form. The moment the solubility of VP7 was increased the equilibrium changes and shifted more towards soluble trimers. Therefore the force behind the equilibrium is the hydrophobicity or insolubility of AHSV VP7.

Examination of the gradient purified particulate structures of VP7 and the VP7 insertion mutants by scanning electron microscopy revealed the following. The mt200 protein, like wild-type VP7, aggregated into flat, disc-shaped, usually hexagonal crystals with dimensions of up to 6 μm in diameter and approximately 200 nm thick. These disc-shaped aggregates of expressed AHSV VP7 have previously been observed in recombinant baculovirus-infected insect cells (Chuma et al., 1992) and are also produced in AHSV-infected BHK cells (Burroughs *et al.*, 1994). These crystals are formed of flat sheets of VP7 trimers. Although not proved it can be assumed that each sheet in the crystal represents a double layer of VP7 trimers where the hydrophobic bottom domains of the trimers are located on the inside away from the aqueous surrounding, while the top domains face

the environment. The bottom domains are probably involved in keeping the two layers together by means of hydrophobic interactions, similar to the interaction with the underlying VP3 molecules in the core. In each layer of the crystal the trimers are arranged as hexagonal rings, similar to the rings of VP7 trimers that are observed of the surface of the core particles (Burroughs *et al.*, 1994; Basak et al., 1996; Grimes *et al.*, 1998; Stuart *et al.*, 1998). The mt200 was arranged in the same lattice of trimeric subunits, described for the VP7 crystal lattice (Burroughs *et al.*, 1994). The hexagonal arrangement observed in the VP7 crystal lattice appears to have a direct structural similarity to the segmented, ring-shaped capsomeres that are visible on the outer surface of the AHSV core (Burroughs *et al.*, 1994), which are also composed of VP7 (Hewat *et al.*, 1992). The particulate form of mt177 does not have the characteristic flat, hexagonal crystal appearance of mt200 and VP7, but the particles have a round ball-like structure. The soluble portion of the protein, recovered from the top of the sucrose gradient did not assemble into any recognisable structure, visible by SEM or TEM analysis. This is not unexpected if the top fractions represent soluble trimers. The fine structure of the ball-like structures was further investigated by TEM analysis and showed the same lattice arrangement of trimeric subunits, observed in VP7 and mt200 crystals. A possible explanation for the round, ball-like structures formed by the mt177 protein, is that when the mt177 trimers aggregate into a highly ordered hexagonal lattice structure, the hydrophilic/soluble mt177 trimers resulted in a weaker interactions between adjacent sheets and the crystal appears round and distorted.

Investigation of the CLP formation when co-expressed with AHSV-9 VP3, revealed that both VP7 insertion mutants assembled onto VP3 scaffolds to form CLPs. These CLPs were morphological identical to CLPs formed by the assembly of wild-type VP7 and VP3. Their biophysical character was also identical to that of normal CLPs, since the CLPs produced by the insertion mutants of VP7 appeared to be equally stable in the same ionic strengths and pH conditions as normal CLPs. However, one unique characteristic about the yield of CLPs produced, was observed. The yield of CLPs produced by mt200 was as low as in the case of VP7, since most of the mt200 protein, like VP7, aggregated to form crystals. The yield of CLPs produced by mt177 was significantly higher. No crystals were present with the co-expression of VP3, although a small amount of mt177 protein did aggregate in the highly ordered lattice described in the previous paragraph. These data indicate that mt177 is indeed more soluble than VP7 and that it still forms the trimeric structure necessary for assembly on theVP3 scaffold and that more trimers are available for CLP formation.

The data observed can be summarised as shown in *Figure 2.23*. The VP7 crystals have no known functional significance in the replication cycle of AHSV and are only a by-product in the viral morphogenesis. The assembly of the trimers (B) into hexagonal crystals (D) is forced by the hydrophobic nature of the protein. This resulted in a low yield of CLPs (C) synthesised when co-expressed with VP3, since only a limited quantity of soluble VP7 trimers is available for CLP formation. When the solubility of VP7 is increased (E), the equilibrium shifts towards more soluble

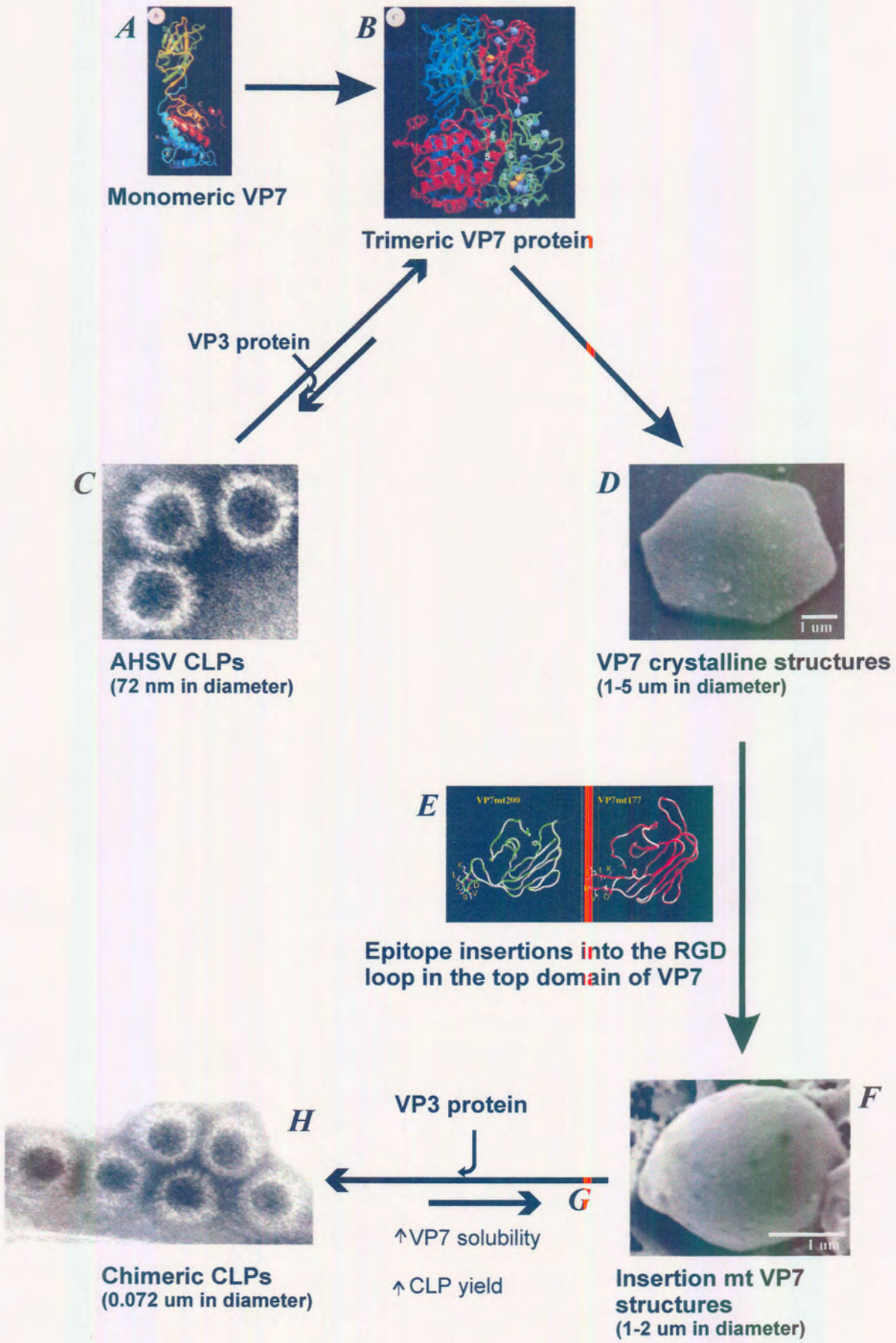

Figure 4.24: Summary of results. See text for details.

trimers. This causes an increase in the effective concentration of the trimers (G) in the cytoplasm of the cell. Therefore, more trimers are available for assembly onto VP3 scaffolds, which resulted in increased yield of CLPs (H) produced.

The next step of the investigation was to determine if the regions chosen for epitope insertion were flexible enough to tolerate additional sequences and what the effect of the insertions will be on the trimerisation and solubility of VP7. The size of the inserts that would be accommodated by the VP7 3-D structure also has be determined. To address these questions two chimeric VP7 mutants were constructed, utilising the restriction enzyme sites introduced into the two specified regions of the VP7 gene. VP7 chimeras with an additional 105 amino acids were prepared, by inserting a region of AHSV-9 VP2, containing at least two neutralising epitopes of the protein. The two VP7/TrVP2 chimeric genes were expressed in insect cells

The chimeric proteins were analysed for their ability to form crystals and their solubility. The two chimeric VP7 proteins (mt177/TrVP2 and mt200/TrVP2) were recovered from the sucrose gradient as a heterogeneous complex with a maximum sedimentation rate of approximately 400 S. The data indicates that the chimeras were present as multiprotein structures, which are larger than the trimeric structures observed in the case of mt177, but also much smaller than the crystals formed by VP7. Examination by SEM revealed small ball-like structures of diameters of approximately 0.5 μm. Since the proteins were more than 90% pure, as analysed by protein gel electrophoresis, it was assumed that these structures represent aggregates of the chimeric proteins.

Data obtained by Roy *et al.* (1997) suggested that the insertion of a number of foreign epitopes into the BTV VP7 at site Gln238 abrogated CLP formation, despite the fact that this site is located on an exposed loop of VP7. Successful insertion of sequences of up to 29 nucleotides could be achieved in the Ala145 site without inhibiting CLP formation. Although CLP formation was not analysed for the chimeras constructed in the study, the successful insertion of a foreign domain into AHSV VP7 resulted in a multimeric protein structure, which resembles structures from highly ordered arrays of protein. Whether the chimeric proteins in this structures are folded correctly and retained the epitopes of the inserted domain, remains to be resolved.

CHAPTER 5

CONCLUDING REMARKS AND FUTURE PROSPECTS

The development of particulate vector systems for the presentation of immunogenic epitopes provides a powerful approach for the delivery of antigens. Some existing particulate vector systems are based on linking an epitope to a carrier protein capable of assembly into a multimeric structure. Examples include hepatitis B particles (Clarke *et al.*, 1987), poliovirus particles (Evans *et al.*, 1989) and yeast Ty-particles (Adams *et al.*, 1987). AHSV is associated with three characteristic structures that could be used as particulate delivery systems. The NS1 tubules were found to be effective carriers for foreign epitopes, in the case of BTV (Mikhailov *et al.*, 1996). The VP7 crystals elicit a strong humoral immune response in an animal model (Wade-Evans *et al.*, 1997; Wade-Evans *et al.*, 1998). Empty virions or particles that simulate the virion surface should also provide a safe way of stimulating protective immunological memory.

The objective of this study was not only to investigate the morphology and assembly of these structures, but also to investigate their use as delivery systems for neutralizing epitopes. Three specific aims were identified and accomplished. The first aim involved the cloning, characterization and expression of the NS1 gene, followed by biochemical and morphological analysis of the NS1 tubules, as well as the identification of potential epitope insertion sites. The second aim was to co-express different combinations of the AHSV genes that encode the four major structural proteins to investigate particle morphogesis in the absence of the other viral components. The last aim involved the identification of epitope insertion sites in VP7 that are not essential for trimer-trimer interactions or CLP formation. The academical and practical value of the results are briefly highlighted and discussed here.

A full-length cDNA copy of the dsRNA segment 5 of AHSV-6 that encodes NS1, was cloned and sequenced. Bioinformatics is the key to understanding the properties and function of AHSV proteins. DNA and protein sequences are amenable to computer analysis, since they can be represented by strings of letters. The NS1 gene contains the conserved terminal hexanucleotides, proposed by Mizukoshi *et al.* (1993), with segment-specific inverted terminal repeats reported for other orbivirus segments. A hydrophilic region, displaying significant antigenicity, was identified in the C-terminus of NS1 and it was postulated that this region may be exposed on the surface of the AHSV NS1 tubules. This was indeed found to be true for BTV NS1 (Du Plessis *et al.*, 1995; Mikhailov *et al.*, 1996). The cloned NS1 gene was epressed *in vitro* and yielded a NS1 protein of the expected size thereby confirming that the ORF was full-length and did not contain any stop codons. Evidence was obtained that the *in vitro* synthesised NS1 protein of AHSV assembled spontaneously to form small tubular structures. This indicates that the ability to form tubules is self-primed and as

such a function of the amino acid sequence of the NS1 protein.

The NS1 gene was expressed to high levels, using a novel Bac-to-Bac™ baculovirus expression system. The use of this expression system has facilitated the rapid and convenient expression of NS1, since the entire recombinant baculovirus genome could be constructed in *E. coli* and did not involve *in vivo* homologous recombination. Heterologous expression of this gene enabled the first assembly studies regarding the AHSV tubule. The baculovirus expressed NS1 assembled into tubular structures in the insect cells with similar morphology to authentic tubules found in AHSV-infected cells (Huismans & Els, 1979). An important finding was that the morphology and biophysical properties differed in many respects from those described for other orbiviruses such as BTV, EHDV and BRDV. The purified tubules reacted in an immuno-labelling assay with anti-AHSV-6 antiserum, as well as with heterologous antiserum. This not only confirmed the AHSV origin of the protein, but also the antigenicity of these multimeric structures.

The subsequent approach for the development of AHSV NS1 tubules as a particulate antigen delivery system is to construct a panel of insertional mutants, by introducing several foreign antigenic sequences of different lengths into the proposed antigenic site of NS1. This would provide the means to identify the maximum length of a foreign peptide that could be inserted into NS1 without disrupting tubule formation. Deletions, point and domain switching analysis of the NS1 protein can be used to identify certain sequences in the NS1 protein that are essential for assembly into tubules. The use of multiple baculovirus gene expression vectors could also enable the formation of multiple epitope tubules, by co-expressing chimeric NS1 proteins with different epitopes. NS1 tubules have many advantages over CLPs as epitope carriers. They are composed of a single protein, in cotrast to CLPs, which consist of VP3 and VP7. In addition, the expression level of recombinant NS1 is generally high (ca. 20% of the proteins synthesised in infected Sf cells) and tubules are easy to purify. Therefore, tubules could provide an efficient and inexpensive system for the presentation of single or multiple foreign epitopes. The tubules are also highly immunogenic and elicit a strong humoral immune response without the use of standard adjuvants.

Using the novel Bac-to-Bac™ baculovirus expression system, dual-gene vectors co-expressing various combinations of AHSV genes under control of either the polh or p10 promoters, were constructed. Co-expression of the VP3 and VP7 genes resulted in the intracellular formation of CLPs, which structurally resembled AHSV cores and reacted strongly with VP7 monoclonal antibodies. In contrast to virus-derived cores, the CLPs were empty, since they lacked the genome and minor core proteins. The problem found with the previous co-infection of VP3 and VP7, regarding the variation in the ratio of VP3 to VP7, which correlates with the variation in the multiplicity of infection of each recombinant virus from cell to cell (Maree *et al.*, 1998) was overcome using this co-expression strategy. The CLPs produced were uniform in structure and the molar

ratios of the two proteins were si VP7 derived from infectious AHSV. However, the yield of CLPs were low, which made the large scale purification of these particles for vaccination purposes or use in high resolution structural studies, very difficult. It should be noted that VP7 aggregates into large distinctive crystals in infected cells, which could impede incorporation into particles. Furthermore, low yields of proteins are generally obtained when AHSV genes are expressed using the baculovirus system in comparison to BTV or EEV genes. These two factors downregulated the assembly of particles.

To investigate the structure and assembly of AHSV VLPs, two dual recombinant baculovirus vectors were used, the one expressing AHSV-9 VP5 and VP7, the other AHSV-9 VP3 and either AHSV-9 or AHSV-3 VP2. The expressed proteins assembled into double capsid particles with a diffuse surface structure. The formation of VLPs in the absence of other AHSV encoded structural or non-structural proteins implies that these proteins are not necessary for the assembly of VLPs in insect cells. The particles, however, were not homogenous, but contained different amounts of the outer capsid proteins and the yield of VLPs was extremely low. This may be due to variable amount of VP7 incorporated during intracellular assembly as a direct result of the variation in the ratio of VP3 to VP7 expression in insect cells co-infected with the two dual recombinant baculoviruses (French *et al.*, 1990; Maree *et al.*, 1998). It is possible that the absence of VP7 capsomeres in partially assembled CLPs resulted in the failure of VP2 or VP5 to associate with the CLPs or in some cases resulted in partial association. This problem could be resolved by constructing a quadruple gene expression vector, which allows the simultaneous expression of all four major structural proteins of AHSV. However, this will not solve the problem of the low expression levels of AHSV proteins. At this stage no information is available on the regulation of AHSV transcription and translation. Dual expression of AHSV genes seems to decrease the expression levels even further, compared to single expression. Quadruple expression could result in even lower expression levels. A large fraction of most of the heterologous expressed AHSV proteins also seems to be insoluble and could also impede the assembly process.

AHSV comprises multiple protein components in non-equimolar ratios, each of which is encoded by a discrete gene (mRNA species). These factors make the mechanism of virus assembly a challenge to unravel. Synthesis of subviral particles in eukaryotic cells by a heterologous expression system, opens up the opportunity to investigate the protein-protein interactions involved in the assembly process, the stages of viral assembly and the contribution of the individual components to that process. An increased understanding of viral morphogenesis may aid the development of antiviral agents, which specifically interfere with the assembly process. The information on the assembly is also important regarding the future development of a recombinant subunit vaccine, utilising the AHSV CLPs and VLPs. For example, by manipulating the structure of various viral proteins, it will be possible to develop particulate antigen delivery systems for the presentation of

immunogenic epitopes against other infectious diseases. Furthermore, it has been reported that BTV VLPs fully protect sheep against BTV, while BTV CLPs induce partial protection not involving neutralising antibodies, implicating a role for cell-mediated immunity. No such information is yet available for AHSV. If this holds true for AHSV VLPs, these particles will not only provide safe and effective vaccination, but also allow differentiation between vaccinated and infected horses, thereby simplifying the international movement of horses.

Another important application is the use of CLPs and VP7 crystals as antigen delivery systems. The VP7 protein, associated with both the CLPs and crystals, was manipulated to receive foreign immunogenic epitopes. The functional significance of two hydrophilic amino acid regions in the structure, trimerisation and solubility of VP7 was subsequently investigated by analysing two insertion mutants of AHSV-9 VP7. A cloning site comprising three unique restriction sites was introduced into two chosen antigenic or hydrophilic regions in the top domain of AHSV-9 VP7, respectively, using the convenient PCR methods for mutagenesis. These cloning sites facilitated the easy insertion of epitopes, for example a truncated fragment of the VP2 protein containing a previously identified immunodominant epitope of VP2, responsible for neutralisation. The effects of inserting as little as 6 amino acids or as much as 105 amino acids in the two chosen sites on protein solubility, folding and trimerisation were investigated. Insertion of six amino acids in the flexible RGD loop located in the top domain of VP7 increased the solubility of VP7, although the protein was still able to form its trimeric structure and to assemble into CLPs. Unlike normal VP7 and insertion mutant mt200, mt177 did not aggregate into highly ordered hexagonal crystals but formed ball-like structures, that could rapidly dissociate into trimers when required by equilibrium. As a result of the increased solubility of the VP7mt177 trimers, the yield of CLPs produced, when co-expressed with VP3, was significantly higher than with normal VP7 or mt200. Preliminary studies indicated that the VP7 structure in this highly flexible loop is able to accommodate up to 105 amino acids without losing the ability to assemble into trimers and ultimately into CLPs. This approach represents a novel strategy and is important for the development of future subunit vaccines, since it was the first report on increased VP7 solubility, as well as on the incorporation of up to 105 amino acids (1/3 of the size of VP7) without obstructing CLP production.

Several contributions regarding the protein-protein interaction in virus assembly, the solubility of VP7, the yield of CLP production and the use of CLPs and VP7 crystals as vehicles for foreign immunogens have been made during this investigation. Subsequent work, following on from that described in this thesis, has been performed on the AHSV-9 VP7 gene and insertion mutants constructed. Firstly, a third insertion mutant of VP7 has been constructed, with three unique restriction enzyme sites in the nucleotide sequence encoding amino acids 144 to 145 (Joanne Riley). Preliminary data indicated that the insertion at 144-145, like mt200, did not influence the solubility of VP7 and that mt144 also forms hexagonal crystals and CLPs. Secondly, three other

chimeric VP7 proteins were also constructed, two of which contained smaller truncated fragments of 33 amino acids of AHSV-9 VP2 inserted in each of the constructed sites, respectively (Lineo Motopi), and a third containing 12 amino acids from NS3 in site 200-201 (Tracey Meiring). These studies have shown that the VP7 chimeras, containing 33 amino acids, remain in a trimeric form that assemble into ball-like structures, similar to those found in this study. This data confirm the results obtained in this study. The insertion of 12 amino acids at position 200-201 (mt200) did not influence the ability of the protein to assemble into hexagonal crystals. The assembly of these chimeras with VP3 is still under investigation.

The immune response elicited by the chimeric VP7 crystals, chimeric CLPs and VLPs will be evaluated in the near future to determine the application of these systems as subunit vaccines. The VP7 crystal and chimeric CLPs may provide the ideal candidate subunit vaccine capable of inducing antibodies against many AHSV serotypes as well as serogroup protection provided by VP7. It is possible that in the future even more elaborate experiments where different sites or domains could be manipulated in a single VP7 protein could result in the expression of more than one epitope onto the VP7 surface. This can also lead to the application of an antigen presentation system for epitopes of a variety of human and animal important viruses.